



Article

Growth Factors VEGF-A₁₆₅ and FGF-2 as Multifunctional Biomolecules Governing Cell Adhesion and Proliferation

Antonín Sedlář^{1,2} , Martina Trávníčková¹ , Roman Matějka^{1,3} , Šimon Pražák^{1,3}, Zuzana Mészáros^{4,5} , Pavla Bojarová^{3,4} , Lucie Bačáková^{1,*} , Vladimír Křen⁴ and Kristýna Slámová^{4,*}

- ¹ Laboratory of Biomaterials and Tissue Engineering, Institute of Physiology of the Czech Academy of Sciences, Vídeňská 1083, CZ 14220 Praha 4, Czech Republic; Antonin.Sedlar@fgu.cas.cz (A.S.); Martina.Travnickova@fgu.cas.cz (M.T.); Roman.Matejka@fgu.cas.cz or roman.matejka@fbmi.cvut.cz (R.M.); simon.prazak@fgu.cas.cz or simon.prazak@fbmi.cvut.cz (Š.P)
 - ² Department of Physiology, Faculty of Science, Charles University, Viničná 7, CZ 12844 Praha 2, Czech Republic
 - ³ Faculty of Biomedical Engineering, Czech Technical University in Prague, CZ 27201 Kladno, Czech Republic; bojarova@biomed.cas.cz
 - ⁴ Laboratory of Biotransformation, Institute of Microbiology of the Czech Academy of Sciences, Vídeňská 1083, CZ 14220 Praha 4, Czech Republic; zuzana.meszaros@biomed.cas.cz (Z.M.); kren@biomed.cas.cz (V.K.)
 - ⁵ Department of Biochemistry, University of Chemistry and Technology Prague, Technická 6, CZ 16628 Praha 6, Czech Republic
- * Correspondence: Lucie.Bacakova@fgu.cas.cz (L.B.); slamova@biomed.cas.cz (K.S.); Tel.: +420-296443743 (L.B.); +420-296442766 (K.S.)



Citation: Sedlář, A.; Trávníčková, M.; Matějka, R.; Pražák, Š.; Mészáros, Z.; Bojarová, P.; Bačáková, L.; Křen, V.; Slámová, K. Growth Factors VEGF-A₁₆₅ and FGF-2 as Multifunctional Biomolecules Governing Cell Adhesion and Proliferation. *Int. J. Mol. Sci.* **2021**, *22*, 1843. <https://doi.org/10.3390/ijms22041843>

Academic Editor: Claudiu T. Supuran

Received: 19 January 2021

Accepted: 10 February 2021

Published: 12 February 2021

Publisher's Note: MDPI stays neutral with regard to jurisdictional claims in published maps and institutional affiliations.



Copyright: © 2021 by the authors. Licensee MDPI, Basel, Switzerland. This article is an open access article distributed under the terms and conditions of the Creative Commons Attribution (CC BY) license (<https://creativecommons.org/licenses/by/4.0/>).

Abstract: Vascular endothelial growth factor-A₁₆₅ (VEGF-A₁₆₅) and fibroblast growth factor-2 (FGF-2) are currently used for the functionalization of biomaterials designed for tissue engineering. We have developed a new simple method for heterologous expression and purification of VEGF-A₁₆₅ and FGF-2 in the yeast expression system of *Pichia pastoris*. The biological activity of the growth factors was assessed in cultures of human and porcine adipose tissue-derived stem cells (ADSCs) and human umbilical vein endothelial cells (HUVECs). When added into the culture medium, VEGF-A₁₆₅ stimulated proliferation only in HUVECs, while FGF-2 stimulated the proliferation of both cell types. A similar effect was achieved when the growth factors were pre-adsorbed to polystyrene wells. The effect of our recombinant growth factors was slightly lower than that of commercially available factors, which was attributed to the presence of some impurities. The stimulatory effect of the VEGF-A₁₆₅ on cell adhesion was rather weak, especially in ADSCs. FGF-2 was a potent stimulator of the adhesion of ADSCs but had no to negative effect on the adhesion of HUVECs. In sum, FGF-2 and VEGF-A₁₆₅ have diverse effects on the behavior of different cell types, which maybe utilized in tissue engineering.

Keywords: heterologous expression; recombinant vascular endothelial growth factor (VEGF); basic fibroblast growth factor (bFGF); adult stem cells; endothelial cells; cell adhesion; cell proliferation; tissue engineering; regenerative medicine; vascular replacements

1. Introduction

Vascular endothelial growth factor A (VEGF-A) is a heparin-binding dimeric protein belonging to the VEGF gene family together with VEGF-B, VEGF-C, VEGF-D, and the placental growth factor. All these factors differ in their affinity for three VEGF receptors, i.e., VEGFR-1, VEGFR-2, and VEGFR-3. VEGF-A binds to VEGFR-1 and VEGFR-2. Among all members of the VEGF family, VEGF-A is most strongly associated with angiogenesis and acts as a signaling protein and as a growth factor promoting specific functions in vascular endothelial cells. It occurs in nine isoforms, namely VEGF₁₂₁, VEGF₁₄₅, VEGF₁₄₈, VEGF₁₆₂, VEGF₁₆₅, VEGF_{165b}, VEGF₁₈₃, VEGF₁₈₉, and VEGF₂₀₆, which are generated by alternative exon splicing of the human VEGF-A gene and differ in the number of amino acids in

their chains. The VEGF-A₁₆₅ isoform is most abundantly expressed and since it plays a key role in enhancing cell proliferation and angiogenesis [1], it is used in commercially available growth media for endothelial cells, or in experimentally-designed media inducing vasculogenesis and differentiation of stem cells towards endothelial cells [2]. VEGF-A₁₆₅ has been used in clinical trials for therapy of refractory coronary artery disease, where it was applied in the form of a gene construct [3], in the form of mRNA [4], or in the form of the protein [5]. Other clinical applications of VEGF-A₁₆₅ (and VEGF in general) include treatment of periodontitis and reparation of jaw bone defects, where this factor has been applied as a component of a concentrated growth factor (CGF) fibrin, i.e., a new generation of platelet concentrate biomaterial, based on autologous fibrin with multiple concentrated growth factors [6]. Recent preclinical applications of VEGF-A₁₆₅ include therapy of spinal cord injury in a rat model [7], regeneration of sciatic nerve in rats, where VEGF-A₁₆₅ was combined with FGF-2 [8], functionalization of artificial blood vessel replacements for promoting spontaneous endothelialization of these grafts in an ovine model [9], treatment of placental insufficiency [10], and healing of cutaneous wounds in mice [11]. VEGF-A₁₆₅ has also been widely used for experimental work in vitro, e.g., creation of vascularized tissue-engineered constructs, intended for bone regeneration [12] or functionalization of a decellularized pericardial matrix, intended for cardiovascular tissue engineering, in order to promote its recellularization with endothelial and stem cells [13]. In this context, it is worth mentioning that VEGF-A₁₆₅ immobilized on cell cultivation substrates can also act as an extracellular adhesion molecule, binding to integrin adhesion receptors on cells [14,15].

Fibroblast growth factor-2 (FGF-2); also known as a basic fibroblast growth factor (bFGF), is a signaling molecule of the family of fibroblast growth factors. It regulates a wide range of biological processes, e.g., cell proliferation, migration, or differentiation [16]. Similar to VEGF-A₁₆₅, it is commonly used as a supplement in commercially available media for endothelial cell growth and expansion. FGF-2 is also a common additive to growth media for adipose tissue-derived stem cells (ADSCs). It maintains the stem cell phenotype of ADSCs, enhances their proliferation, and thus it is suitable for ADSC expansion and maintenance of their therapeutic potential [17]. In addition, it is a component of media for the expansion of various cell types, e.g., chondrocytes [18] or induced pluripotent stem cells [19]. FGF-2 has been widely applied in clinical practice, particularly in cutaneous wound healing, such as second-degree burns and chronic ulcers [20,21], and in bone regenerative therapies, such as treatment of bone fractures, osteotomies, and osteonecrosis (for a review, see [22]), or treatment of periodontitis with intrabony defects ([23]; for a review, see [24]). FGF-2 also proved its efficacy in the treatment of oral lichen planus [25] or vitiligo [26]. Animal studies also proved that FGF-2 is promising for regenerative therapy of spinal cord injury [27], of liver injury and liver diseases [28], or for treatment of alopecia [29]. It also enhanced the tendon-to-bone healing in a rabbit model [30]. In studies in vitro, FGF-2 has also been shown to promote the adhesion of various cell types, including endothelial cells and ADSCs [31,32]. Immobilization of VEGF-A₁₆₅ and FGF-2 to the surface of various synthetic and nature-derived biomaterials enhanced adhesion and proliferation of various cell types, mainly of endothelial cells, and improved the biocompatibility of these materials [33–36]. Together with VEGF-A₁₆₅, FGF-2 has been recently used for functionalization of a fibrin/heparin coating on the inner surface of an ePTFE vascular prosthesis to promote its endothelialization [37].

VEGF-A₁₆₅ and FGF-2 are challenging proteins to be expressed in microbial expression systems. Although they are commercially available, their prices are rather inhibitory, namely for larger experiments. When these proteins are produced in *Escherichia coli*, the formation of inclusion bodies and the necessary protein refolding are inconvenient and result in low yields of the active growth factors [38–40]. In addition, purification of the growth factors from an *E. coli* lysate requires total removal of bacterial endotoxins [41], which is extremely important for any in cellulo or ex vivo experiments. Therefore, we aimed to develop a simple and generally accessible method for heterologous expression and purification of native VEGF-A₁₆₅ and FGF-2 in a eukaryotic expression system in

methylotrophic yeast *Pichia pastoris*, which is generally more suitable for the expression of eukaryotic proteins [42,43]. VEGF-A₁₆₅ has been produced in *P. pastoris* previously, however, the produced protein was fused with hydrophobin, and the biological activity of this chimeric protein was not verified [44].

Here, we describe a facile and high-yielding method for the extracellular expression of VEGF-A₁₆₅ and FGF-2 in *P. pastoris* KM71H, followed by a single purification step to obtain proteins of sufficient quantity and quality even for large-scale experiments. Moreover, the respective proteins were also expressed with the N-terminal 8 amino acid substrate sequence for Factor XIIIa (NQE_QVSPL), which is useful for covalent attachment of the growth factors into a fibrin network used for coating of cardiovascular prostheses [45]. The functionality of recombinant growth factors was verified and quantified *in vitro* by evaluating the metabolic activity and the cell number of human and porcine ADSCs and human umbilical vein endothelial cells (HUVECs) cultivated in media containing the newly produced growth factors. The effect of substrate-bound growth factors on cell adhesion and proliferation was evaluated as well because these factors are often used for immobilization on various biomaterials intended for tissue engineering.

2. Results and Discussion

2.1. Expression and Purification of Vascular Endothelial Growth Factor (VEGF)-A₁₆₅ and Fibroblast Growth Factor (FGF)-2M Growth Factors

Due to the increasing number of biological research studies employing human cells that require supplementation by human growth factors, such as VEGF-A₁₆₅ and FGF-2, efficient production of these factors has become a challenge to reduce the costs of the experiments. The major advantage of the yeast expression system (*Pichia pastoris*) is a high-yielding production of the target protein, which is secreted into the culture media, thus facilitating a simple one-step purification by, e.g., ion-exchange chromatography [42,43].

For the efficient expression of human FGF-2, its sequence was slightly genetically modified as it naturally comprises two LysArg dibasic cleavage sites recognized by the Kex2 protease important for the processing of extracellularly targeted proteins [46]. These sites had to be removed by mutagenesis (R31K/R129K), where two arginine residues were replaced by lysines to maintain the basic character. The resulting protein has been designated FGF-2M (for respective sequences see the Supplementary Materials). Moreover, both VEGF-A₁₆₅ and FGF-2M were also designed and expressed with the N-terminal 8 amino acid substrate sequence for Factor XIIIa (NQE_QVSPL), which can be used for covalent attachment of the growth factors into a fibrin network used for coating cardiovascular prostheses or implants [45].

The genes of the respective growth factors were obtained by commercial synthesis and cloned into the yeast expression vector pPICZA via the 5⁰-EcoRI and 3⁰-KpnI restriction sites. The plasmids were electroporated into the methylotrophic expression host *Pichia pastoris* KM71H, and the transformants were selected based on zeocin resistance. The extracellular expression of the individual growth factors was screened in nutrient-rich media and the best producing clones were cryopreserved. Subsequently, the conditions for the large-scale production were explored to reach good yields of the target proteins.

VEGF-A₁₆₅ and its variant comprising the substrate sequence for Factor XIIIa (VEGF-A₁₆₅-FXIIIa) were expressed in the minimal media upon induction by methanol for three days. After that, the culture media were collected and the amounts of proteins in the crude media were determined (35 mg/L for VEGF-A₁₆₅; 37 mg/L for VEGF-A₁₆₅-FXIIIa). VEGF-A₁₆₅ was purified from the culture media using cation exchange chromatography at pH 6.0; the final yield of the purified VEGF-A₁₆₅ was 15 mg per 1 L of the original culture medium (43%). The multiple bands of VEGF-A₁₆₅ probably represent different O-glycosylation variants of the protein (Supplementary Materials Figure S1). For the production of FGF-2M and FGF-2M-FXIIIa, the initial cultivation of *P. pastoris* cells in the nutrient-rich medium was required; then the cells were transferred into the minimal medium to facilitate the subsequent purification, and the expression of the desired proteins was induced by methanol for three days. Even under these conditions, the production was generally lower than in the case of

VEGF-A₁₆₅, e.g., 18 mg/L of FGF-2M and 15 mg/L of FGF-2M-FXIIIa were obtained from the crude media. FGF-2M was purified employing the cation exchange chromatography at pH 4.0, and the final yield of the purified protein reached 7 mg per 1 L of the original culture medium (39%; for sodium dodecyl sulfate polyacrylamide gel electrophoresis (SDS-PAGE) of the purified growth factors see Supplementary Materials Figure S1). To make the production process biotechnologically straightforward, VEGF-A₁₆₅-FXIIIa and FGF-2M-FXIIIa were not further purified; the crude media were concentrated and used for the assay of biological activity as such. After sterilization by syringe filters, the protein solutions were supplemented with 20% (v/v) of sterile glycerol, were shock-frozen in liquid nitrogen, and stored at -80 °C without loss of biological activity.

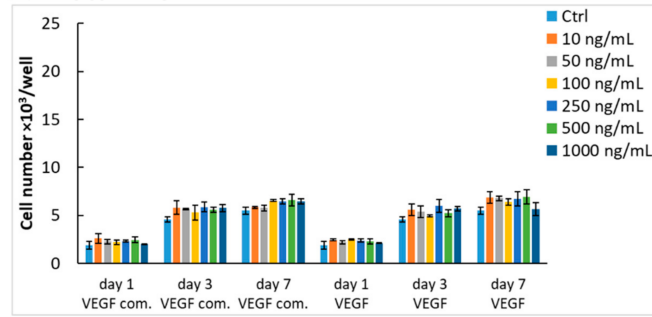
2.2. Mitogenic Activity of Soluble VEGF-A₁₆₅ and FGF-2M

2.2.1. Number of Cells in Media with Growth Factors

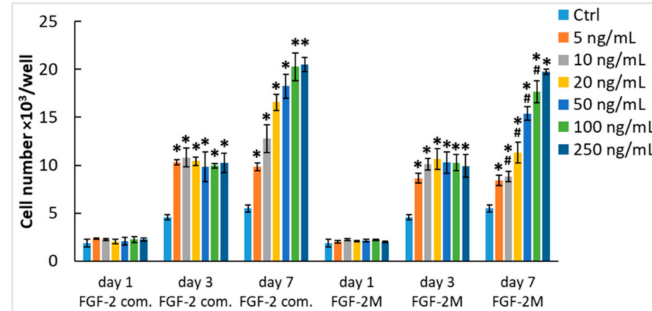
First, we verified the mitogenic activity of our recombinant VEGF-A₁₆₅ and FGF-2M by using these factors as supplements of the growth media for ADSCs and HUVECs. In the case of ADSCs, the mitogenic response to the two investigated growth factors markedly differed. The addition of VEGF-A₁₆₅ in concentrations from 10 to 1000 ng/mL into the Dulbecco's modified Eagle medium (DMEM) with 10% fetal bovine serum (FBS) did not have any significant impact on the number of ADSCs (Figure 1A). This result correlates well with a study by Khan et al. [47] where the addition of VEGF-A₁₆₅ (50 ng/mL) into the cultivation medium did not enhance the number of ADSCs. A possible explanation is that VEGFs, in general, are endothelial-cell specific mitogens, and in different cell types, they may have different functions. Khan et al. [47] showed that VEGF-A₁₆₅ stimulated differentiation of ADSCs towards endothelial cell phenotype, and it is known that cell differentiation is often accompanied by a decrease in cell proliferation activity. Similarly, the differentiation towards endothelial cells was observed in dental pulp stem cells exposed to a medium containing VEGF-A₁₆₅ [2], and also in circulating monocytes adhered to tissue-engineered vascular grafts, immobilized with VEGF-A₁₆₅ and implanted into the carotid arteries of sheep [9]. Another explanation for the insufficiency of VEGF-A₁₆₅ to stimulate the ADSC proliferation is a lack of the VEGFR2 receptor on human ADSCs, resulting in a decreased sensitivity of these cells to VEGF, as suggested in a study by Bassaneze et al. (2010) [48]. Nevertheless, in our recent study, VEGF-A₁₆₅ attached to a decellularized pericardium through a fibrin mesh increased its recellularization with ADSCs and subsequent endothelialization in comparison with a pericardium modified only with fibrin [13].

When ADSCs were exposed to FGF-2M in concentrations from 5 to 250 ng/mL in the same medium, they showed significantly higher cell numbers at all tested FGF-2M concentrations after 3 and 7 days of cultivation compared with the cells in the control medium without FGF-2M (Figure 1B). Moreover, on day 7, a clear positive correlation of the cell number with the FGF-2 concentration was apparent. These results are in accordance with the study by Khan et al. [47], where a simultaneous increase in both proliferation and differentiation of ADSCs were obtained when VEGF-A₁₆₅ was combined with FGF-2. In general, our results are in line with all studies, in which FGF-2 is used for expansion of various cell types, such as mesenchymal stem cells including ADSCs [17], induced pluripotent stem cells [19] or chondrocytes [18], or for various regenerative therapies, in which the cell proliferation is needed, such as healing of cutaneous wounds [20,21], regeneration of damaged or diseased bone tissue [22,24], or treatment of vitiligo, requiring proliferation of melanocytes [26].

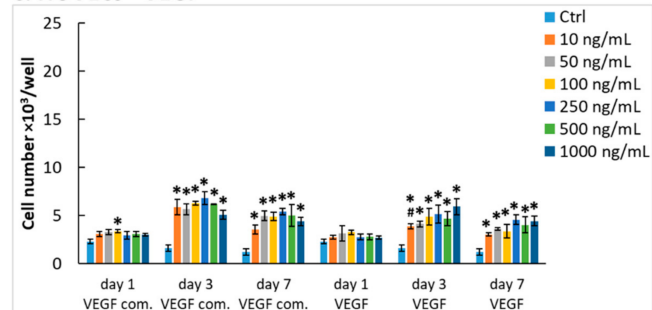
A. ADSCs - VEGF



B. ADSCs - FGF-2



C. HUVECs - VEGF



D. HUVECs - FGF-2

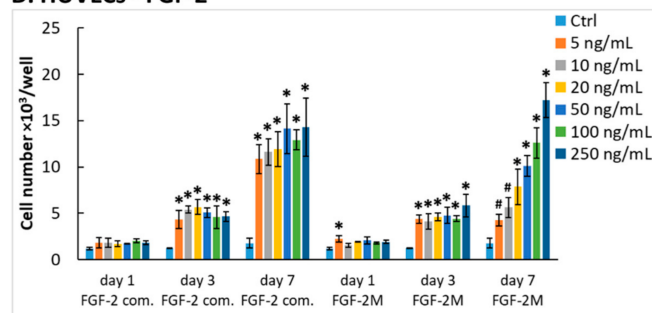


Figure 1. The mitogenic activity of vascular endothelial growth factor VEGF-A₁₆₅ and fibroblast growth factor FGF-2M diluted in the culture medium. The adipose tissue-derived stem cells (ADSCs) (A,B) or human umbilical vein endothelial cells (HUVECs) (C,D) were grown in media enriched with commercial VEGF-A₁₆₅ (VEGF com.) or our recombinant VEGF-A₁₆₅ in concentrations from 10 to 1000 ng/mL (A,C); in media enriched with commercial FGF-2 (FGF-2 com.) or our recombinant FGF-2M in concentrations from 5 to 250 ng/mL (B,D). The growth factors were added into Dulbecco’s modified Eagle medium (DMEM) with 10% fetal bovine serum (FBS) for ADSCs (A,B), and into EGM2-weak for HUVECs (C,D). Control cells were grown in media without growth factors (Ctrl). The cell number was determined on days 1, 3, and 7 after seeding. Mean standard deviation (SD) from 3 wells. Holm–Sidak method, p 0.05. The samples were statistically compared on the indicated day after seeding. Statistically significant differences are depicted above the columns. * statistically significant difference versus control sample (Ctrl). # statistically significant difference versus sample containing a corresponding concentration of commercial growth factor.

In the case of HUVECs, the mitogenic response to the two investigated growth factors was basically similar. On days 3 and 7 of cultivation, these cells showed increased numbers both in the medium containing VEGF-A₁₆₅ and in the medium containing FGF-2M in comparison with the control medium without the growth factors. On day 7, this increase was more pronounced in the medium with FGF-2. In addition, similar to ADSCs, the number of HUVECs also increased proportionally to the FGF-2 concentration, especially in the medium with our recombinant FGF-2M factor. In contrast, all concentrations of the commercial and our recombinant VEGF-A₁₆₅ increased the number of HUVECs to similar values (Figure 1C,D). Also, HUVECs treated with all the concentrations of VEGF-A₁₆₅ showed the highest cell number on day 3, and longer cultivation (7 days) led to a slight decrease in the cell numbers. This suggests that VEGF cannot maintain a desired proliferation rate of cells for longer time periods. This confirms the hypothesis that VEGF should be used in combination with other growth factors, as it is common in commercially available media for the growth of endothelial cells, such as Endothelial Cell Growth Medium 2 (EGM2) containing the recommended growth medium-2 supplement pack (EGM2-full; see Section 3.4. in the Materials and Methods). Among other factors, this pack contains FGF-2, which proved in our study to be capable, in both commercial and our recombinant form, to boost the proliferation of both ADSCs and HUVECs in a concentration-dependent manner. This result is in line with the fact that FGF-2 is an important component of various growth media for ADSCs and endothelial cells [17,49]. Thus, our recombinant protein behaves in full accordance with its commercial counterpart.

2.2.2. Comparison of Our Recombinant and Commercial Growth Factors

In cell proliferation studies, we also compared our recombinant VEGF-A₁₆₅ and FGF-2M prepared in *P. pastoris* with commercially available VEGF-A₁₆₅ produced in human embryonic kidney 293 (HEK 293) cells (GenScript, Cat. No. Z03073-1) and with FGF-2 produced in *E. coli* (GenScript, Cat. No. Z03116-1). From the obtained cell numbers it is clear that both commercial growth factors generally show increased mitogenic activity at lower concentrations than our recombinant VEGF-A₁₆₅ and FGF-2M (Figure 1). As already mentioned above, our recombinant FGF-2M contained two anti-protease amino acid mutations (R31K/R129K). FGF-2 contains two heparin-binding sites, mainly formed by clusters of basic amino acids in the positions of 102–129 and 128–144 [50]. In the literature, FGF-2 containing a single mutation in the first heparin-binding site (lysine changed for neutral amino acid alanine—K129A) showed a slightly lower capacity to bind low molecular weight heparin [51]. Quadruple mutation of residues in heparin-binding sites (R118Q/K119Q/K128Q/K129Q) caused almost no change in the mitogenic activity of FGF-2 but decreased the ability to induce chemotaxis and production of urokinase-type plasminogen activator (uPA) [52]. FGF-2 deletion mutant lacking residues 27–32 remained highly mitogenic and chemotactic but failed to induce the activity of uPA [53]. From the studies published so far, it is apparent that minor changes in the amino acid sequence of the heparin-binding site or the N-terminal part of FGF-2 do not alter its mitogenic activity [52,53]. Therefore, we presume that lower mitogenic activity of our recombinant FGF-2M per mg is caused by a non-negligible amount of impurities present in the protein solution even after purification by cation exchange chromatography (see Supplementary Materials Figure S1); thus, the actual amount, especially of FGF-2M molecules, is lower in the protein solution. A similar explanation can apply for a lower mitogenic activity of our recombinant VEGF-A₁₆₅ per mg in comparison with the activity of the commercial VEGF-A₁₆₅ produced in HEK 293 cells. Thus, we estimated the real amount of our recombinant growth factors by densitometric measurement of the bands with the use of ImageJ software (Figure S1). According to the densitometric analysis of lines containing samples of our recombinant growth factors, the content of VEGF-A₁₆₅ and FGF-2M corresponds approximately to 85% and 56% of the total proteins in solution, respectively.

Despite the impurities found, our recombinant growth factors were still able to significantly increase the cell number in comparison with control cells grown without these

factors, as was apparent mainly in ADSCs in the medium with FGF-2M (Figure 1B) and in HUVECs in the medium with VEGF-A₁₆₅ or FGF-2M (Figure 1C,D). Moreover, our recombinant growth factors were able to reach comparable mitogenic activity as their commercial counterparts when used in higher concentrations, i.e., 250 ng/mL of FGF-2M in the medium for ADSCs, and 50–1000 ng/mL of VEGF-A₁₆₅ or 20–250 ng/mL of FGF-2M in the medium for HUVECs. When the densitometric measurements are taken into account, the real concentration of our recombinant growth factors in these solutions is lower by 15% in VEGF, i.e., approx. 42–850 ng/mL instead of 50–1000 ng/mL, and by 44% lower in FGF-2M, i.e., approx. 11–140 ng/mL instead of 20–250 ng/mL.

2.2.3. Morphology of Cells in Media with Soluble Growth Factors

Our results on cell numbers were further reflected in the morphology of ADSCs and HUVECs grown in the media with VEGF-A₁₆₅ or FGF-2M for 7 days. The ADSCs in all tested media, i.e., in the media without VEGF-A₁₆₅, or with VEGF-A₁₆₅ of commercial or lab-made origin, were almost confluent with similar spindle-shaped morphology, random orientation, and distribution on the cultivation substrate (Figure 2A). Similar morphology and distribution of ADSCs were also found in the medium without FGF-2, with commercially-available FGF-2 or with our recombinant FGF-2M. However, in the media with both types of FGF-2, the number of cell nuclei was apparently higher than in the control non-supplemented medium, particularly in cultures with commercial FGF-2, where the cells seemed to form multilayered clusters with cells often oriented in parallel. Interestingly, the multilayered clusters were less pronounced in higher concentrations (from 100 ng/mL) of both types of FGF-2, particularly in commercial FGF-2 (Figure 2A).

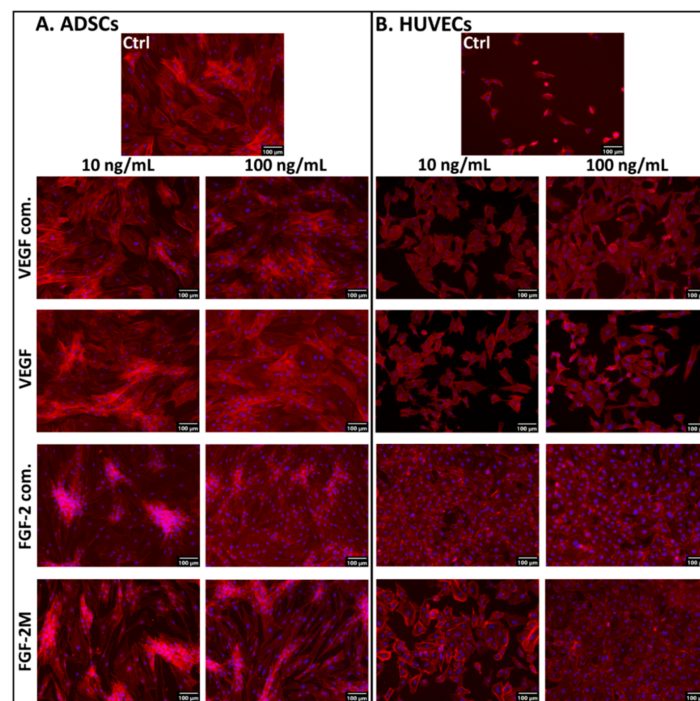


Figure 2. Microphotographs of ADSCs (A) and HUVECs (B) on day 7 after seeding in media enriched with commercial VEGF-A₁₆₅ (VEGF com.) or our recombinant VEGF-A₁₆₅, and in media enriched with commercial FGF-2 (FGF-2 com.) or our recombinant FGF-2M. The growth factors were added into DMEM with 10% FBS for ADSCs and into EGM2-weak for HUVECs. Representative low and high concentrations (i.e., 10 ng/mL and 100 ng/mL, respectively) of the tested growth factors were selected. Control cells were grown in media without growth factors (Ctrl). The filamentous actin in cells was stained with phalloidin-tetramethylrhodamine (TRITC) to visualize the cell morphology. The nuclei were counterstained with Hoechst 33258. Olympus IX 71 microscope, DP 70 digital camera, obj. 10, scale bar 100 m.

In HUVECs cultivated in the medium without growth factors, the cells were only sparsely distributed even on day 7 after seeding, although they were well-spread and polygonal. In contrast, in the medium with commercially available or our recombinant VEGF-A₁₆₅, the cell population density markedly increased (Figure 2B). Admittedly, the cells were not able to reach confluence at any concentration of both commercial and lab-made VEGF-A₁₆₅. On the contrary, in the medium with commercial FGF-2, the cells reached confluence even at low FGF-2 concentrations (up to 10 ng/mL). In the medium with our recombinant FGF-2M in low concentrations, the cell population density markedly increased in comparison with the control medium, and in high concentrations (from 100 ng/mL), the cells were able to reach full confluence (Figure 2B). Taken together, the commercial FGF-2 was more efficient for obtaining the confluence of endothelial cells than our recombinant FGF-2M, which can be attributed to the fact that the real concentration of our FGF-2M in the medium is lower due to the presence of impurities in its stock solution (see above the Section 2.2.2).

Since the HUVECs did not reach confluence after 7 days of cultivation with both types of VEGF-A₁₆₅ (i.e., commercial and our recombinant), and their number even decreased when compared with day 3 of cultivation (Figure 1C), we decided to perform an additional experiment. In a set of samples, we exchanged the medium on day 3 for a fresh medium with corresponding concentrations of the commercial or our recombinant growth factor (Figure 3). The results showed that the replacement of the medium with a medium with fresh growth factor maintained or even slightly improved the proliferation of HUVECs but the cell number values still did not surpass the values on day 3. This suggests that VEGF-A₁₆₅ becomes depleted from the medium in a relatively short time period and cannot stimulate proliferation for longer incubation times, which is in contrast with FGF-2 where the cell number values were the highest on day 7 of cultivation (Figure 1D). Taken all together, it is apparent that VEGF is only a weak mitogen for endothelial cells. When expanding endothelial cells in vitro, it is important to exchange the growth medium at least twice a week and to enrich the medium also with other growth factors (e. g., FGF-2, EGF, or IGF-1) to induce rapid and continuous cell growth.

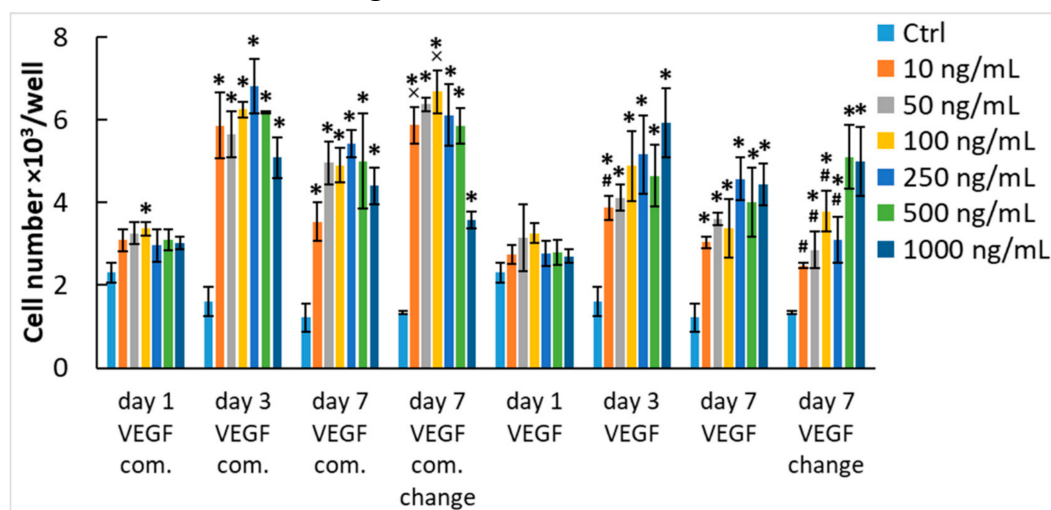


Figure 3. The effect of medium exchange on the mitogenic activity of VEGF-A₁₆₅ diluted in the culture medium. The HUVECs were grown in media enriched with commercial VEGF-A₁₆₅ (VEGF com.) or our recombinant VEGF-A₁₆₅ in the concentration range from 10 to 1000 ng/mL. VEGF-A₁₆₅ was added into EGM2-weak. Control cells were grown in media without growth factors (Ctrl). The cell number was determined on days 1, 3, and 7 after seeding. In some of the samples, the medium containing the corresponding concentration of growth factor was exchanged for a fresh one on day 3 after cell seeding. Mean SD from 3 wells. Holm–Sidak method, $p < 0.05$. The samples were statistically compared on the indicated day after seeding. Statistically significant differences are depicted above the columns. * statistically significant difference versus control sample (Ctrl). # statistically significant difference versus sample containing the corresponding concentration of commercial growth factor. ** statistically significant difference versus sample containing the corresponding concentration of growth factor without medium exchange.

2.2.4. Metabolic Activity of Cells in Media with Soluble VEGF-A₁₆₅ and FGF-2M

The results on the cell numbers were further verified by evaluating the metabolic activity of cells, measured by the resazurin assay (Supplementary Materials Figure S2). Cell metabolic activity is generally accepted as an indirect marker of cell proliferation activity and number. We found out that in HUVECs, the cell metabolic activity correlated well with the cell numbers, corresponding also with significant differences in the cell numbers observed between the samples with our recombinant growth factors and with the commercial ones in lower concentrations. Also after the medium exchange, the numbers of HUVECs in media with VEGF-A₁₆₅ generally corresponded to the values of cell metabolic activity (Supplementary Materials Figure S3).

However, in ADSCs, the direct cell counting and the assay of cell metabolic activity gave some different results. Interestingly, the metabolic activity of ADSCs was significantly increased by VEGF (both commercial and our recombinant) even on day 1 after seeding, while the direct cell counting did not show any differences (Figure 1A and Figure S2A). This indicates that ADSCs are responsive to this factor, although not by activating their proliferation. As mentioned above, Khan et al. [47] described the differentiation of ADSCs towards endothelial cell phenotype in a medium with VEGF-A₁₆₅. Cell differentiation, in general, is manifested by the synthesis of phenotype-specific protein markers, which can be associated with the increased enzymatic activity of cells. Second, the metabolic activity of ADSCs in the medium with FGF-2 was almost similar to the medium with VEGF-A (Supplementary Materials Figure S2A,B), while the cell number was markedly higher in the medium with FGF-2 than in the medium with VEGF-A (Figure 1A,B). In addition, the metabolic activity of ADSCs in the FGF-2-supplemented medium was generally lower than in HUVECs (Supplementary Materials Figure S2B,D), while direct cell counting gave opposite results (Figure 1B,D). These disproportions could be explained by the fact that the resazurin assay and related assays (such as MTT, MTS, XTT, or WST—see List of Abbreviations) measure the activity of dehydrogenases in cells, which is not always linearly correlated with the cell number. The cell metabolic activity can be influenced by a wide range of factors, such as the size of cells, their nuclei and their mitochondrial area, the specific phase of the cell cycle, cell–cell contacts, 2D or 3D cultivation systems, cell population density, working volume of resazurin or incubation time. For example, in bigger cells, the activity of dehydrogenases can be relatively high at lower cell densities, while in the S-phase of the cell cycle, this activity can be relatively low [54]. The cells with relatively tight cell–cell contacts, such as cells at higher population densities or cells in 3D systems including organoids, can also show a relatively low metabolic activity, which is due to lower penetration of resazurin into the cells [55]. Besides, high cell population densities, low resazurin working volumes, or long incubation times contribute to a quick depletion of resazurin from the culture media before all cells are sufficiently stained with resorufin, a conversion product of resazurin [56].

Due to the disproportionate results on the cell number and cell metabolic activity, we decided to perform another independent and more detailed analysis of the growth of ADSCs in FGF-2-supplemented media. This analysis was also based on counting the fluorescently-stained cell nuclei, but the growth factors were added in three different concentrations, and the cells were counted in five intervals from days 1 to 7. Moreover, FGF-2M was compared not only with the commercially available FGF-2 (Genscript, Piscataway, NJ, USA, Cat. No. Z03116-1) but also with FGF-2M-FXIIIa. Moreover, the analysis was performed not only in human ADSCs but also in porcine ADSCs, i.e., in stem cells from another source widely used in experimental biomedical research.

We found that (1) all three tested forms of FGF-2 increased the number of human and porcine ADSCs in comparison with the control non-supplemented medium; (2) this increase was less apparent in both types of our recombinant FGF-2M than in the commercially-available FGF-2, except for day 7 in human ADSCs, where the effect of the highest concentration (20 ng/mL) was similar in all three forms of FGF-2; and (3) the effect of FGF-2M was usually slightly lower than in FGF-2M-FXIIIa, which was more pronounced in human than

in porcine ADSCs (Supplementary Materials Figure S4). Three global trends were apparent in this data set, although some results are non-significant. First, the FGF-2 promoted cell growth in contrast to media containing only FBS. Second, there is an increased cell count with a higher concentration of all forms of FGF-2. Third, lower cell count in FGF-2M and FGF-2M-FXIIIa than in commercial FGF-2 was possibly caused by lower factor concentration due to the presence of impurities. Therefore, it can be summarized that this analysis confirmed our results on the mitogenic activity of the investigated growth factors based on the direct counting of cells on microphotographs.

2.3. Mitogenic Activity of Adsorbed VEGF-A₁₆₅ and FGF-2M

2.3.1. Number and Metabolic Activity of Cells on Cultivation Substrates Pre-Adsorbed with Growth Factors

In biomaterial science and tissue engineering, growth factors are often immobilized on various biomaterials to increase their bioactivity and to mimic the extracellular matrix-bound growth factors. Therefore, we evaluated whether the mitogenic activity of the studied growth factors remains preserved after adsorption on an experimental plastic surface. We measured the proliferation of ADSCs and HUVECs in wells of 96-well plates pre-adsorbed with our recombinant VEGF-A₁₆₅ or FGF-2M in concentrations from 0.01 M to 10 M, which corresponded to approximately 0.192–192 g/mL of VEGF-A₁₆₅ and to approx. 0.172–172 g/mL of FGF-2.

We found that the proliferation response of both cell types to the adsorbed growth factors was similar as if the growth factors were diluted in the culture media. ADSCs in wells pre-adsorbed with VEGF-A₁₆₅ did not show almost any increase in their number and metabolic activity in comparison with control cells in the medium without the growth factor (Figure 4A and Supplementary Materials Figure S5A). Only the highest concentrations of VEGF-A₁₆₅ (1 to 10 M) caused a slightly elevated metabolic activity of ADSCs (Figure S5A). In contrast, the number and metabolic activity of ADSCs on immobilized FGF-2M were significantly elevated, as apparent already on day 1 after cell seeding, at least in wells with the highest FGF-2M concentrations. On day 7 after seeding, the cell numbers and metabolic activity reached the highest values at the concentrations from 1 to 10 M (Figure 4B and Figure S5B).

In contrast to ADSCs, HUVECs displayed an increase in cell number and metabolic activity in wells pre-adsorbed with both types of growth factor, more apparently on wells pre-adsorbed with FGF-2M, especially considering the cell number. This result is rather surprising because the immobilization of VEGF to biomaterial surfaces is widely used in cardiovascular tissue engineering to enhance the growth of endothelial cells [33,34,57,58]. In these studies, the immobilized VEGF accelerated endothelialization of polymeric substrates promising for fabrication of blood vessel prostheses [33] or promoted penetration and proliferation of endothelial cells inside porous 3D collagen scaffolds in vitro [34]. Collagen scaffolds with immobilized VEGF-A₁₆₅ were also used for the repair and vascularization of myocardial defects in rats in vivo [58]. VEGF-A₁₆₅ in the form of a gene construct, mRNA, or protein was also clinically used for vascularization of ischemic myocardial tissue in human patients [3–5]. Nevertheless, in some of these cases, the effect of VEGF was further enhanced by an additional factor promoting the growth of endothelial cells, such as angiopoietin-1 [57], and particularly FGF-2 [3,5]. In a recent study, a combination of VEGF-A₁₆₅ and FGF-2, immobilized on a fibrin mesh, was used for endothelialization of an ePTFE vascular prosthesis in vitro and is also promising for self-endothelialization of an implanted ePTFE vascular graft in vivo [37].

On FGF-2M-modified wells in our experiments, the number and metabolic activity of HUVECs clearly increased with increasing concentration of the growth factor (Figure 4C,D and Supplementary Materials Figure S5C,D). Moreover, as mentioned above, FGF-2M stimulates not only the growth of endothelial cells but also of stem cells. These cells can be used for differentiation towards various cell types used in cardiovascular tissue engineering, e.g., towards endothelial cells or vascular smooth muscle cells (for a review, see [59]). Other studies also confirmed that adsorption of FGF-2 to tissue culture polystyrene greatly

enhanced the proliferation of human vascular endothelial cells [59] or human mesenchymal stem cells [60]. Similar results were also observed in studies performed on FGF-2 immobilized on non-tissue culture polystyrene, where the fetal bovine endothelial cells showed an increased proliferation rate [31,61]. In these studies, the mitogenic activity of adsorbed FGF-2 was mediated by α_3 integrin and FGF receptor 1, and FGF-2 was expressed in *E. coli* without any mutations in its structure [31,61]. Immobilization of FGF-2 to biomaterial surfaces, such as various synthetic and nature-derived polymers, has repeatedly been proven beneficial for adhesion and proliferation of various cell types (e.g., fibroblasts, endothelial cells) [35,36,62].

It is also noteworthy that, similar to the growth factors diluted in the culture medium, the metabolic activity of HUVECs in wells with pre-adsorbed growth factors is markedly higher than in ADSCs, albeit direct cell counting gave the opposite results (Figure 4 and Figure S5). The explanation is that the cell metabolic activity is not always linearly correlated with the cell number, although it is generally used as a marker of the cell proliferation activity (see Section 2.2.4).

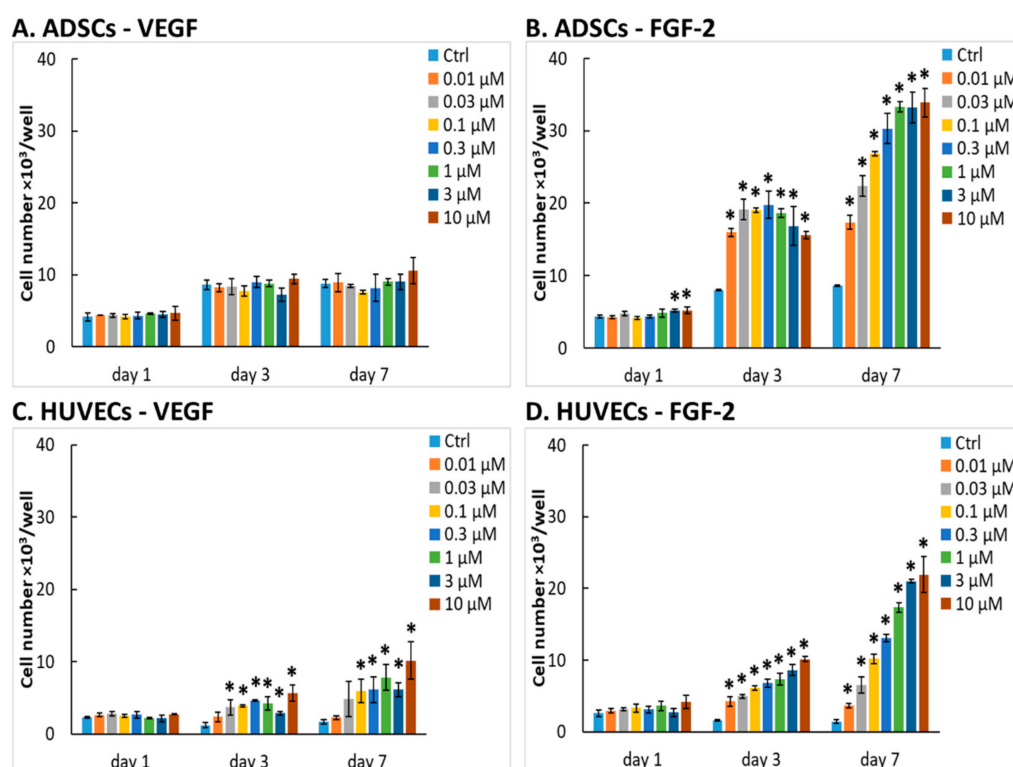


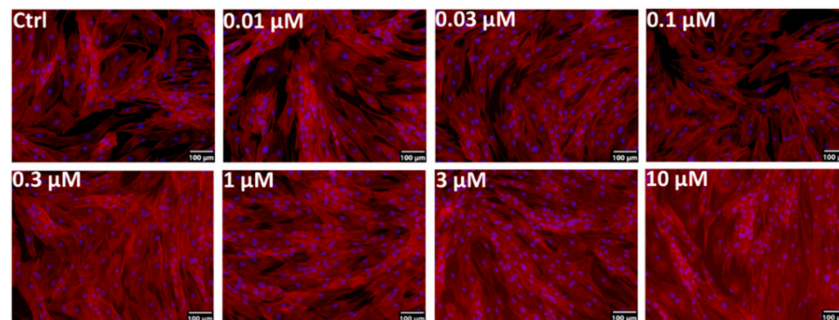
Figure 4. The mitogenic activity of VEGF-A₁₆₅ or FGF-2M adsorbed on the cultivation substrate. The ADSCs (A,B) or HUVECs (C,D) were seeded in wells of 96-well polystyrene tissue culture plates pre-adsorbed with VEGF-A₁₆₅ (A,C) or FGF-2M (B,D) in concentrations from 0.01 to 10 M. Pristine wells without growth factors served as control substrates (Ctrl). ADSCs were grown in DMEM with 10% FBS. HUVECs were grown in EGM2-weak. The cell number was determined on days 1, 3, and 7 after seeding. Mean ± SD from 3 wells. Holm–Sidak method, $p < 0.05$. The samples were statistically compared on the indicated day after seeding. *statistically significant difference in comparison with the control sample (Ctrl).

2.3.2. Morphology of Cells on Cultivation Substrates Pre-Adsorbed with Growth Factors

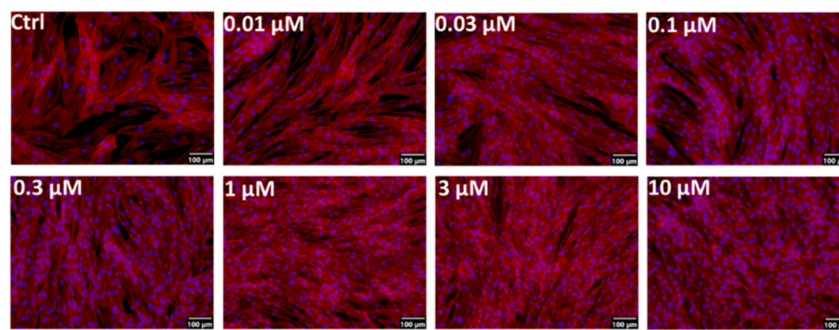
The morphology of cells on the substrate-bound growth factors was also generally similar to the morphology of cells grown in the media with diluted growth factors. The ADSCs cultivated on surfaces pre-adsorbed with VEGF-A₁₆₅ or FGF-2M were mostly elongated, spindle-shaped, and randomly oriented. There was an apparent increase in the number of cell nuclei with the increasing concentration of both growth factors, especially

of FGF-2M. At the highest concentrations of the adsorbed growth factors (1 to 10 M), the cells on FGF-2M reached full confluence, while the cells on VEGF-A₁₆₅ were rather subconfluent (Figure 5A,B).

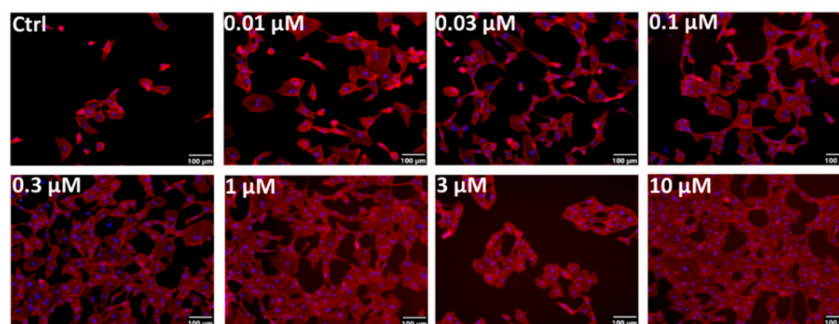
A. ADSCs - VEGF



B. ADSCs - FGF-2M



C. HUVECs - VEGF



D. HUVECs - FGF-2M

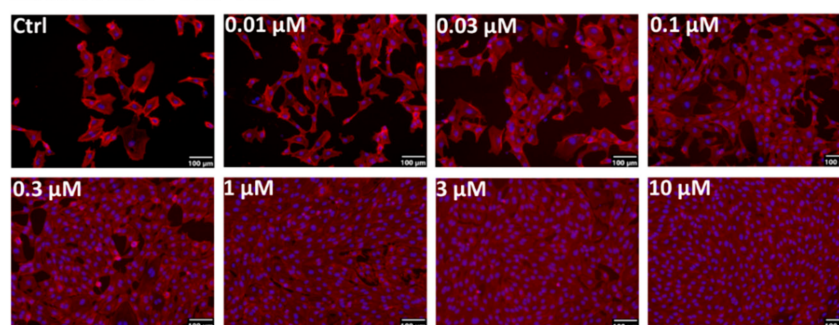


Figure 5. Microphotographs of ADSCs (A,B) and HUVECs (C,D) on day 7 after seeding into wells pre-adsorbed with VEGF-A₁₆₅ (A,C) or FGF-2M (B,D) in concentrations from 0.01 to 10 M. The filamentous actin in cells was stained with phalloidin-TRITC to visualize the cell morphology. The nuclei were counterstained with Hoechst 33258. Olympus IX 71 microscope, DP 70 digital camera, obj. 10, scale bar 100 m.

In HUVECs, the microphotographs confirmed a generally lower cell population density than in ADSCs, especially on the surfaces pre-adsorbed with VEGF-A₁₆₅. Even on the highest concentrations (1 to 10 M) of VEGF-A₁₆₅, the cells were not able to reach confluence, while on the corresponding surfaces with FGF-2M, they were fully confluent on day 7 after seeding. HUVECs on the pre-adsorbed surfaces were mostly polygonal but a considerable number of them were elongated, i.e., of a migratory and proliferative phenotype (Figure 5C,D).

2.4. VEGF-A₁₆₅ and FGF-2M as Adhesion Ligands for Cells

It is known that VEGF-A₁₆₅ and FGF-2, important growth factors, can also influence the cell adhesion when immobilized on cultivation substrates [14,32]. To investigate and compare the role of our recombinant VEGF-A₁₆₅ and FGF-2M in the adhesion of ADSCs and HUVECs, we allowed these factors to adsorb on the bottoms of wells in 96-well E-plates, and the initial adhesion of ADSCs and HUVECs during the first 4 h after seeding was monitored in real-time using an xCELLigence sensory system.

2.4.1. Adhesion of ADSCs on Cultivation Substrates Pre-Adsorbed with Growth Factors

(1) Adhesion to VEGF-A₁₆₅

As revealed by xCELLigence studies, the adhesion response of ADSCs to VEGF-A₁₆₅ was similar to the growth response of ADSCs to VEGF-A₁₆₅ in free or substrate-immobilized forms. In wells non-blocked with BSA, VEGF-A₁₆₅ had no significant effect on the adhesion of ADSCs in comparison with control wells without the growth factor. In wells where non-specific binding sites for cells were blocked with BSA, VEGF-A₁₆₅ slightly improved the initial adhesion of ADSCs with the optimal value at the concentration of 0.1 M; it was significant only in comparison with wells coated with BSA alone, but not with control unmodified wells (Figure 6A). The morphology of cells was similar in all tested samples, the cells being well-spread and polygonal (Supplementary Materials Figure S6A).

The relatively low effect of VEGF-A₁₆₅ on the adhesion of ADSCs is in accordance with previous studies by Kang et al. [32,60] who observed poor adhesion of ADSCs or other types of mesenchymal stem cell to adsorbed VEGF-A₁₆₅. The poor adhesion-mediating ability of VEGF-A₁₆₅ might be explained by the lack of any canonical adhesion motif, recognizable by integrin and non-integrin cell adhesion receptors in its amino acid sequence (e.g., RGD, DGEA, KQAGDV, VAPG, REDV, YIGSR, IKVAV, or KRSR; see the amino acid sequence of VEGF-A₁₆₅ in Supplementary Materials). However, the adsorbed VEGF-A₁₆₅ enhanced the adhesion of lymphocytic leukemia cells and B lymphocytes, mediated with the direct association of α_4 integrin with vascular endothelial growth factor receptor-2 (VEGFR-2). The adhesion of B lymphocytes to adsorbed VEGF-A₁₆₅ was optimal at a concentration of 8 g/mL (0.4 M) [15].

(2) Adhesion to FGF-2M

When the wells were pre-adsorbed with FGF-2M, the initial adhesion of ADSCs was significantly elevated at the highest concentrations of FGF-2M, i.e., from 1 to 10 M, and increased in a concentration-dependent manner (Figure 6B). This cell response became more apparent in wells where non-specific cell adhesion sites were blocked with bovine serum albumin (BSA). In these wells, the cell adhesion to wells pre-adsorbed with 10 M FGF-2M exceeded the value obtained in control unmodified wells, which suggested a strong affinity of ADSCs to the substrate-bound FGF-2M. These xCELLigence results were reflected by the cell morphology, especially in samples blocked with BSA. In these samples, the cells were relatively sparse and rounded in wells without FGF-2M, and their number and spreading increased with increasing FGF-2M concentration (Figure S6B). Similar results were obtained in a study by Kang et al. (2012) [32], where the adhesion of human ADSCs increased in a concentration-dependent manner up to the concentration of 10 g/mL (ca. 0.6 M), and then reached a plateau [32]. There, FGF-2 was co-expressed with maltose-binding protein to enhance its adsorption to a polystyrene surface. The substrate-bound

FGF-2 also stimulated the adipogenic differentiation of ADSCs but not the osteogenic differentiation of these cells [32].

The positive effect of FGF-2 on the adhesion of ADSCs could be explained by the presence of two DGR sequences (positions 46–48 and 88–90), which are reverse to RGD (Arg-Gly-Asp), i.e., a well-known adhesion motif recognized by integrin adhesion receptors (see the amino acid sequence of FGF-2M in Supplementary Materials). Similarly, the DGR sequence is also recognized by integrin adhesion receptors (e.g., including α_3), especially in its isoDGR form, which is formed by deamidation of asparagine in the NGR sequence [63,64].

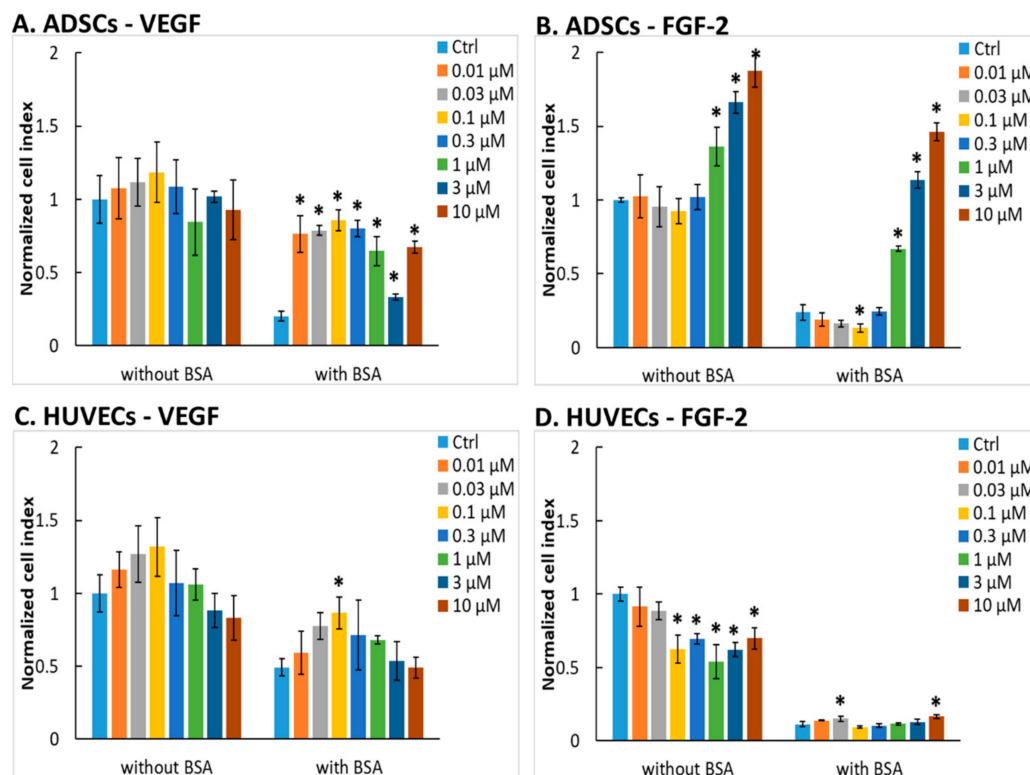


Figure 6. Initial adhesion of ADSCs (A,B) and HUVECs (C,D) 4 h after seeding into wells of E-plates in the xCELLigence system pre-adsorbed with VEGF-A₁₆₅ (A,C) or with FGF-2M (B,D) in concentrations from 0.01 to 10 M. The wells were either left unblocked, i.e. without bovine serum albumin (BSA) or were blocked with 0.5% BSA (with BSA). Cell index values were normalized to the control sample without adsorbed growth factors and BSA (Ctrl without BSA). Mean SD from 3 wells. Holm-Sidak method, $p < 0.05$. The statistical comparison was made amongst the samples with or without BSA. * statistically significant difference in comparison with the control sample (Ctrl).

2.4.2. Adhesion of Human Umbilical Vein Endothelial Cells (HUVECs) on Cultivation Substrates Pre-Adsorbed with Growth Factors

(1) Adhesion to VEGF-A₁₆₅

The adhesion response of HUVECs to VEGF-A₁₆₅ was similar to ADSCs (Figure 6C). In wells non-blocked with BSA, the cell adhesion was improved only slightly at the intermediate VEGF-A₁₆₅ concentration of 0.1 M, and then it decreased again. Moreover, this improvement was statistically significant only in comparison with the highest concentration of VEGF-A₁₆₅, but not in comparison with control wells without VEGF-A₁₆₅ (Figure 6C). The difference between the wells without VEGF-A₁₆₅ and those with 0.1 M VEGF-A₁₆₅ became significant when the non-specific cell-binding sites in wells were blocked with BSA. However, the cell adhesion in wells with VEGF-A₁₆₅ did not surpass the control value in wells without any modification. The cells were well-spread and polygonal, but this morphology was similar in all tested samples irrespective of the presence and con-

centration of VEGF-A₁₆₅ (Figure S6C). These results were rather unexpected because it is known that VEGF-A stimulates the adhesion of endothelial cells by interacting with integrin adhesion receptors on these cells [14]. However, not all isoforms of VEGF-A can bind the cells through these receptors. As mentioned above, VEGF-A is expressed in nine splice variants encoded by a single gene. These VEGF-A isoforms differ in the length of their amino acid chains, i.e., in the number of amino acids in their chains [1]. The shorter isoforms, i.e., variants with 121, 145, and 165 amino acids, are mainly diffusible, whereas the longer ones, i.e., with 189 and 206 amino acids, are sequestered in the cell membranes after secretion [14]. In the mentioned study, HUVECs seeded in plastic wells pre-coated with VEGF-A₁₂₁, VEGF-A₁₆₅, or the full-length or cleaved forms of VEGF-A₁₈₉, adhered well to the VEGF-A₁₈₉ isoforms (cleaved or full-length), moderately to VEGF-A₁₆₅, but not at all to VEGF-A₁₂₁. Experiments with blocking antibodies and tumstatin, an antiangiogenic peptide, revealed that in VEGF-A₁₆₅, the cell adhesion was mediated by $\alpha_3\beta_1$ and $\alpha_v\beta_3$ integrins, and in VEGF-A₁₈₉ also by other α_v integrins [14]. However, this adhesion was not fully complete, which was manifested by a lack of actin stress fibers in adhering cells [14]. The binding of VEGF-A₁₆₅ to $\alpha_v\beta_3$ integrin receptors of cells can be markedly improved by fusion of this growth factor with the 10th type III domain of fibronectin (FNIII10). This construct was able to activate strongly and simultaneously both VEGFR-2 and the $\alpha_v\beta_3$ integrin, and thus it was more efficient in mediating cell adhesion than VEGF-A₁₆₅ or FNIII10 alone [65].

(2) Adhesion to FGF-2M

Surprisingly, the adsorbed FGF-2M suppressed in a concentration-dependent manner the adhesion of HUVECs on wells non-blocked with BSA and showed almost no interaction with these cells in wells blocked with BSA (Figure 6D). These results were reflected in the cell morphology (Figure S6). In samples non-blocked with BSA, the cells were well-spread and polygonal, but apparently, the cell population density decreased with increasing FGF-2M concentration. In samples blocked with BSA, the cells with all tested FGF-2M concentrations were less spread and mostly rounded.

The negative effect of FGF-2M on the adhesion of HUVECs is in contrast with its strong mitogenic effect on these cells. An explanation could be the presence of an RSRK sequence in the position 116–119 in the FGF-2M molecule (see the Supplementary Materials). RSRK is the reverse sequence of KRSR. KRSR is known to bind non-integrin adhesion receptors on the cell surface, namely heparan sulfate proteoglycans, and to promote the adhesion of osteoblasts but not the adhesion of other cell types, including endothelial cells [66]. However, some studies reported a positive influence of FGF-2 on the adhesion of endothelial cells [31,61], and this adhesion was mediated by the FGF-2 fragments 24–68 and 93–120 [67], which, according to our study, contains the DGR and RSRK sequences, respectively. To the best of our knowledge, the role of RSRK in the adhesion of various cell types, stimulatory or inhibitory, has not yet been described and needs to be investigated.

2.5. Limitation of an In Vitro Study

Translation of recombinant growth factors into clinical applications is associated with several limitations, which arise from the growth factor preparation as well as from the system, where the potency of these factors is tested. Recombinant synthesis of growth factors can suffer from insufficient yields of recombinant expression, presence of impurities, short-term stability, and low efficiency of the final product or high production costs (for a review, see [68]). The first system of choice, in which the newly prepared growth factors are tested, is usually cell culture in vitro, which precedes the tests on animal models in vivo. This approach is in accordance with the 3R principle of the ethical use of animals in a testing (i.e., replacement, reduction, refinement). The cell cultures are believed to enable the screening of a wide range of protein variants and concentrations and to save the laboratory animals, on which only the most promising results obtained in vitro can be verified. However, it is often difficult to translate the results obtained in vitro to the conditions in vivo. It is generally known that cultured cells, especially those in a

conventional static culture system in serum-supplemented media, undergo phenotypic changes (e.g., changes in the spectrum, amount, and distribution of the surface receptors), which can alter their responsiveness to various stimuli, including growth factors. After establishing the method of cell cultivation *in vitro*, the main advantage of this system was seen in the possibility to evaluate the biological activity of various factors on a specific single cell type without the influence of the complex and less-defined environment of the whole organism. However, this endeavor could be counterproductive, because *in vivo* the observed reactivity to a given factor can be modulated by the presence of other adjacent or remote cell types. For example, under *in vivo* conditions, the growth factors in the blood are exposed to various cell types, which could modulate their effect on endothelial cells. Conversely, one cell type can be influenced simultaneously with several growth factors. Therefore, it is difficult to extrapolate a proper growth factor concentration from studies *in vitro* to the conditions *in vivo*.

Our study aimed, at least partly, to mitigate some of these limitations. Specifically, we focused on the cost-effective recombinant expression followed by a single-step purification method resulting in high yields of the obtained growth factors. In addition, modern engineering of growth factors *in vitro*, in general, enables improvement of several important properties of growth factors, such as their stability, half-life, binding affinity to receptors, internalization into cells, biodistribution, and tissue penetration, and it can also modulate the binding of growth factors to the extracellular matrix (ECM) [68]. The production of human recombinant factors also paves the way to the development of novel xeno-free media for the cultivation of various cell types, particularly stem cells, needed for applications in cell therapies and tissue engineering.

In our study, we used a conventional static cells culture system with serum-supplemented media and with monocultured cells. However, the effect of our recombinant growth factors was tested on two cell types (with different results obtained for each cell type) and in a wide range of concentrations. These concentrations were inspired by the literature, where lower concentrations (5–100 ng/mL) have been usually used for studies with soluble growth factors (e.g., [2,12,15,17–19,47,49]), while higher concentrations (0.5–10 g/mL) have been used for functionalization of various biomaterials (e.g., [12,14,15,33,34,36,37]) to simulate a local concentration of growth factors bound to the natural ECM *in vivo*, which can act as reservoirs of these factors, enabling their continuous release and delivery to cells [68].

The translatability of *in vitro* studies to the real situation in the organism *in vivo* can be further improved by co-cultivation of two or more cell types, by the use of chemically defined serum-free media, including media supplemented by recombinant growth factors and other recombinant proteins, and particularly by the use of dynamic cell culture systems. These systems provide the cells with adequate mechanical stimulation similar to that to which the cells are exposed *in vivo*. This stimulation can also be substituted by electrical, magnetic, gravity, or ultrasound stimulation, and is important for proper cell differentiation and phenotypic maturation. In addition, the media flow in dynamic cell culture systems enables a better supply of cells with oxygen and nutrients and quick waste removal, which further improves the physiological functions of cells [69,70]. Dynamic cultivation is, therefore, indispensable in advanced tissue engineering, which aims to create replacements of damaged tissues, closely mimicking the well-functioning tissues in a healthy organism.

3. Materials and Methods

3.1. Expression and Purification of VEGF-A₁₆₅

The gene of the 165-amino acid splice variant of human vascular endothelial growth factor (VEGF-A₁₆₅) was prepared synthetically (Generay, Shanghai, China); both the nucleotide and amino acid sequences are given in the Supplementary Materials. The gene was cloned into the yeast expression vector pPICZA comprising zeocin resistance gene downstream of the -factor-encoding DNA segment for extracellular protein targeting using 5⁰-KpnI and 3⁰-EcoRI restriction sites. Fifteen g of plasmid DNA were linearized employing SacI (New England Biolabs, Ipswich, US) and electroporated into the competent

P. pastoris KM71H cells prepared according to the manufacturer's instruction manual (Easy-Select *Pichia* Expression Kit, Invitrogen, Waltham, MA, US). The resulting transformants were grown on yeast extract peptone dextrose (YPD) plates under the pressure of zeocin for three days at 28 C. For a screening of the production of VEGF-A₁₆₅ in *P. pastoris* KM71H at a small-scale, a combination of BMGY (buffered glycerol complex medium) and BMMY (buffered methanol complex medium) was used. Selected colonies were inoculated into 100 mL of BMGY and incubated at 28 C and 220 rpm overnight. Then the cultures were centrifuged (5000 rpm, 10 min, 4 C) and the pellets were resuspended in 30 mL of BMMY. The extracellular expression of the target protein was induced by methanol (0.5% v/v); methanol was supplemented every 24 h. The cultures were shaken at 28 C and 220 rpm for three days. On day 5 after inoculation, the cultures were tested for the presence of VEGF-A₁₆₅ by 15% SDS-PAGE. Clones providing the highest protein production were cryopreserved at 80 C and employed in the large-scale production of VEGF-A₁₆₅.

For the preparative production of VEGF-A₁₆₅, BMGH (buffered minimal glycerol medium) and BMMH (buffered minimal methanol medium) were used starting with a preculture. The cryopreserved cultures obtained from the screening (100 L) were inoculated into 15 mL of YPD medium and incubated at 28 C and 220 rpm for 5 h. This preculture was inoculated into 1 L of BMGH medium in 3 L Erlenmeyer flasks and cultivated overnight at 28 C on a rotary shaker. Then the cells were collected by centrifugation (5000 rpm, 10 min, 4 C) and resuspended in 200 mL of BMMH medium in 1 L Erlenmeyer flasks. The culture was shaken at 28 C and 220 rpm, the expression of VEGF-A₁₆₅ was induced by methanol (0.5% v/v) every 24 h.

On day 5 after the first inoculation, the target protein was purified using a cation exchange chromatography column (Fractogel EMD-SO³⁻, Merck, Darmstadt, Germany) connected to the Äkta Purifier chromatography system (GE Healthcare, Chicago, IL, USA). The column was equilibrated with 10 mM sodium citrate-phosphate buffer pH 6.0. The proteins were eluted with a linear gradient of 0–2 M NaCl (60 mL, 2 mL/min). The protein concentration was assayed according to Bradford [71] using Protein Assay Dye Reagent Concentrate (Bio-Rad, Watford, UK) calibrated for -globulin from bovine plasma (IgG, BioRad, Watford, UK). The purity of protein fractions was determined by SDS-PAGE using 15% polyacrylamide gel. The real content of our recombinant VEGF in protein fractions after purification was determined by densitometric analysis of the gels using ImageJ software. The content was determined according to the following calculation: area under the peak corresponding to VEGF in lane histogram/sum of areas under all peaks in the lane. Fractions containing VEGF-A₁₆₅ were collected; the buffer was changed for 100 mM Tris/HCl pH 7.4 and sterilized using 0.22 m sterile syringe filters (Carl Roth, Karlsruhe, Germany). The protein solution was aliquoted into 1.5 mL tubes, 20% (v/v) of sterile glycerol was added and aliquoted VEGF-A₁₆₅ was shock-frozen in liquid nitrogen and stored at 80 C.

3.2. Expression and Purification of FGF-2M

The expression of human fibroblast growth factor-2 (FGF-2) was performed analogously to VEGF-A₁₆₅, in the yeast expression system of *P. pastoris* KM71H. Two potential LysArg dibasic cleavage sites for the yeast protease Kex2 were removed by replacing Arg for Lys, and the gene of R31K/R129K FGF-2, further designated FGF-2M, was optimized and synthesized commercially (Generay, Shanghai, China; for respective sequences see the Supplementary Materials). The gene was cloned into the pPICZA expression vector (KpnI/ EcoRI), the plasmid pPICZA-FGF-2M was electroporated into *P. pastoris* and individual colonies were screened for FGF-2M extracellular production as described for VEGF-A₁₆₅. The most producing clones were cryopreserved at 80 C and used for large scale production of FGF-2M.

For the large-scale production of FGF-2M, a combination of BMGY and BMMH in smaller flasks was used. Cryopreserved cells (100 L) were inoculated into 10 mL of YPD medium and precultures were incubated for 5 h at 28 C with vigorous shaking. After

that, 2.5 mL of precultures were inoculated into 100 mL of BMGY medium in 1 L flasks and cultivated at 28 C and 220 rpm overnight. After centrifugation (5000 rpm, 10 min, 4 C), the pellets were resuspended in 30 mL of BMMH medium in 300 mL baffled flasks to ensure high oxygen supply. The extracellular expression of the target protein was induced by methanol (0.5% v/v) every 24 h. The cultures were shaken at 28 C and 220 rpm for three days.

On day 5 after the first inoculation, the FGF-2M produced was purified using a cation exchange chromatography column (Fractogel EMD-SO³⁻, Merck, Darmstadt, DE) connected to the Äkta Purifier chromatography system (GE Healthcare, Chicago, IL, USA). The column was equilibrated with 10 mM sodium citrate-phosphate buffer pH 4.0. The proteins were eluted with a linear gradient of 0–2 M NaCl (60 mL, 2 mL/min). The protein concentration was assayed according to Bradford and its purity was analyzed as described for VEGF-A₁₆₅. Fractions comprising FGF-2M were collected, re-buffered, aliquoted, and stored as described for VEGF-A₁₆₅.

3.3. Expression of VEGF-A₁₆₅-FXIIIa and FGF-2M-FXIIIa

The constructs for the expression of VEGF-A₁₆₅-FXIIIa and FGF-2M-FXIIIa containing an additional N-terminal 8 amino acid substrate sequence for Factor XIIIa (NQEQVSPL) were prepared commercially (Generay, Shanghai, China) and cloned into the pPICZA vector. The expression of these prolonged forms of the growth factors was performed in the same way as described for the native factors. The VEGF-A₁₆₅-FXIIIa and FGF-2M-FXIIIa obtained were concentrated from the culture media without purification in 100 mM Tris/HCl pH 7.4 buffer, sterilized, aliquoted, and stored as described above.

3.4. Cell Models

Human adipose tissue-derived stem cells (ADSCs) were isolated from a lipoaspirate obtained by liposuction from the thigh region of a patient (woman, aged 46 years) at a negative pressure (−200 mmHg). The isolation was conducted in compliance with the tenets of the Declaration of Helsinki for experiments involving human tissues and under ethical approval issued by the Ethics Committee in “Na Bulovce” Hospital in Prague (11 June 2019). Written informed consent was obtained from the patient before the liposuction procedure. The ADSCs were isolated by a procedure described by Estes et al. [49] with minor modifications described in our previous studies [69,72,73]. The cells were expanded in Dulbecco’s modified Eagle’s Medium (DMEM, Thermo Fisher Scientific, Waltham, MA, USA) supplemented with 10% of fetal bovine serum (FBS, Thermo Fisher Scientific, Waltham, MA, USA), 40 g/mL of gentamicin and 10 ng/mL of FGF-2 (GenScript, Piscataway, NJ, USA, Cat. No. Z03116-1). In passage 2, the cells were characterized by flow cytometry (Accuri C6 Flow Cytometer, BD Biosciences, San José, CA, USA), using antibodies against the specific cluster of differentiation (CD) markers of mesenchymal stem cells. This method revealed the presence of standard surface markers of ADSCs, namely CD105 (endoglin, 99.9%), CD90 (immunoglobulin Thy-1, 99.5%), CD73 (ecto-5⁰-nucleotidase, 100%) and CD29 (fibronectin receptor, 100%). At the same time, the ADSCs were negative or almost negative for CD31, also referred to as platelet-endothelial cell adhesion molecule-1, PECAM-1 (0.5%), CD34 (antigen of hematopoietic progenitor cells, 0.2%) and CD45 (protein tyrosine phosphatase receptor type C, 3.8%), which are markers of hematopoietic or endothelial cells, and also for CD146 (4.7%), referred to as melanoma cell adhesion molecule or receptor for laminin; also considered to be a marker of pericytes [69].

Porcine adipose tissue-derived stem cells (PrADSCs) were isolated from fat surgically extracted from the neck area of experimental pigs (breed Prestice black pied pigs with a weight of approximately 35–40 kg; Institute of Animal Science, Přeštice, Czech Republic) during the surgery under general anesthesia. The protocol for cell isolation was also set according to Estes et al. [49] with some modifications developed in studies focused on adipose-derived stem or stromal cells [74,75] and is described in our previous study by Matejka et al., 2020 [70]. The cells were expanded in a standard way until the 2nd passage in

DMEM-F12K (Sigma-Aldrich, St. Louis, MO, USA) medium (ratio 1:1) supplemented with 10% of FBS (Sigma-Aldrich, St. Louis, MO, USA), 1% of ABAM (Antibiotic Antimycotic Solution, contains 100 units penicillin, 0.1 mg streptomycin, and 0.25 g amphotericin B per mL of culture media, Sigma-Aldrich, St. Louis, MO, USA) and 10 ng/mL of FGF-2 (GenScript, Piscataway, NJ, USA, Cat. No. Z03116-1). Similarly, as human ADSCs, they were characterized by flow cytometry for the presence or absence of specific CD markers, namely CD105 (96–99%), CD90 (99%), and CD29 (99%). CD73 was present only in 0.3–2.6% of the cells but is known from the literature that this marker is very low or absent in porcine ADSCs, and instead of it, CD44, i.e., hyaluronan receptor, has been usually evaluated. The prADSCs were almost negative for CD34 (0.5–1%) and CD45 (1–3%) but they showed a relatively high positivity for CD31 (29–35%) [70].

For studies on the effect of our recombinant FGF-2M, the commercial FGF-2 was removed from the medium. The cells were grown until 80% confluence and then used for testing. This was done to minimize the pooling effect of FGF-2 used in cell expansion. The fat isolation from experimental pigs was approved by the Ministry of Health of the Czech Republic, reference No. MZDZ 23132/2018-4/OVZ, approval No. 37/2018 in the Institute of Clinical and Experimental Medicine. A minimal number of animals were used. All procedures described were undertaken under general anesthesia and according to ethical guidelines to minimize the pain and discomfort of the animals. The Institute of Clinical and Experimental Medicine has authorized facilities and fully equipped operating theatres for performing these animal experiments.

Human umbilical vein endothelial cells (HUVECs) were purchased from Lonza (Basel, Switzerland, Cat. No. C2517A). The cells were grown in the endothelial cell growth medium 2 (EGM2), which was prepared from the endothelial cell basal medium 2 (EBM2, PromoCell, Heidelberg, Germany, Cat. No. C-22111) supplemented with 1% of antibiotic-antimycotic solution (v/v, Sigma-Aldrich, St. Louis, MO, USA, A5955) and the growth medium-2 supplement pack (PromoCell, Heidelberg, Germany, Cat. No. C-39211) containing hydrocortisone, heparin, ascorbic acid, EGF, VEGF, IGF-1, FGF-2 and 2% of FBS. For the purpose of this study, we decided to term this medium “EGM2-full”.

3.5. Cell Cultivation with Recombinant Growth Factors Diluted in Culture Medium

To confirm the mitogenic activity of the newly prepared recombinant growth factors, the cells were seeded in 96-well tissue culture plates (TPP, Trasadingen, Switzerland, Cat. No. 92096) at a density of 3×10^3 cells/well. ADSCs were grown in DMEM with 10% of FBS and HUVECs in EGM2 medium containing hydrocortisone, heparin, ascorbic acid, and 2% of FBS from the growth medium-2 supplement pack (PromoCell, Heidelberg, Germany, Cat. No. C-39211). However, EGF, VEGF, IGF-1, and FGF-2 that are also components of the supplement pack were not added to the medium to prevent their interference with the tested recombinant growth factors. This medium was further termed “EGM2-weak”. This cultivation medium was further enriched with our recombinant VEGF-A₁₆₅ or FGF-2M in the range of concentrations from 10 to 1000 ng/mL or 5 to 250 ng/mL respectively, and the cells were cultivated for 1, 3, or 7 days. In selected wells, the medium was exchanged for a fresh one with a corresponding concentration of the growth factor on day 3 after cell seeding.

An additional experiment focused on the mitogenic activity of the tested growth factors was performed on human and porcine ADSCs. The cells were seeded in 24-well tissue culture plates (Jet Bio-Filtration Co., Guangzhou, China) with an initial density of 5×10^3 cells per cm². As a basic culture medium, the DMEM-F12K (1:1 ratio) with 10% FBS and 1% ABAM was used. This mixture was also set as a control. Then, three different types of FGF-2 (commercial FGF-2, our recombinant FGF-2M, and FGF-2M-FXIIIa) at concentrations 5, 10, and 20 ng/mL were added. The cultivation ran for 1, 2, 3, 5, and 7 days.

3.6. Cell Cultivation with Recombinant Growth Factors Adsorbed on Culture Wells

The mitogenic effect of the substrate-bound growth factors was determined in the 96-well polystyrene tissue culture plates pre-adsorbed overnight at 4 °C with recombinant growth factors diluted in a phosphate-buffered saline (PBS) at concentrations ranging from 0.01 to 10 nM. The wells were then washed twice in PBS. The cells were seeded at a density of 3×10^3 cells/well in 200 μ L of the medium designated for each cell type. ADSCs were grown in DMEM containing 10% of FBS and HUVECs in EGM2-weak for 1, 3, or 7 days.

3.7. Monitoring the Initial Cell Adhesion to Adsorbed VEGF-A₁₆₅ and FGF-2M Using xCELLigence System

The cell-adhesive properties of the tested growth factors were monitored with the use of xCELLigence Real-Time Cell Analysis - Single Plate (RTCA SP) sensing device (Agilent Technologies, Waltham, MA, USA). Wells in an E-plate (E-plate view 96 PET, ACEA Biosciences, San Diego, CA, USA, Cat. No. 300600910) were adsorbed with VEGF-A₁₆₅ or FGF-2M (0.01 to 10 nM) overnight at 4 °C in PBS. Then, the wells were incubated with 0.5% bovine serum albumin (BSA) in PBS at 37 °C for 1 h to block the non-specific binding on the well bottoms. Some of the wells were left unblocked to observe the effect of the respective growth factor on the non-specific cell adhesion to the plastic surface (i.e., mediated by other factors, such as electrostatic interactions or adsorption of cell membrane-bound adhesion-mediating proteins, e.g., fibronectin and vitronectin, to the well bottom). The cells were seeded at the density of 10^4 cells/well in 200 μ L of pure medium without any supplements (DMEM for ADSCs; EBM2 for HUVECs). The cell adhesion was monitored every 3 min for 4 h in a cell incubator at 37 °C in a humidified atmosphere containing air with 5% CO₂.

3.8. Fluorescence Staining and Counting of Cells

After the cultivation of cells with free and substrate-bound growth factors, and also after monitoring the initial cell adhesion in the xCELLigence system, the cells were processed for the evaluation of their number and morphology. The cells were fixed in 4% paraformaldehyde (10 min). The cells were blocked and permeabilized in PBS containing 1% BSA and 0.1% Triton X-100 (20 min), and then in PBS with 1% Tween-20 (20 min). The cells were stained with phalloidin-TRITC (100 ng/mL in PBS; 1 h; 25 °C) to visualize the filamentous actin (F-actin), which is a component of the cell cytoskeleton. The nuclei were counterstained with Hoechst 33258 (10 μ g/mL in PBS; 1 h; 25 °C). The cells were observed in the Olympus IX71 epifluorescence microscope (DP71 digital camera, objective magnification 10). The number of cells grown with free or substrate-bound growth factors was evaluated on days 1, 3, and 7 after cell seeding by counting the cell nuclei on four randomly selected microphotographs for every well. The cell number was then presented as a mean from 3 wells for each experimental group and time interval. The morphology of initially adhering cells monitored in xCELLigence system was evaluated at the end of monitoring, i.e., 4 h after seeding.

In the additional experiment with human and porcine ADSCs, the fixed cells were counterstained with DAPI (Sigma-Aldrich, St. Louis, MO, USA). Then 10 randomly selected fields of view were taken of each sample using a Leica DMI8 epifluorescence microscope with a 5 objective and digital camera. Custom MATLAB (MathWorks, Natick, MA, USA) script was used to batch count cell nuclei at each image.

3.9. Metabolic Activity Assay

The metabolic activity of ADSCs and HUVECs cultured in 96-well plates was measured with a resazurin assay. Resazurin (Sigma-Aldrich, St. Louis, MO, USA, Cat. No. R7017) is a non-toxic redox indicator. In metabolically active cells, intracellular reductases reduce resazurin to fluorescent resorufin, and this fluorescence is then detected spectrophotometrically. The cell metabolic activity was determined on days 1, 3, and 7 after seeding. The stock solution of resazurin in PBS (4 mM) was diluted to the final concentration of

40 M in the fresh cultivation medium (DMEM without phenol red containing 10% FBS for ADSCs and EGM2-weak for HUVECs). The cells were incubated for 4 h at 37 C in a medium containing resazurin (0.1 mL/well). Fluorescence (Ex/Em = 530/590 nm) was measured on Synergy™ HT Multi-Mode Microplate reader (BioTek, Winooski, VT, USA). Every sample was measured in triplicate. Resazurin solution in a medium without cells was used as a background control. The cell metabolic activity was regarded as an indirect marker of the cell proliferation and the cell number.

3.10. Statistical Analysis

In experiments determining the cell number (Figures 1, 3 and 4), the cell index (Figure 6) and the cell metabolic activity (Figures S2, S3 and S5), the data are presented in bar graphs as mean standard deviation (SD) from 3 wells. The samples were statistically compared using one-way analysis of variance (ANOVA), Holm-Sidak method. The statistical comparison was carried out using SigmaPlot 14.0 software (Systat Software Inc., San Jose, CA, USA). In Figure S4, showing the influence of FGF-2 on the growth of human and porcine ADSCs, the data are presented as mean SD from 10 randomly selected fields of view, and the statistical significance was evaluated using non-parametric Kruskal–Wallis one-way ANOVA on ranks, Dunn's method, in MATLAB. In all used methods of statistics, the value of $p < 0.05$ was considered significant.

4. Conclusions

Our study presents a new and cost-effective method for extracellular expression of VEGF-A₁₆₅ and FGF-2 in a eukaryotic system of *P. pastoris*. FGF-2 was produced as a double mutant termed FGF-2M (R31K/R129K) to avoid degradation by Kex2 proteases. When added to the culture media (VEGF-A₁₆₅: 10–1000 ng/mL, FGF-2: 5–250 ng/mL), both recombinant growth factors showed mitogenic activity, which was stronger in FGF-2; this factor supported the growth of both ADSCs and HUVECs, while VEGF-A₁₆₅ supported the growth of HUVECs only. When the factors were adsorbed to a plastic surface in concentrations from 0.01 M to 10 M (corresponding to approximately 0.192–192 g/mL for VEGF-A₁₆₅ and 0.172–172 g/mL for FGF-2), their mitogenic activity remained unaltered. The mitogenic activity of our recombinant growth factors was slightly lower than that of their commercially available counterparts, which can be explained by the presence of some impurities, and thus by a lower actual concentration of the growth factors in the solution. Furthermore, the effect of the adsorbed growth factors on the initial adhesion of ADSCs and HUVECs was determined. Both cell types, especially ADSCs, showed a relatively low affinity to adsorbed VEGF-A₁₆₅. Interestingly, recombinant FGF-2 enhanced the adhesion of ADSCs but not the adhesion of HUVECs, which even tended to decrease with increasing FGF-2 concentration. Our results suggest that the coating of the biomaterial surface with VEGF-A₁₆₅ and FGF-2 can direct the adhesion and growth of different cell types in different ways. This knowledge can be utilized in regenerative medicine, particularly in tissue engineering, where the cell adhesion, growth and further differentiation should be modulated by a controllable manner.

Supplementary Materials: The following are available online at <https://www.mdpi.com/1422-0067/22/4/1843/s1>, Figure S1: Amino acid and nucleotide sequences of growth factors expressed in *P. pastoris* KM71H. Figure S2: Sodium dodecyl sulfate polyacrylamide gel electrophoresis (SDS-PAGE) of purified VEGF-A₁₆₅ and FGF-2M. Figure S3: Metabolic activity of ADSCs and HUVECs in media containing VEGF-A₁₆₅ or FGF-2M. Figure S4: Influence of FGF-2 on the growth of human and porcine adipose tissue-derived stem cells. Figure S5: Metabolic activity of ADSCs and HUVECs cultivated in wells coated with FGF-2M or VEGF-A₁₆₅. Figure S6: The initial adhesion of ADSCs and HUVECs to wells coated with FGF-2M or VEGF-A₁₆₅.

Author Contributions: Conceptualization, A.S., R.M., L.B., P.B., V.K. and K.S.; methodology, A.S., R.M., M.T., Z.M. and K.S.; software, A.S. and Š.P.; validation, A.S., R.M., L.B., P.B. and K.S.; formal analysis, L.B., R.M. and V.K.; investigation, A.S., R.M., M.T., Š.P., Z.M. and K.S.; resources, L.B., R.M. and V.K.; data curation, A.S., R.M., M.T. and K.S.; writing—original draft preparation, A.S., R.M., L.B. and K.S.; writing—review and editing, A.S., R.M., M.T., P.B., L.B., V.K. and K.S.; supervision, L.B., R.M., K.S. and V.K.; project administration, L.B. and V.K.; funding acquisition, L.B., P.B. and V.K. All authors have read and agreed to the published version of the manuscript.

Funding: This study was supported by the Czech Science Foundation (Grant No. 18-01163S). Further support was provided by the Ministry of Health of the Czech Republic (Grant No. NV18-02-00422) and by the Ministry of Education, Youth, and Sports of CR (Project “BIOCEV” No. CZ.1.05/1.1.00/02.0109 and BIOCEV-FAR Project within LQ1604 National Sustainability Program II). P.B. acknowledges the support from the mobility grant project LTC18038 by the Ministry of Education, Youth and Sports of the Czech Republic.

Institutional Review Board Statement: The study on human ADSCs was conducted according to the guidelines of the Declaration of Helsinki, and approved by the Ethics Committee of “Na Bulovce” Hospital in Prague (11 June 2019). The study on porcine ADSCs was approved by the Ministry of Health of the Czech Republic (reference No. MZDZ 23132/2018-4/OVZ, approval No. 37/2018) in the Institute of Clinical and Experimental Medicine, Prague, Czech Republic.

Informed Consent Statement: Written informed consent has been obtained from the patient(s) to publish this paper.

Data Availability Statement: The data presented in this study are available on request from the corresponding authors.

Conflicts of Interest: The authors declare no conflict of interest.

Abbreviations

ABAM	Antibiotic antimycotic solution
ADSC	Adipose tissue-derived stem cell
BMGH	Buffered minimal glycerol medium
BMMH	Buffered minimal methanol medium
BMGY	Buffered glycerol complex medium
BMMY	Buffered methanol complex medium
BSA	Bovine serum albumin
DAPI	2-(4-Amidinophenyl)-1H-indole-6-carboxamidine
DMEM	Dulbecco’s modified Eagle’s medium
EBM2	Endothelial cell basal medium 2
EGF	Epidermal growth factor
EGM2	Endothelial cell growth medium 2
FBS	Fetal bovine serum
FGF-2	Fibroblast growth factor 2
FGF-2M	Fibroblast growth factor 2 double mutant
HEK	Human embryonic kidney
HUVEC	Human umbilical vein endothelial cell
IGF-1	Insulin-like growth factor 1
MTS	3-(4,5-Dimethylthiazol-2-yl)-5-(3-carboxymethoxyphenyl)-2-(4-sulfophenyl)-2H-tetrazolium
MTT	3-[4,5-Dimethylthiazol-2-yl]-2,5-diphenyltetrazolium bromide
PBS	Phosphate-buffered saline
PrADSC	Porcine adipose tissue-derived stem cell
SDS-PAGE	Sodium dodecyl sulfate-polyacrylamide gel electrophoresis
TRITC	Tetramethylrhodamine
VEGF	Vascular endothelial growth factor
VEGF-A	Vascular endothelial growth factor A
VEGFR2	Vascular endothelial growth factor receptor 2
WST	Water-soluble tetrazolium salt
XTT	2,3-bis-(2-Methoxy-4-nitro-5-sulfophenyl)-2H-tetrazolium-5-carboxanilide
YPD	Yeast extract peptone dextrose

References

1. Bhisitkul, R.B. Vascular endothelial growth factor biology: Clinical implications for ocular treatments. *Br. J. Ophthalmol.* **2006**, *90*, 1542–1547. [[CrossRef](#)]
2. Luzuriaga, J.; Irurzun, J.; Irastorza, I.; Unda, F.; Ibarretxe, G.; Pineda, J.R. Vasculogenesis from human dental pulp stem cells grown in matrigel with fully defined serum-free culture media. *Biomedicines* **2020**, *8*, 483. [[CrossRef](#)]
3. Kukula, K.; Urbanowicz, A.; Klopotoski, M.; Dabrowski, M.; Pregowski, J.; Kadziela, J.; Chmielak, Z.; Witkowski, A.; Ruzyllo, W. Long-term follow-up and safety assessment of angiogenic gene therapy trial VIF-CAD: Transcatheter intramyocardial administration of a bicistronic plasmid expressing VEGF-A₁₆₅/bFGF cDNA for the treatment of refractory coronary artery disease. *Am. Heart J.* **2019**, *215*, 78–82. [[CrossRef](#)] [[PubMed](#)]
4. Anttila, V.; Saraste, A.; Knuuti, J.; Jaakkola, P.; Hedman, M.; Svedlund, S.; Lagerstrom-Fermer, M.; Kjaer, M.; Jeppsson, A.; Gan, L.M. Synthetic mRNA encoding VEGF-A in patients undergoing coronary artery bypass grafting: Design of a phase 2a clinical trial. *Mol. Ther. Methods Clin. Dev.* **2020**, *18*, 464–472. [[CrossRef](#)]
5. Kastrup, J. Therapeutic angiogenesis in ischemic heart disease: Gene or recombinant vascular growth factor protein therapy? *Curr. Gene Ther.* **2003**, *3*, 197–206. [[CrossRef](#)] [[PubMed](#)]
6. Xu, Y.; Qiu, J.L.; Sun, Q.F.; Yan, S.G.; Wang, W.X.; Yang, P.S.; Song, A.M. One year results evaluating the effects of concentrated growth factors on the healing of intrabony defects treated with or without bone substitute in chronic periodontitis. *Med. Sci. Monit. Int. Med J. Exp. Clin. Res.* **2019**, *25*, 4384–4389. [[CrossRef](#)]
7. Fadeev, F.O.; Bashirov, F.V.; Markosyan, V.A.; Izmailov, A.A.; Povysheva, T.V.; Sokolov, M.E.; Kuznetsov, M.S.; Eremeev, A.A.; Salafutdinov, I.I.; Rizvanov, A.A.; et al. Combination of epidural electrical stimulation with ex vivo triple gene therapy for spinal cord injury: A proof of principle study. *Neural Regen. Res.* **2021**, *16*, 550–560. [[CrossRef](#)]
8. Masgutov, R.; Zeinalova, A.; Bogov, A.; Masgutova, G.; Salafutdinov, I.; Garanina, E.; Syromiatnikova, V.; Idrisova, K.; Mul-lakhmetova, A.; Andreeva, D.; et al. Angiogenesis and nerve regeneration induced by local administration of plasmid pBud-coVEGF165-coFGF2 into the intact rat sciatic nerve. *Neural Regen. Res.* **2021**, *16*, 1882–1889. [[CrossRef](#)] [[PubMed](#)]
9. Smith, R.J.; Nasiri, B.; Kann, J.; Yergeau, D.; Bard, J.E.; Swartz, D.D.; Andreadis, S.T. Endothelialization of arterial vascular grafts by circulating monocytes. *Nat. Commun.* **2020**, *11*, 1622. [[CrossRef](#)] [[PubMed](#)]
10. Rossi, C.; Lees, M.; Mehta, V.; Heikura, T.; Martin, J.; Zachary, I.; Spencer, R.; Peebles, D.M.; Shaw, R.; Karhinen, M.; et al. Comparison of efficiency and function of vascular endothelial growth factor adenovirus vectors in endothelial cells for gene therapy of placental insufficiency. *Hum. Gene Ther.* **2020**, *31*, 1190–1202. [[CrossRef](#)] [[PubMed](#)]
11. Ishihara, J.; Ishihara, A.; Starke, R.D.; Peghaire, C.R.; Smith, K.E.; McKinnon, T.A.J.; Tabata, Y.; Sasaki, K.; White, M.J.V.; Fukunaga, K.; et al. The heparin binding domain of von Willebrand factor binds to growth factors and promotes angiogenesis in wound healing. *Blood* **2019**, *133*, 2559–2569. [[CrossRef](#)] [[PubMed](#)]
12. Knaack, S.; Lode, A.; Hoyer, B.; Rosen-Wolff, A.; Gabrielyan, A.; Roeder, I.; Gelinsky, M. Heparin modification of a biomimetic bone matrix for controlled release of VEGF. *J. Biomed. Mater. Res. Part A* **2014**, *102*, 3500–3511. [[CrossRef](#)] [[PubMed](#)]
13. Filova, E.; Steinerova, M.; Travnickova, M.; Knitlova, J.; Musilkova, J.; Eckhardt, A.; Hadraba, D.; Matejka, R.; Prazak, S.; Stepanovska, J.; et al. Accelerated in vitro recellularization of decellularized porcine pericardium for cardiovascular grafts. *Biomed. Mater.* **2020**. [[CrossRef](#)]
14. Hutchings, H.; Ortega, N.; Plouet, J. Extracellular matrix-bound vascular endothelial growth factor promotes endothelial cell adhesion, migration, and survival through integrin ligation. *FASEB J.* **2003**, *17*, 1520–1522. [[CrossRef](#)] [[PubMed](#)]
15. Gutierrez-Gonzalez, A.; Aguilera-Montilla, N.; Ugarte-Berzal, E.; Bailon, E.; Cerro-Pardo, I.; Sanchez-Maroto, C.; Garcia-Campillo, L.; Garcia-Marco, J.A.; Garcia-Pardo, A. 41 integrin associates with VEGFR2 in CLL cells and contributes to VEGF binding and intracellular signaling. *Blood Adv.* **2019**, *3*, 2144–2148. [[CrossRef](#)]
16. Bikfalvi, A.; Klein, S.; Pintucci, G.; Rifkin, D.B. Biological roles of fibroblast growth factor-2. *Endocr. Rev.* **1997**, *18*, 26–45. [[CrossRef](#)]
17. Gharibi, B.; Hughes, F.J. Effects of medium supplements on proliferation, differentiation potential, and in vitro expansion of mesenchymal stem cells. *Stem Cells Transl. Med.* **2012**, *1*, 771–782. [[CrossRef](#)]
18. Al-Masawa, M.E.; Zaman, W.S.W.K.; Chua, K.H. Biosafety evaluation of culture-expanded human chondrocytes with growth factor cocktail: A preclinical study. *Sci. Rep.* **2020**, *10*. [[CrossRef](#)]
19. Vahdat, S.; Pahlavan, S.; Mahmoudi, E.; Barekat, M.; Ansari, H.; Bakhshandeh, B.; Aghdami, N.; Baharvand, H. Expansion of human pluripotent stem cell-derived early cardiovascular progenitor cells by a cocktail of signaling factors. *Sci. Rep.* **2019**, *9*. [[CrossRef](#)] [[PubMed](#)]
20. Ahn, H.N.; Kang, H.S.; Park, S.J.; Park, M.H.; Chun, W.; Cho, E. Safety and efficacy of basic fibroblast growth factors for deep second-degree burn patients. *Burns* **2020**, *46*, 1857–1866. [[CrossRef](#)] [[PubMed](#)]
21. Fu, X.B.; Shen, Z.Y.; Chen, Y.L.; Xie, J.H.; Guo, Z.R.; Zhang, M.L.; Sheng, Z.Y. Recombinant bovine basic fibroblast growth factor accelerates wound healing in patients with burns, donor sites and chronic dermal ulcers. *Chin. Med. J.* **2000**, *113*, 367–371.
22. Kuroda, Y.; Kawai, T.; Goto, K.; Matsuda, S. Clinical application of injectable growth factor for bone regeneration: A systematic review. *Inflamm. Regen.* **2019**, *39*. [[CrossRef](#)] [[PubMed](#)]
23. Yoshida, W.; Takeuchi, T.; Imamura, K.; Seshima, F.; Saito, A.; Tomita, S. Treatment of chronic periodontitis with recombinant human fibroblast growth factor-2 and deproteinized bovine bone mineral in wide intrabony defects: 12-month follow-up case series. *Bull. Tokyo Dent. Coll.* **2020**, *61*, 231–241. [[CrossRef](#)]

24. Fiorillo, L.; Cervino, G.; Galindo-Moreno, P.; Herford, A.S.; Spagnuolo, G.; Cicciu, M. Growth factors in oral tissue engineering: New perspectives and current therapeutic options. *BioMed Res. Int.* **2021**, 2021, 8840598. [[CrossRef](#)]
25. Wang, H.; Zhou, W.X.; Huang, J.F.; Zheng, X.Q.; Tian, H.J.; Wang, B.; Fu, W.L.; Wu, A.M. Endocrine therapy for the functional recovery of spinal cord injury. *Front. Neurosci.* **2020**, *14*, 590570. [[CrossRef](#)] [[PubMed](#)]
26. Salem, S.A.M.; Fezeaa, T.A.; El Khazragy, N.; Soltan, M.Y. Effect of platelet-rich plasma on the outcome of mini-punch grafting procedure in localized stable vitiligo: Clinical evaluation and relation to lesional basic fibroblast growth factor. *Dermatol. Ther.* **2021**, e14738. [[CrossRef](#)]
27. Edamura, K.; Takahashi, Y.; Fujii, A.; Masuhiro, Y.; Narita, T.; Seki, M.; Asano, K. Recombinant canine basic fibroblast growth factor-induced differentiation of canine bone marrow mesenchymal stem cells into voltage- and glutamate-responsive neuron-like cells. *Regen. Ther.* **2020**, *15*, 121–128. [[CrossRef](#)]
28. Kurniawan, D.W.; Booiijink, R.; Pater, L.; Wols, I.; Vrynas, A.; Storm, G.; Prakash, J.; Bansal, R. Fibroblast growth factor 2 conjugated superparamagnetic iron oxide nanoparticles (FGF2-SPIONs) ameliorate hepatic stellate cells activation in vitro and acute liver injury in vivo. *J. Control. Release* **2020**, *328*, 640–652. [[CrossRef](#)] [[PubMed](#)]
29. Kapoor, R.; Shome, D.; Vadera, S.; Kumar, V.; Ram, M.S. QR678 & QR678 neo hair growth formulations: A cellular toxicity & animal efficacy study. *Plast. Reconstr. Surg. Glob. Open* **2020**, *8*. [[CrossRef](#)]
30. Zhang, J.; Liu, Z.; Tang, J.; Li, Y.; You, Q.; Yang, J.; Jin, Y.; Zou, G.; Ge, Z.; Zhu, X.; et al. Fibroblast growth factor 2-induced human amniotic mesenchymal stem cells combined with autologous platelet rich plasma augmented tendon-to-bone healing. *J. Orthop. Transl.* **2020**, *24*, 155–165. [[CrossRef](#)]
31. Rusnati, M.; Tanghetti, E.; Dell’Era, P.; Gualandris, A.; Presta, M. α_3 integrin mediates the cell-adhesive capacity and biological activity of basic fibroblast growth factor (FGF-2) in cultured endothelial cells. *Mol. Biol. Cell* **1997**, *8*, 2449–2461. [[CrossRef](#)]
32. Kang, J.M.; Han, M.; Park, I.S.; Jung, Y.; Kim, S.H.; Kim, S.H. Adhesion and differentiation of adipose-derived stem cells on a substrate with immobilized fibroblast growth factor. *Acta Biomater.* **2012**, *8*, 1759–1767. [[CrossRef](#)] [[PubMed](#)]
33. Shin, Y.M.; Lee, Y.B.; Kim, S.J.; Kang, J.K.; Park, J.C.; Jang, W.; Shin, H. Mussel-inspired immobilization of vascular endothelial growth factor (VEGF) for enhanced endothelialization of vascular grafts. *Biomacromolecules* **2012**, *13*, 2020–2028. [[CrossRef](#)]
34. Shen, Y.H.; Shoichet, M.S.; Radisic, M. Vascular endothelial growth factor immobilized in collagen scaffold promotes penetration and proliferation of endothelial cells. *Acta Biomater.* **2008**, *4*, 477–489. [[CrossRef](#)]
35. Robinson, D.E.; Smith, L.E.; Steele, D.A.; Short, R.D.; Whittle, J.D. Development of a surface to enhance the effectiveness of fibroblast growth factor 2 (FGF-2). *Biomater. Sci.* **2014**, *2*, 875–882. [[CrossRef](#)]
36. Firoozi, N.; Kang, Y. Immobilization of FGF on poly(xylitol dodecanedioic acid) polymer for tissue regeneration. *Sci. Rep.* **2020**, *10*, 10419. [[CrossRef](#)]
37. Taborska, J.; Riedelova, Z.; Brynda, E.; Majek, P.; Riedel, T. Endothelialisation of ePTFE vessel prosthesis modified with an antithrombogenic fibrin/heparin coating enriched with bound growth factors. *RSC Adv.* **2021**, *11*, 5903–5913. [[CrossRef](#)]
38. Kaplan, O.; Zarubova, J.; Mikulova, B.; Filova, E.; Bartova, J.; Bacakova, L.; Brynda, E. Enhanced mitogenic activity of recombinant human vascular endothelial growth factor VEGF₁₂₁ expressed in *E. coli* Origami B (DE3) with molecular chaperones. *PLoS ONE* **2016**, *11*, e0163697. [[CrossRef](#)]
39. Taktak-BenAmar, A.; Morjen, M.; Ben Mabrouk, H.; Abdelmaksoud-Dammak, R.; Guerfali, M.; Fourati-Masmoudi, N.; Marrakchi, N.; Gargouri, A. Expression, purification and functionality of bioactive recombinant human vascular endothelial growth factor VEGF₁₆₅ in *E. coli*. *AMB Express* **2017**, *7*, 33. [[CrossRef](#)] [[PubMed](#)]
40. Lee, J.H.; Lee, J.E.; Kang, K.J.; Jang, Y.J. Functional efficacy of human recombinant FGF-2s tagged with (His)₆ and (His-Asn)₆ at the N- and C-termini in human gingival fibroblast and periodontal ligament-derived cells. *Protein Expr. Purif.* **2017**, *135*, 37–44. [[CrossRef](#)] [[PubMed](#)]
41. Sauer, D.G.; Mosor, M.; Frank, A.C.; Weiss, F.; Christler, A.; Walch, N.; Jungbauer, A.; Durauer, A. A two-step process for capture and purification of human basic fibroblast growth factor from *E. coli* homogenate: Yield versus endotoxin clearance. *Protein Expr. Purif.* **2019**, *153*, 70–82. [[CrossRef](#)]
42. Slamova, K.; Bojarova, P.; Gerstorferova, D.; Fliedrova, B.; Hofmeisterova, J.; Fiala, M.; Pompach, P.; Kren, V. Sequencing, cloning and high-yield expression of a fungal -N-acetylhexosaminidase in *Pichia pastoris*. *Protein Expr. Purif.* **2012**, *82*, 212–217. [[CrossRef](#)] [[PubMed](#)]
43. Krejzova, J.; Kulik, N.; Slamova, K.; Kren, V. Expression of human -N-acetylhexosaminidase B in yeast eases the search for selective inhibitors. *Enzym. Microb. Technol.* **2016**, *89*, 1–6. [[CrossRef](#)]
44. Arjmand, S.; Tavasoli, Z.; Siadat, S.O.R.; Saeidi, B.; Tavana, H. Enhancing chimeric hydrophobin II-vascular endothelial growth factor A₁₆₅ expression in *Pichia pastoris* and its efficient purification using hydrophobin counterpart. *Int. J. Biol. Macromol.* **2019**, *139*, 1028–1034. [[CrossRef](#)]
45. Zisch, A.H.; Schenk, U.; Schense, J.C.; Sakiyama-Elbert, S.E.; Hubbell, J.A. Covalently conjugated VEGF-fibrin matrices for endothelialization. *J. Control. Release* **2001**, *72*, 101–113. [[CrossRef](#)]
46. Rockwell, N.C.; Krysan, D.J.; Komiyama, T.; Fuller, R.S. Precursor processing by Kex2/furin proteases. *Chem. Rev.* **2002**, *102*, 4525–4548. [[CrossRef](#)] [[PubMed](#)]
47. Khan, S.; Villalobos, M.A.; Choron, R.L.; Chang, S.; Brown, S.A.; Carpenter, J.P.; Tulenko, T.N.; Zhang, P. Fibroblast growth factor and vascular endothelial growth factor play a critical role in endotheliogenesis from human adipose-derived stem cells. *J. Vasc. Surg.* **2017**, *65*, 1483–1492. [[CrossRef](#)] [[PubMed](#)]

48. Bassaneze, V.; Barauna, V.G.; Lavini-Ramos, C.; Kalil, J.; Schettert, I.T.; Miyakawa, A.A.; Krieger, J.E. Shear stress induces nitric oxide-mediated vascular endothelial growth factor production in human adipose tissue mesenchymal stem cells. *Stem Cells Dev.* **2010**, *19*, 371–378. [[CrossRef](#)] [[PubMed](#)]
49. Estes, B.T.; Diekman, B.O.; Gimble, J.M.; Guilak, F. Isolation of adipose-derived stem cells and their induction to a chondrogenic phenotype. *Nat. Protoc.* **2010**, *5*, 1294–1311. [[CrossRef](#)] [[PubMed](#)]
50. Ori, A.; Free, P.; Courty, J.; Wilkinson, M.C.; Fernig, D.G. Identification of heparin-binding sites in proteins by selective labeling. *Mol. Cell. Proteom.* **2009**, *8*, 2256–2265. [[CrossRef](#)]
51. Thompson, L.D.; Pantoliano, M.W.; Springer, B.A. Energetic characterization of the basic fibroblast growth factor-heparin interaction: Identification of the heparin binding domain. *Biochemistry* **1994**, *33*, 3831–3840. [[CrossRef](#)]
52. Presta, M.; Statuto, M.; Isacchi, A.; Caccia, P.; Pozzi, A.; Gualandris, A.; Rusnati, M.; Bergonzoni, L.; Sarmientos, P. Structure-function relationship of basic fibroblast growth factor: Site-directed mutagenesis of a putative heparin-binding and receptor-binding region. *Biochem. Biophys. Res. Commun.* **1992**, *185*, 1098–1107. [[CrossRef](#)]
53. Isacchi, A.; Bergonzoni, L.; Statuto, M.; Rusnati, M.; Chiesa, R.; Caccia, P.; Sarmientos, P.; Presta, M.; Ragnotti, G. A mutant of basic fibroblast growth factor that has lost the ability to stimulate plasminogen activator synthesis in endothelial cells. *Ann. N. Y. Acad. Sci.* **1991**, *638*, 369–377. [[CrossRef](#)] [[PubMed](#)]
54. Tahara, H.; Matsuda, S.; Yamamoto, Y.; Yoshizawa, H.; Fujita, M.; Katsuoka, Y.; Kasahara, T. High-content image analysis (HCIA) assay has the highest correlation with direct counting cell suspension compared to the ATP, WST-8 and Alamar blue assays for measurement of cytotoxicity. *J. Pharmacol. Toxicol. Methods* **2017**, *88*, 92–99. [[CrossRef](#)]
55. Walzl, A.; Unger, C.; Kramer, N.; Unterleuthner, D.; Scherzer, M.; Hengstschlager, M.; Schwanzler-Pfeiffer, D.; Dolznig, H. The resazurin reduction assay can distinguish cytotoxic from cytostatic compounds in spheroid screening assays. *J. Biomol. Screen* **2014**, *19*, 1047–1059. [[CrossRef](#)]
56. Uzarski, J.S.; DiVito, M.D.; Wertheim, J.A.; Miller, W.M. Essential design considerations for the resazurin reduction assay to noninvasively quantify cell expansion within perfused extracellular matrix scaffolds. *Biomaterials* **2017**, *129*, 163–175. [[CrossRef](#)] [[PubMed](#)]
57. Chiu, L.L.; Radisic, M. Scaffolds with covalently immobilized VEGF and angiopoietin-1 for vascularization of engineered tissues. *Biomaterials* **2010**, *31*, 226–241. [[CrossRef](#)] [[PubMed](#)]
58. Miyagi, Y.; Chiu, L.L.; Cimini, M.; Weisel, R.D.; Radisic, M.; Li, R.K. Biodegradable collagen patch with covalently immobilized VEGF for myocardial repair. *Biomaterials* **2011**, *32*, 1280–1290. [[CrossRef](#)]
59. Underwood, P.A.; Whitelock, J.M.; Bean, P.A.; Steele, J.G. Effects of base material, plasma proteins and FGF2 on endothelial cell adhesion and growth. *J. Biomater. Sci. Polym. Ed.* **2002**, *13*, 845–862. [[CrossRef](#)] [[PubMed](#)]
60. Kang, J.; Park, H.M.; Kim, Y.W.; Kim, Y.H.; Varghese, S.; Seok, H.K.; Kim, Y.G.; Kim, S.H. Control of mesenchymal stem cell phenotype and differentiation depending on cell adhesion mechanism. *Eur. Cell Mater.* **2014**, *28*, 387–403. [[CrossRef](#)] [[PubMed](#)]
61. Tanghetti, E.; Ria, R.; Dell’Era, P.; Urbinati, C.; Rusnati, M.; Ennas, M.G.; Presta, M. Biological activity of substrate-bound basic fibroblast growth factor (FGF2): Recruitment of FGF receptor-1 in endothelial cell adhesion contacts. *Oncogene* **2002**, *21*, 3889–3897. [[CrossRef](#)] [[PubMed](#)]
62. Kumorek, M.; Kubies, D.; Filova, E.; Houska, M.; Kasoju, N.; Mazl Chanova, E.; Matejka, R.; Kryslova, M.; Bacakova, L.; Rypacek, F. Cellular responses modulated by FGF-2 adsorbed on albumin/heparin layer-by-layer assemblies. *PLoS ONE* **2015**, *10*, e0125484. [[CrossRef](#)]
63. Spitaleri, A.; Mari, S.; Curnis, F.; Traversari, C.; Longhi, R.; Bordignon, C.; Corti, A.; Rizzardi, G.P.; Musco, G. Structural basis for the interaction of isoDGR with the RGD-binding site of v3 integrin. *J. Biol. Chem.* **2008**, *283*, 19757–19768. [[CrossRef](#)]
64. Corti, A.; Curnis, F. Isoaspartate-dependent molecular switches for integrin-ligand recognition. *J. Cell Sci.* **2011**, *124*, 515–522. [[CrossRef](#)]
65. Traub, S.; Morgner, J.; Martino, M.M.; Honing, S.; Swartz, M.A.; Wickstrom, S.A.; Hubbell, J.A.; Eming, S.A. The promotion of endothelial cell attachment and spreading using FNIII10 fused to VEGF-A₁₆₅. *Biomaterials* **2013**, *34*, 5958–5968. [[CrossRef](#)]
66. Dee, K.C.; Andersen, T.T.; Bizios, R. Design and function of novel osteoblast-adhesive peptides for chemical modification of biomaterials. *J. Biomed. Mater. Res.* **1998**, *40*, 371–377. [[CrossRef](#)]
67. Baird, A.; Schubert, D.; Ling, N.; Guillemin, R. Receptor-binding and heparin-binding domains of basic fibroblast growth factor. *Proc. Natl. Acad. Sci. USA* **1988**, *85*, 2324–2328. [[CrossRef](#)]
68. Mitchell, A.C.; Briquez, P.S.; Hubbell, J.A.; Cochran, J.R. Engineering growth factors for regenerative medicine applications. *Acta Biomater.* **2016**, *30*, 1–12. [[CrossRef](#)]
69. Bacakova, L.; Zarubova, J.; Travnickova, M.; Musilkova, J.; Pajorova, J.; Slepicka, P.; Kasalkova, N.S.; Svorcik, V.; Kolska, Z.; Motarjemi, H.; et al. Stem cells: Their source, potency and use in regenerative therapies with focus on adipose-derived stem cells—A review. *Biotechnol. Adv.* **2018**, *36*, 1111–1126. [[CrossRef](#)] [[PubMed](#)]
70. Matejka, R.; Konarik, M.; Stepanovska, J.; Lipensky, J.; Chlupac, J.; Turek, D.; Prazak, I.; Broz, A.; Simunkova, Z.; Mrazova, I.; et al. Bioreactor processed stromal cell seeding and cultivation on decellularized pericardium patches for cardiovascular use. *Appl. Sci.* **2020**, *10*, 5473. [[CrossRef](#)]
71. Bradford, M.M.; Williams, W.L. New, Rapid, sensitive method for protein determination. *Fed. Proc.* **1976**, *35*, 274.

72. Przekora, A.; Vandrovцова, M.; Travnickova, M.; Pajorova, J.; Molitor, M.; Ginalska, G.; Bacakova, L. Evaluation of the potential of chitosan/-1,3-glucan/hydroxyapatite material as a scaffold for living bone graft production in vitro by comparison of ADSC and BMDSC behaviour on its surface. *Biomed. Mater.* **2017**, *12*, 015030. [[CrossRef](#)] [[PubMed](#)]
73. Travnickova, M.; Pajorova, J.; Zarubova, J.; Krocilova, N.; Molitor, M.; Bacakova, L. The influence of negative pressure and of the harvesting site on the characteristics of human adipose tissue-derived stromal cells from lipoaspirates. *Stem Cells Int.* **2020**, *2020*, 1016231. [[CrossRef](#)] [[PubMed](#)]
74. Bunnell, B.A.; Flaas, M.; Gagliardi, C.; Patel, B.; Ripoll, C. Adipose-derived stem cells: Isolation, expansion and differentiation. *Methods* **2008**, *45*, 115–120. [[CrossRef](#)] [[PubMed](#)]
75. Megaloikonomos, P.D.; Panagopoulos, G.N.; Bami, M.; Igoumenou, V.G.; Dimopoulos, L.; Milonaki, A.; Kyriakidou, M.; Mitsiokapa, E.; Anastassopoulou, J.; Mavrogenis, A.F. Harvesting, isolation and differentiation of rat adipose-derived stem cells. *Curr. Pharm. Biotechnol.* **2018**, *19*, 19–29. [[CrossRef](#)] [[PubMed](#)]



Article

Interaction between Galectin-3 and Integrins Mediates Cell-Matrix Adhesion in Endothelial Cells and Mesenchymal Stem Cells

Antonín Sedlář^{1,2}, Martina Trávníčková¹ , Pavla Bojarová^{3,4,*} , Miluše Vlachová³, Kristýna Slámová³, Vladimír Křen³ and Lucie Bačáková^{1,*}

- ¹ Laboratory of Biomaterials and Tissue Engineering, Institute of Physiology of the Czech Academy of Sciences, Vídeňská 1083, CZ 142 20 Prague 4, Czech Republic; antonin.sedlar@fgu.cas.cz (A.S.); martina.travnickova@fgu.cas.cz (M.T.)
 - ² Department of Physiology, Faculty of Science, Charles University, Viničná 7, CZ 128 44 Prague 2, Czech Republic
 - ³ Laboratory of Biotransformation, Institute of Microbiology of the Czech Academy of Sciences, Vídeňská 1083, CZ 142 20 Prague 4, Czech Republic; miluse.vlachova@biomed.cas.cz (M.V.); slamova@biomed.cas.cz (K.S.); kren@biomed.cas.cz (V.K.)
 - ⁴ Department of Health Care Disciplines and Population Protection, Faculty of Biomedical Engineering, Czech Technical University in Prague, Nám. Sítná, CZ 272 01 Kladno, Czech Republic
- * Correspondence: bojarova@biomed.cas.cz (P.B.); lucie.bacakova@fgu.cas.cz (L.B.); Tel.: +420-296442360 (P.B.); +420-296443743 (L.B.)



Citation: Sedlář, A.; Trávníčková, M.; Bojarová, P.; Vlachová, M.; Slámová, K.; Křen, V.; Bačáková, L. Interaction between Galectin-3 and Integrins Mediates Cell-Matrix Adhesion in Endothelial Cells and Mesenchymal Stem Cells. *Int. J. Mol. Sci.* **2021**, *22*, 5144. <https://doi.org/10.3390/ijms22105144>

Academic Editor: Sonia Melino

Received: 23 February 2021

Accepted: 9 May 2021

Published: 13 May 2021

Publisher's Note: MDPI stays neutral with regard to jurisdictional claims in published maps and institutional affiliations.



Copyright: © 2021 by the authors. Licensee MDPI, Basel, Switzerland. This article is an open access article distributed under the terms and conditions of the Creative Commons Attribution (CC BY) license (<https://creativecommons.org/licenses/by/4.0/>).

Abstract: Galectin-3 (Gal-3) is a -galactoside-binding protein that influences various cell functions, including cell adhesion. We focused on the role of Gal-3 as an extracellular ligand mediating cell-matrix adhesion. We used human adipose tissue-derived stem cells and human umbilical vein endothelial cells that are promising for vascular tissue engineering. We found that these cells naturally contained Gal-3 on their surface and inside the cells. Moreover, they were able to associate with exogenous Gal-3 added to the culture medium. This association was reduced with a -galactoside LacdiNac (GalNAc1,4GlcNAc), a selective ligand of Gal-3, which binds to the carbohydrate recognition domain (CRD) in the Gal-3 molecule. This ligand was also able to detach Gal-3 newly associated with cells but not Gal-3 naturally present on cells. In addition, Gal-3 preadsorbed on plastic surfaces acted as an adhesion ligand for both cell types, and the cell adhesion was resistant to blocking with LacdiNac. This result suggests that the adhesion was mediated by a binding site different from the CRD. The blocking of integrin adhesion receptors on cells with specific antibodies revealed that the cell adhesion to the preadsorbed Gal-3 was mediated, at least partially, by 1 and V integrins—namely 51, V3, and V1 integrins.

Keywords: galectin; HUVEC; ADSC; integrin; carbohydrate

1. Introduction

Galectins are -galactosyl-binding proteins, which belong to lectins, i.e., carbohydrate-binding (glyco)proteins, interacting specifically with carbohydrate groups on other molecules, including those on the cell surface. Galectins were discovered in mammals, birds, amphibians, fish, nematodes, sponges, and also, in fungi. In mammals, sixteen types of galectins were found. Galectin-1, -2, -3, -4, -7, -8, -9, -10, -12, -13, -14, and -16 were identified in humans; galectin-5 and -6 were found in rats and mice; and galectin-11, -14, and -15 were found in ruminants [1–5].

Galectins are multifunctional pleiotropic molecules with a wide range of physiological and pathophysiological effects on cells, tissues, and organs. For example, galectins are involved in cell apoptosis, e.g., apoptosis of T cells (galectin-1 and -2); in cell–cell and cell–matrix adhesion (galectin-3 and -8); in cell proliferation (galectin-3); in inflammatory diseases, e.g.,

Crohn's disease and ulcerative colitis (galectin-4); in cell differentiation, e.g., the differentiation of keratinocytes, and in the regeneration of epidermis and cornea (galectin-7) or the differentiation of adipocytes (galectin-12). Galectin-9 is involved in the defense against tuberculosis, and also in rheumatoid arthritis and metabolic disorders like diabetes. Galectin-10 is expressed in eosinophils and basophils and is involved in asthma. Galectins 13, -14, and -16 are expressed in the placenta and are supposed to be important for pregnancy tolerance development [1–8].

This study is focused on the role of galectin-3 (Gal-3) in cell–matrix adhesion. Gal-3 is present in many cell types, such as vascular, bone, adipose, fibroblast, and tumor cells, and it is involved in cell–cell and cell–matrix adhesion, cell proliferation, differentiation, phenotypic modulation, and also in cardiovascular diseases, tumor metastasis, and tumor vascularization. Although Gal-3 is involved in inflammation [9], venous thromboembolism [10], or cancer progression [3,7,11–13], it has also been reported to have many positive effects. These effects include, e.g., re-epithelialization of corneal, intestinal, and skin wounds (for review, see [14]), or a protective role in the uptake and removal of modified lipoproteins, accompanied with the downregulation of the proinflammatory pathways responsible for the initiation and progression of atherosclerosis [15]. Besides, the binding of Gal-3 to galactoside-capped ligands on endothelial progenitor cells (EPCs) promotes differentiation of these cells into mature endothelial cells and endothelial tube formation [16].

Gal-3 binds not only -galactoside-capped glycans displayed on the surface of glycoproteins, but it can also bind synthetic carbohydrates and glycomimetics, which can be produced in relatively large quantities. The simplest ligands are represented by disaccharides LacNAc (Gal1,4GlcNAc), LacdiNAc (GalNAc1,4GlcNAc), or thiodigalactoside (Gal1,1-S-Gal), which can be attached to various biocompatible carriers [17,18] or derivatized [19,20]. In earlier studies, poly-LacNAc-based oligosaccharide ligands were bound, e.g., to a scaffold of bovine serum albumin [21], or LacdiNAc was attached to hydrophilic N-(2-hydroxypropyl) methacrylamide (HPMA) copolymers and used in the form of a glyconanomaterial [11]. These ligand–biomaterial complexes are promising for diagnostic and therapeutic purposes, e.g., for the selective recognition of Gal-3 both on the cell surface and in blood serum, and for the treatment of various disorders, particularly cancer [13].

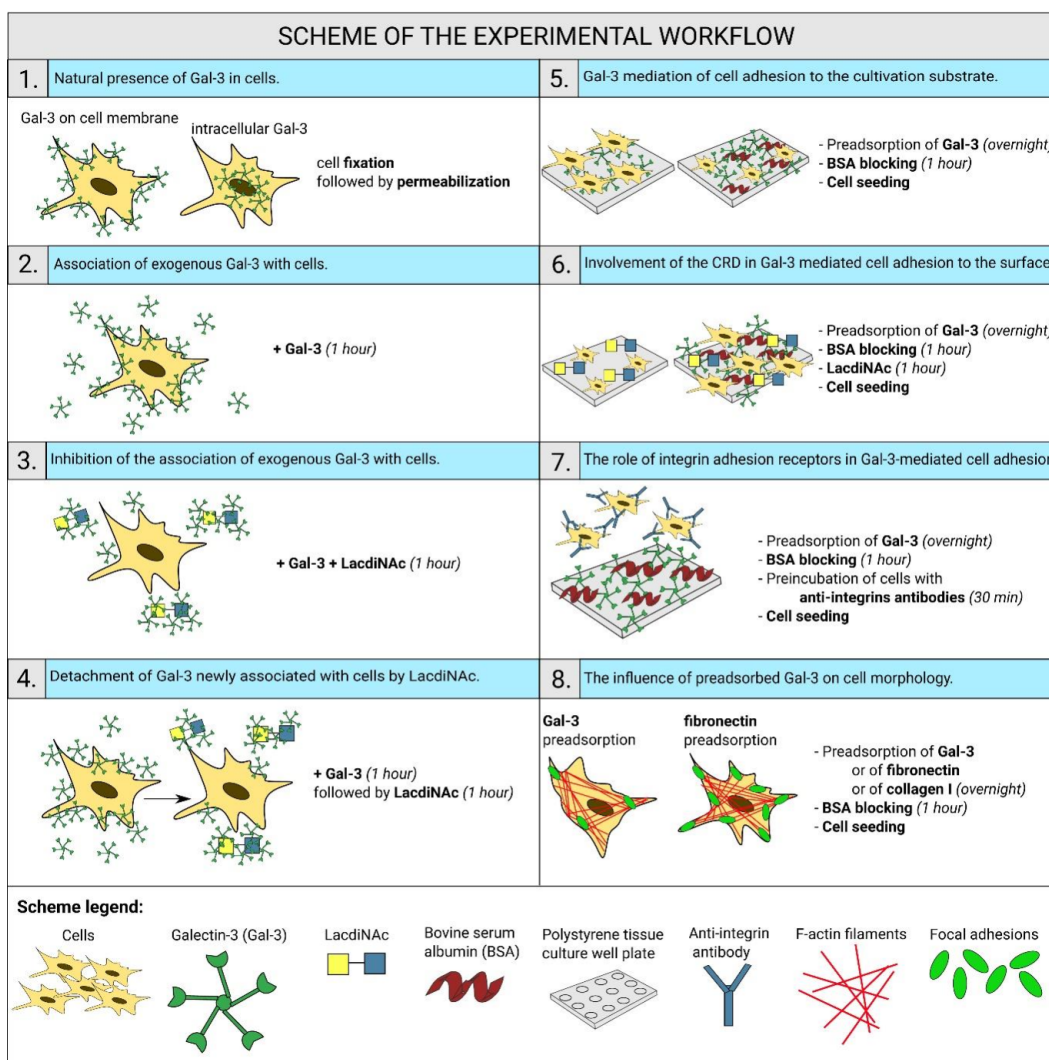
In addition to cellular localization, Gal-3 is also secreted from cells to the extracellular environment, e.g., into the extracellular matrix (ECM), interstitial fluid, or circulation [13]. In the extracellular space, Gal-3 can act as an adhesion ligand for cells. It has been reported that the cells can bind Gal-3 with their integrin adhesion receptors, e.g., with some integrins with the 1 chain; with other transmembrane molecules, such as CD7, CD43, and CD45; and with glycoproteins associated with the cell membrane, such as fibronectin, vitronectin, and laminin [1–3]. From this point of view, Gal-3 ligands, such as LacNAc and LacdiNAc, as well as Gal-3 molecules themselves, could be attached to various biomaterials to colonize them with cells, e.g., for the purpose of tissue engineering.

However, in the context of possible biomaterial functionalization, it should be considered that Gal-3 can play a dual role in cell–matrix adhesion. Gal-3, and also other galectins, such as galectin-1 and galectin-8, can act as either positive or negative modulators of cell–matrix adhesion [1,3,6]. On the one hand, Gal-3 can enhance the cell–matrix adhesion by direct binding to integrin–adhesion receptors on the cells and by promoting the clustering of these receptors into focal adhesion plaques, which is a prerequisite of functional cell adhesion. On the other hand, Gal-3 can mediate the endocytosis of integrins, and thus their lower availability for cell adhesion. In addition, Gal-3 can weaken the cell–matrix adhesion by steric hindrance, when it is bound either to integrins or their ECM ligands [1,3]. The dual role of Gal-3 (and also other galectins) in cell adhesion has not yet been fully elucidated. It may depend on the cell type, type of integrin receptor, and, particularly, on the Gal-3 concentration. Moderate sub-micromolar concentrations of Gal-3 inhibited the adhesion of fibroblasts and tumor cells, while higher concentrations stimulated it [1]. Moreover, the form of galectin either as a soluble ligand or immobilized on the cell adhesion substrate also matters [6].

This study aims to systematically investigate the behavior of Gal-3 in cell–matrix adhesion as an extracellular adhesion ligand for cells, adsorbed on a cultivation substrate in a wide

concentration range from 0.1 to 33 M. We used human adipose tissue-derived stem cells (ADSCs) and human umbilical vascular endothelial cells (HUVECs) as the cell models. These two cell types were selected due to their importance in the tissue engineering of blood vessels. It is known that Gal-3 is expressed in immature cell types, such as endothelial progenitor cells [22] and mesenchymal stem cells [23], including ADSCs, from which it can be secreted into the extracellular space and can influence the adhesion and growth of other cell types [24]. In HUVEC cells *in vitro*, Gal-3 induced the formation of tubular capillary-like structures, which was associated with an increased expression of V3 integrins on these cells [16].

First, we verified the natural presence of Gal-3 in the used cell types, and then, we investigated (i) the ability of exogenous Gal-3 added to the culture medium to associate with cells and (ii) the ability of Gal-3 immobilized on the cultivation substrate to mediate cell adhesion. We found that exogenous free Gal-3 was able to associate with cells, and this association was reduced with Gal-3 ligand LacdiNac in a concentration-dependent manner, while, importantly, cell adhesion to the substrate-immobilized Gal-3 was insensitive to LacdiNac. These results indicate that while the free Gal-3 binds cells through its carbohydrate-binding site on the CRD domain, the Gal-3 immobilized on the cultivation substrate binds cells by another yet not fully explored site on its molecule; apparently, this binding site interacts with 1 and V integrins on the surface of the cells, such as 51, V3, and V1 integrins. A comprehensive summary of our experimental work with its main findings is shown in Scheme 1.



Scheme 1. Summary of the experimental workflow with its main findings.

2. Results

2.1. Gal-3 Is Naturally Present in ADSCs and HUVECs

As a starting point in this study, it was vital to check whether Gal-3 is present in our ADSCs and HUVECs. In order to distinguish the distribution of Gal-3 in the cell membrane and in the cytoplasm, the cells were first fixed, and without permeabilization, they were stained with an anti-Gal-3 antibody. Thus, this antibody bound only the Gal-3 present in the cell membrane (Figure 1A, green fluorescence). Then, the cells were permeabilized and incubated with an anti-Gal-3 antibody to visualize the intracellular Gal-3 (red fluorescence). The microphotographs show that Gal-3 is localized homogeneously in the cell membrane but to a lesser extent than in the cytoplasm. In the cytoplasm, Gal-3 is homogeneously distributed throughout the cells, with clear accumulation in the region of the cell nuclei. The cytosolic fraction of Gal-3 was further quantified by the Western blot method. The cytosolic Gal-3 expression detected by Western blotting is lower in HUVECs than in ADSCs (Figure 1B).

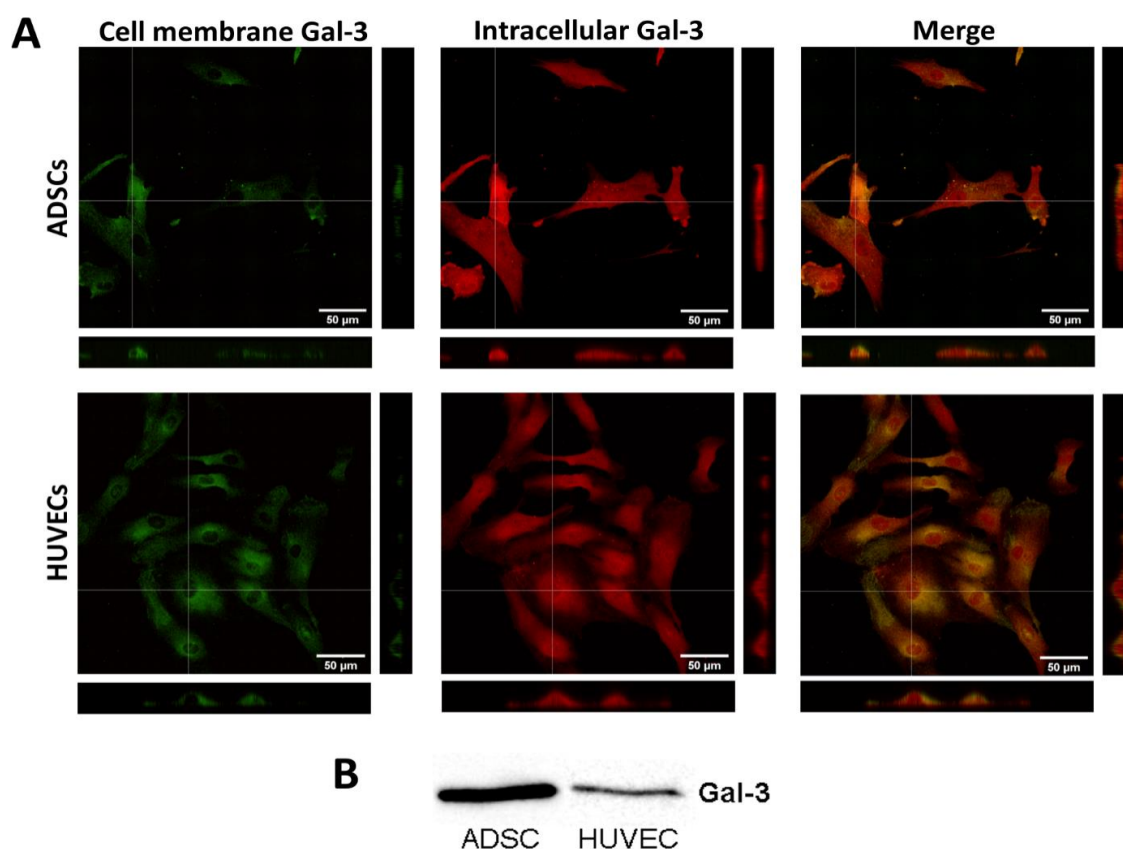


Figure 1. Localization of endogenous Gal-3 in ADSCs and HUVECs. **(A)** Immunofluorescence of Gal-3 in ADSCs and HUVECs in 1-day-old cultures. Cells were stained for Gal-3 present in the cell plasma membrane (green fluorescence) and for intracellular Gal-3 (red fluorescence). For Gal-3 staining, an anti-Gal-3 antibody produced in rabbits (Sigma-Aldrich, Cat. No. SAB4501746) was used. Orthogonal projections depict the localization of Gal-3 in the cell plasma membrane or the intracellular space. Andor Dragonfly 503 scanning disc confocal microscope; Zyla 4.2 PLUS sCMOS camera; objective HC PL APO 40/1.10 W CORR CS2; scale bar 50 μ m. **(B)** Western blot of Gal-3 expression in the cytosol of ADSCs and HUVECs. In both tested cell types, a Gal-3 band was detected at a size of 28 kDa.

2.2. Exogenous Gal-3 Associates with ADSCs and HUVECs

Furthermore, we tested whether ADSCs and HUVECs can associate with Gal-3 molecules in the extracellular environment when it was present in the cell culture media. For this purpose, confluent cells in 96-well tissue culture plates were incubated for 1 h with various concentrations (0.03 to 30 M) of Gal-3 diluted in the cell culture medium, and the membrane-bound Gal-3 was stained by immunofluorescence (after fixation with PFA

and without the use of detergents, i.e., without permeabilization of the cell membrane). After staining, it was apparent that, in the galectin-free medium, ADSCs were more intensively stained than HUVECs, which suggests a higher basal content of Gal-3 in the cell membrane of ADSCs (Figure 2). A similar pattern was observed in permeabilized cells (Figure 1A,B), which implies that the basal content of Gal-3 was also higher inside the ADSCs. When exposed to Gal-3 in the culture medium, the intensity of fluorescence of Gal-3 in cells gradually increased with the increasing Gal-3 concentration, and this increase became statistically significant (in comparison with untreated cell samples) at 0.3 M and 3 M Gal-3 concentrations in ADSCs and HUVECs, respectively (Figure 2). At the 3 M concentration, the intensity of the fluorescence of Gal-3 in ADSCs was still higher than in HUVECs. However, at the 10 M concentration, the intensity of the fluorescence of Gal-3 was similar in ADSCs and HUVECs, and at 30 M of Gal-3 in the cell culture medium, HUVECs showed a stronger ability to bind Gal-3, reaching a higher intensity of the fluorescence signal than ADSCs (Figure 2A).

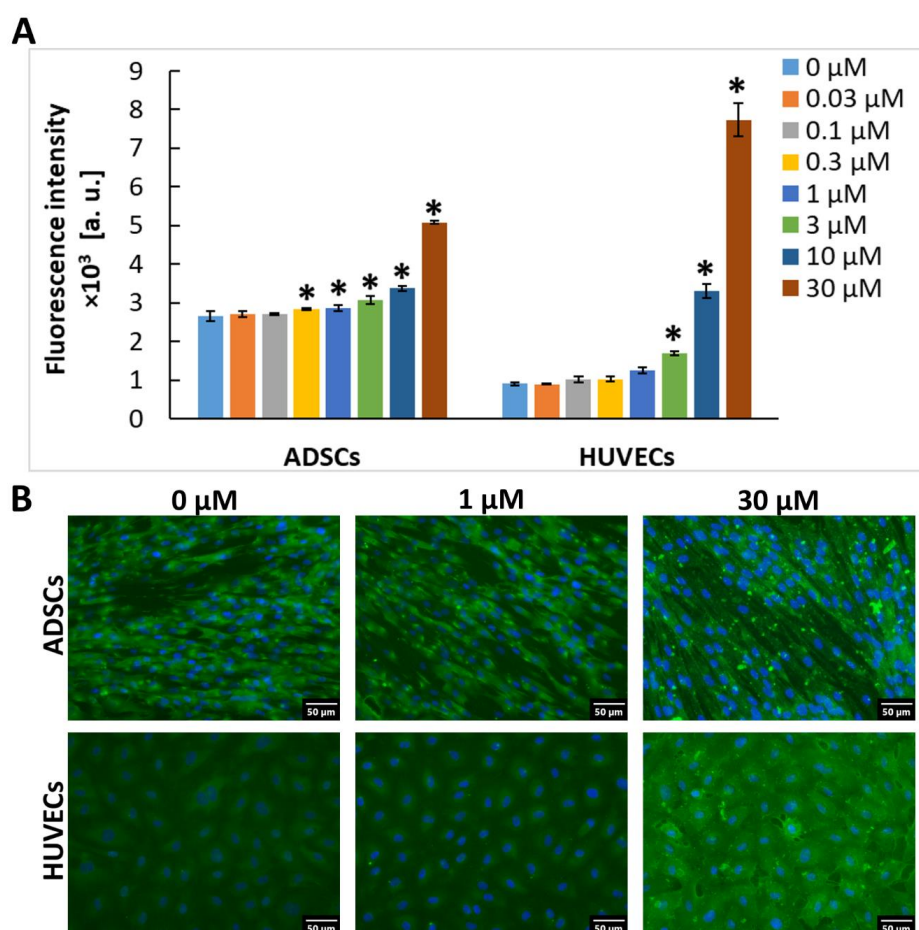


Figure 2. Association of exogenous Gal-3 with cells. For Gal-3 staining, the anti-Gal-3 antibody [EP2775Y] produced in rabbits (Abcam, Cambridge, UK; Cat. No. ab76245) was used. **(A)** The intensity of the fluorescence signal in wells with ADSCs and HUVECs after 1 h of incubation in a cultivation medium containing Gal-3 in a concentration range from 0 to 30 M. The data are presented as the mean SD from 3 wells. Holm-Sidak test, $p < 0.05$. The samples were statistically compared within the group of the indicated cell type. * Statistically significant difference in comparison with the control sample without the added Gal-3 (0 M). **(B)** Representative images of immunofluorescence of Gal-3 in ADSCs and HUVECs after 1 h of incubation in a pure cultivation medium without Gal-3 (0 M) and in the medium with 1 M or 30 M Gal-3. The cell nuclei were counterstained with Hoechst 33258. Olympus IX 71 microscope, DP 70 digital camera, obj. 20, scale bar 50 μm.

2.3. The Association of Gal-3 with Cells Is Reduced by LacdiNAc

We aimed to reveal the mechanism of association of exogenous recombinant Gal-3 with the cell surface. We supposed that this association can be mediated by α -galactoside ligands on the cell surface, including the disaccharide LacdiNAc. This disaccharide is naturally present in a variety of glycoproteins in cells and acts as a specific ligand for the carbohydrate-binding site at the CRD domain of Gal-3 [25]. HUVECs were grown to confluence and incubated with a cultivation medium containing Gal-3 (30 nM) and various concentrations of LacdiNAc (0 to 100 mM), which were added to the medium 1 h before its exposure to the cells. The presence of LacdiNAc in the cultivation medium strongly decreased the ability of Gal-3 to bind to HUVECs in a concentration-dependent manner. Despite this, LacdiNAc was not capable of inhibiting the association of Gal-3 with the cells completely. Even at the highest (100 mM) concentration of LacdiNAc, the immunofluorescence of Gal-3 was still significantly higher than in control cells without exposure to Gal-3 (Figure 3A,B). Nevertheless, this result suggests that recombinant Gal-3 binds to α -galactoside ligands present on the cells by its CRD domain.

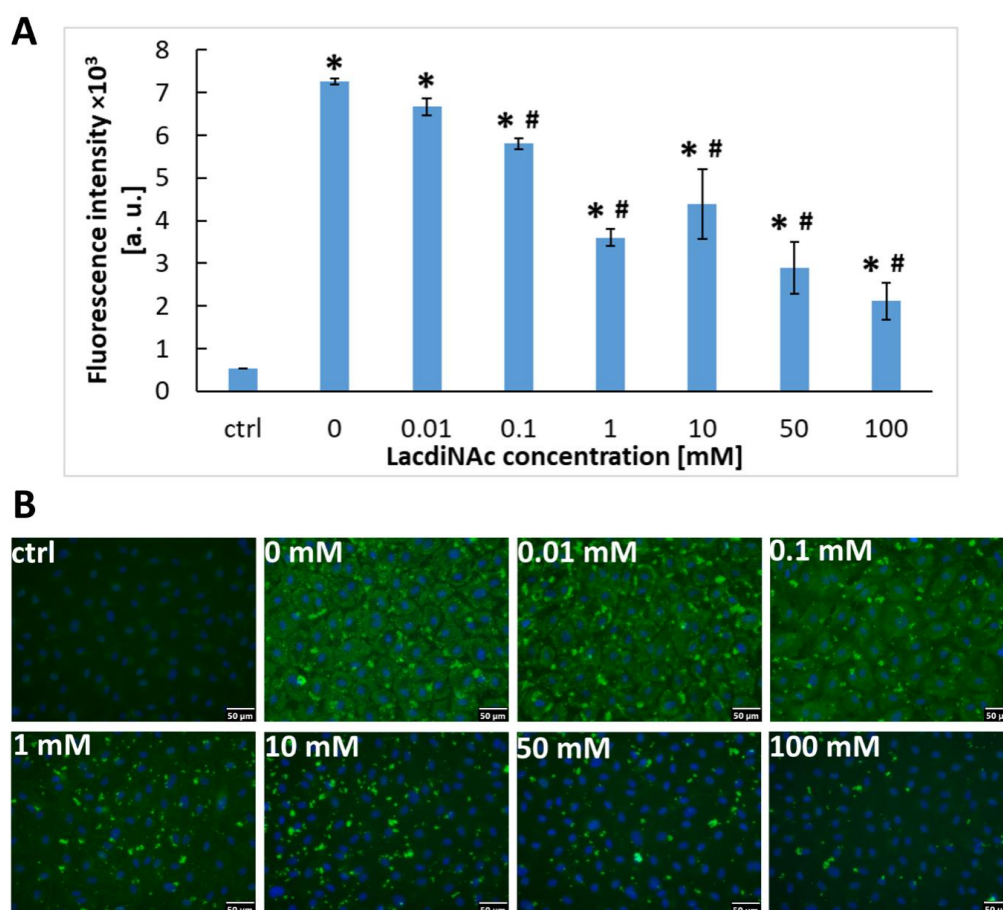


Figure 3. HUVECs after 1 h of incubation in a cultivation medium containing Gal-3 (30 nM) and various concentrations of LacdiNAc (0–100 mM). Control cells were incubated with a pure cultivation medium without Gal-3 and LacdiNAc. **(A)** Intensity of the fluorescence signal in HUVECs stained for Gal-3 (ex./em. = 485/528 nm). The data are shown as the mean \pm SD from 3 wells. Holm-Sidak test, $p < 0.05$. * Statistically significant difference in comparison with the control cells in the pure cultivation medium (ctrl). # Statistically significant difference in comparison with cells without LacdiNAc (0). **(B)** Immunofluorescence of Gal-3 in the cells compared in graph A. Anti-Gal-3 antibody (EP2775Y) produced in rabbits (Abcam, Cambridge, UK; Cat. No. ab76245) was used. The cell nuclei were counterstained with Hoechst 33258. Olympus IX 71 microscope, DP 70 digital camera, obj. 20, scale bar 50 μ m.

2.4. LacdiNac Is Capable to Detach Gal-3 Newly Associated with the Cell Membrane

To further elucidate the exact mechanism of the inhibitory effect of LacdiNac on the association of Gal-3 with the cells, we incubated confluent HUVECs with a cultivation medium containing either Gal-3 (30 M) alone or LacdiNac (1 mM) alone or both agents added either together or in a different order.

After the addition of Gal-3 into the cultivation medium for 1 h, Gal-3 was massively associated with the cells, as indicated by a markedly increased intensity of their immunofluorescence (Figure 4). When incubated for 1 h with LacdiNac, the cells showed a similar presence of Gal-3 as in the control cells cultivated in the pure medium, which suggests that LacdiNac was not capable of detaching Gal-3 naturally present on the plasma membrane. However, when the cells were incubated with a mixture of Gal-3 and LacdiNac, the association of Gal-3 with the cells was markedly reduced, similar to the experiments described in Section 2.3. Moreover, when the cells were first incubated with Gal-3 for 1 h and then exposed to LacdiNac for an additional 1 h, it was apparent that LacdiNac was capable of detaching the newly associated recombinant Gal-3 from the cells. In contrast, when the cells were first treated for 1 h with LacdiNac, then washed with PBS and incubated with Gal-3 for another 1 h, the fluorescence intensity remained comparable to the cells treated only with Gal-3 (Figure 4).

2.5. Gal-3 Mediates Cell Adhesion to the Cultivation Substrate

We decided to adsorb Gal-3 on cultivation surfaces free of other adhesion ligands to test its ability to act as a mediator of adhesion of ADSCs or HUVECs to these surfaces. These surfaces were represented by plastic culture plates used, e.g., for ELISA. The evaluation of the cell-adhesive properties of Gal-3 was performed using an xCELLigence RTCA SP sensing device. The initial adhesion and spreading of ADSCs were measured in wells of E-plates adsorbed with various concentrations of Gal-3, ranging from 0.1 to 33 M. The cells were incubated in DMEM without any additives to avoid the adsorption of cell adhesion-mediating molecules from the serum supplement, such as vitronectin and fibronectin or growth factors, which can also influence the cell adhesion [26]. The cell adhesion and spreading were monitored for four hours. One hour after cell seeding, i.e., after the time interval necessary for the initial adhesion of the cells, mediated by the interactions of the cell surface adhesion receptors (e.g., integrins) with ligands on the cultivation surface, Gal-3 significantly enhanced cell adhesion to the well bottoms in concentrations of 3.3 to 33 M, as indicated by the increasing cell index (Figure 5A). However, in the negative control assay in the absence of Gal-3, the control wells allowed the initial adhesion to a similar extent as in lower concentrations of Gal-3, i.e., from 0.1 to 1 M. Similar results were also obtained four hours after cell seeding, which is the time interval when the spreading of the adhered cells typically happens (Figure S1A, Supplementary Materials). This suggests nonspecific cell adhesion mediated by weak chemical bonds, e.g., electrostatic interactions, polar interactions, hydrogen bonding, van der Waals forces, etc., between the cell membrane and the well material [27]. In addition, some cell adhesion-mediating molecules, such as fibronectin, vitronectin, collagen, and laminin, can be retained on the cell surface even after trypsinization, which preceded cell seeding, and these molecules can also contribute to nonspecific cell adhesion. Therefore, the wells adsorbed with Gal-3 were blocked with 0.5% w/v BSA, a protein nonadhesive for cells, to prevent nonspecific interactions of cells with the well bottom surface (Figure 5A and Figure S1A). After blocking the nonspecific binding sites in the wells by BSA, the highest cell adhesion and spreading were observed at the 1 M concentration of Gal-3, and the lower or higher concentrations were not optimal for cell adhesion mediated by Gal-3 (Figure 5A and Figure S1A). At the same time, the well bottoms without Gal-3 or with its lowest concentration (0.1 M) did not promote almost any cell adhesion or any cell spreading.

The same set of experiments was then performed with HUVECs (Figure 5B and Figure S1B), and the adhesion behavior of these cells was compared with that of ADSCs. Interestingly, ADSCs and HUVECs showed a comparable affinity to Gal-3, which is in

contrast to our previous results (Figure 2), where the binding of Gal-3 from the culture medium to the cell surface appeared to be higher in HUVECs. On the other hand, a higher association of Gal-3 with HUVECs occurred only at the 30 M concentration of Gal-3, while at lower concentrations, this association was similar (10 M) or even lower (0.03–3 M) in comparison with ADSCs (Figure 2). Nonetheless, all these results are promising, because they suggest that Gal-3 acts as an adhesive molecule, and it could be further used for coating biomaterials, e.g., the inner surface of artificial vascular grafts, to enhance the adhesion of endothelial cells or their potential precursors in the form of stem cells, and thus to promote the formation of a confluent endothelial cell layer.

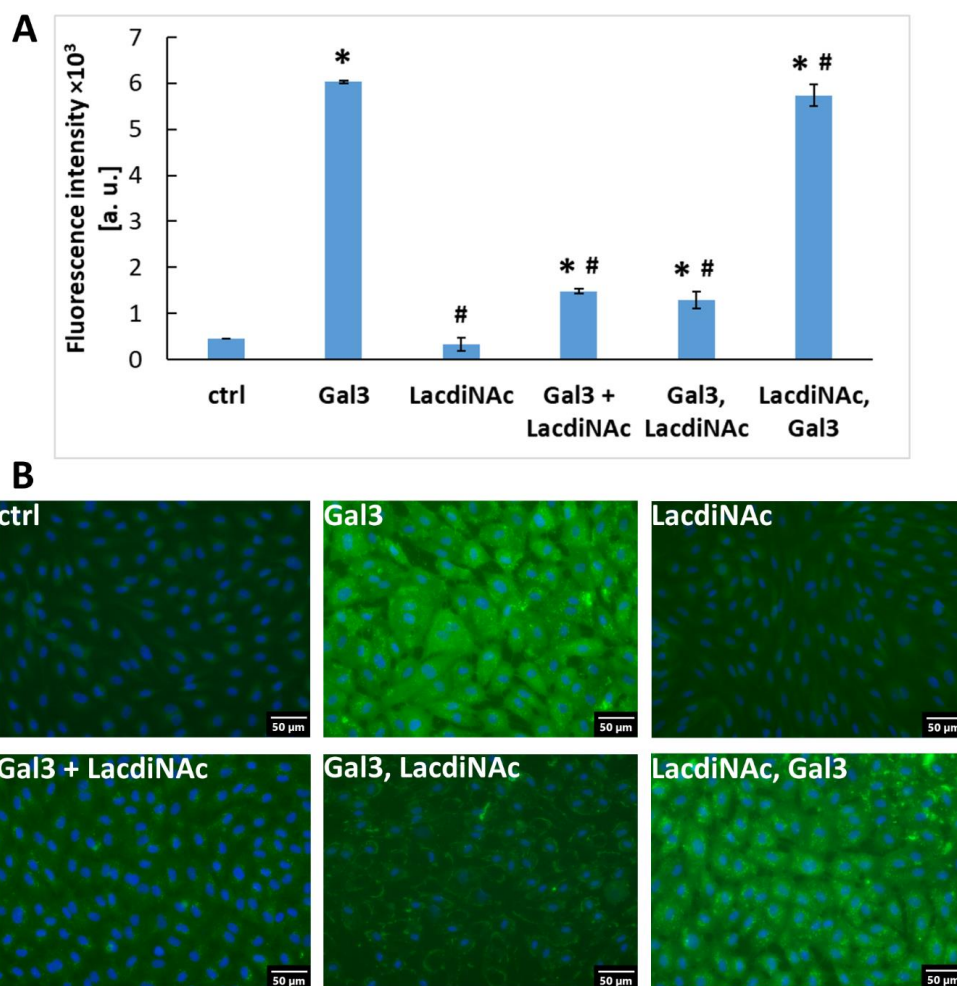


Figure 4. HUVECs after incubation in a cultivation medium containing Gal-3 (30 M) or LacdiNAc (1 mM) or both molecules added together or in a different order. Control cells were incubated for 1 h in a pure cultivation medium. **(A)** Intensity of the fluorescence signal in HUVECs stained for Gal-3 (ex./em. = 485/528 nm). The data are shown as the mean SD from 3 wells. Holm-Sidak test, $p < 0.05$. * Statistically significant difference in comparison with cells in the pure medium (ctrl), # Statistically significant difference in comparison with cells incubated with Gal-3 (Gal-3). **(B)** Immunofluorescence of Gal-3 in the cells compared in graph A. Anti-Gal-3 antibody (EP2775Y) produced in rabbits (Abcam, Cambridge, UK; Cat. No. ab76245) was used. The cell nuclei were counterstained with Hoechst 33258. Olympus IX 71 microscope, DP 70 digital camera, obj. 20, scale bar 50 μ m. Ctrl: cells in the pure medium; Gal3: cells incubated for 1 h in the medium with Gal-3; LacdiNAc: cells incubated for 1 h in the medium with 1-mM LacdiNAc; Gal3 + LacdiNAc: cells incubated for 1 h in the mixture of Gal-3 and LacdiNAc; LacdiNAc, Gal3: cells incubated for 1 h in the medium with LacdiNAc, then for 1 h in the medium with Gal-3; Gal3, LacdiNAc: cells incubated for 1 h in the medium with Gal-3, then for 1 h in the medium with LacdiNAc.

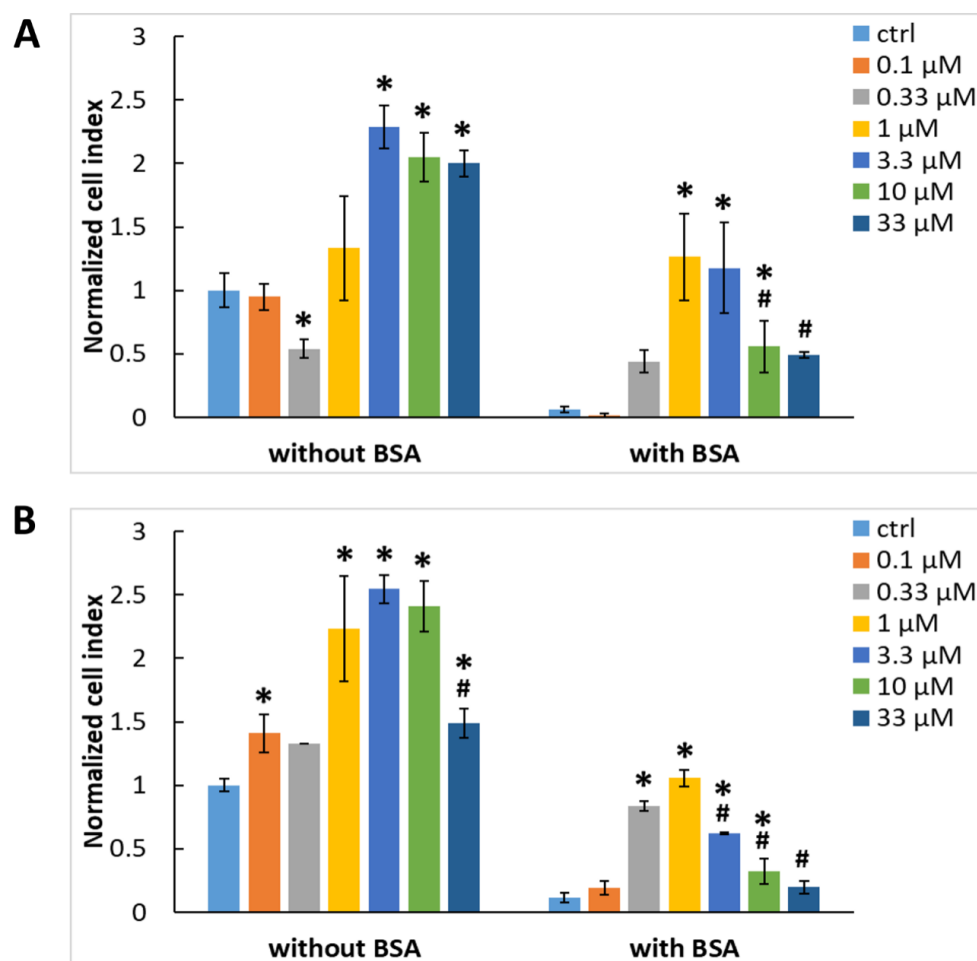


Figure 5. Initial adhesion of ADSCs (A) and HUVECs (B) to the wells of the E-plates in the xCELLigence system 1 h after seeding. The wells were adsorbed with various concentrations of Gal-3 (0.1–33 M) either without blocking or with blocking using 0.5% w/v BSA. Cell index values were normalized to the control cell sample without adsorbed Gal-3 and BSA (ctrl without BSA). Mean SD (n = 3). Holm-Sidak test, p 0.05. The cell samples were statistically compared either within the group without BSA or within the group with BSA. * Statistically significant difference in comparison with the control samples without adsorbed Gal-3 (ctrl). # Statistically significant difference in comparison with the sample exhibiting the highest average value of the cell index.

2.6. Gal-3-Mediated Cell Adhesion to the Surface Does Not Involve the CRD-Domain

Our experiments then continued with testing the potential inhibitory activity of LacdiNac, a -galactoside ligand for Gal-3, on Gal-3-mediated cell adhesion. Wells in the xCELLigence E-plates were adsorbed with 1 M Gal-3, blocked with 0.5% v/w BSA, and preincubated with various concentrations of LacdiNac (1 to 40 mM) before cell seeding. The results showed that LacdiNac did not inhibit the initial adhesion of ADSCs to the Gal-3-adsorbed well bottoms one hour after seeding (Figure 6) or the cell spreading after four hours of incubation (Figure S2), except for the highest concentration of LacdiNac, which slightly but significantly decreased the cell adhesion to the wells preadsorbed with Gal-3.

The effect of LacdiNac on nonspecific adhesion (i.e., adhesion not mediated by Gal-3) was also evaluated with ADSCs cells. The results showed that, similarly, LacdiNac did not considerably affect the initial cell adhesion and spreading on the well bottoms non-adsorbed with Gal-3 (Figure 6 and Figure S2).

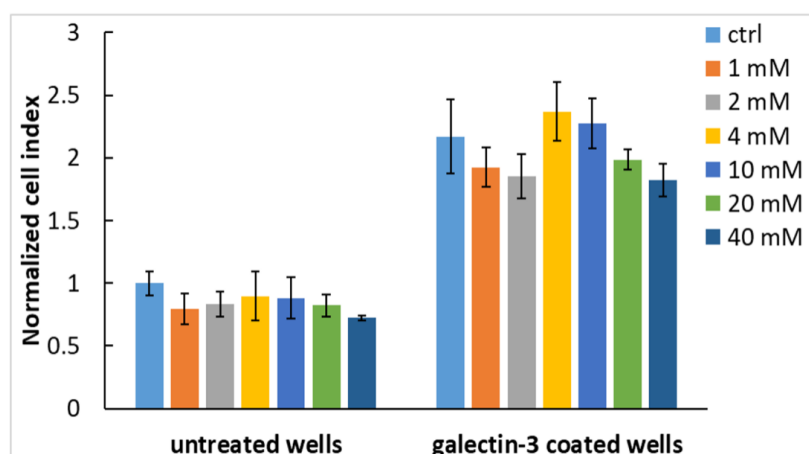


Figure 6. The effect of LacdiNAC on the initial adhesion of ADSCs one hour after seeding into untreated wells or wells preadsorbed with 1 M Gal-3 and blocked with BSA. Before cell seeding, both groups of wells were preincubated with LacdiNAC in concentrations from 1 to 40 mM. Wells without LacdiNAC served as control samples (ctrl). Cell index values were normalized to the sample without Gal-3 adsorption and without LacdiNAC in the medium (ctrl - untreated wells). Mean \pm SD from 3 wells. Holm-Sidak test, $p < 0.05$. The cell samples were statistically compared either within the group of untreated wells or within the group of Gal-3-adsorbed wells. * Statistically significant difference in comparison with the control cells (ctrl).

2.7. Integrins Are Cell Receptors for the Substrate-Bound Galectin

Our experiments continued with searching for receptors on the cell surface that are responsible for binding to Gal-3 preadsorbed on the cell surface. It is generally known that cell adhesion is mainly mediated by integrin receptors, which are heterodimeric transmembrane proteins formed by α and β subunits, and that these receptors are also involved in the galectin-mediated cell-matrix adhesion [1–3]. Here, we show that the highest concentrations of EDTA (10 mM), a potent calcium chelator and a well-known inhibitor of integrin receptors, inhibited the initial cell adhesion and spreading on Gal-3-coated surfaces (Figure 7A and Figure S3A). These results indicate the involvement of integrins in Gal-3-mediated adhesion of both studied cell types because calcium is essential for the adhesion function of integrins.

To further specify the involvement of particular integrin types in Gal-3-mediated cell adhesion, we preincubated the cells with various blocking antibodies against the integrin subunits, and then we seeded the cells on Gal-3-coated surfaces. We used antibodies against the integrin subunits most commonly involved in the cell–matrix interaction and expressed by a wide range of cell types—namely, the 1, 3, and V subunits—and also an antibody against the α_3 integrin subunit. The latter is a component of the $\alpha_3\beta_1$ integrin, a promiscuous receptor expressed mainly by endothelial cells, mediating the adhesion to laminin, fibronectin, or collagen [28]. As indicated by flow cytometry, these integrin subunits were also present in the ADSCs and HUVECs used in our study (Figures S4 and S5 in the Supplementary Materials). Our results showed that the adhesion of ADSCs was strongly blocked both with the V and 1 integrin antibodies but only slightly with the 3 integrin antibody whereas the adhesion of HUVECs was significantly inhibited by all three antibodies (Figure 7B). The inhibition of the cell spreading four hours after seeding of both cell types was more pronounced with the V and 1 integrin antibodies (Figure S3B). In contrast, the adhesion of ADSCs was not blocked with the 3 integrin antibody. This is in line with the results from the flow cytometry analysis, which showed only a weak expression of the 3 integrin subunit in ADSCs. In contrast, the adhesion of HUVECs was partially but significantly blocked with the 3 integrin antibody, mainly 4 h after cell seeding (Figure S3B).

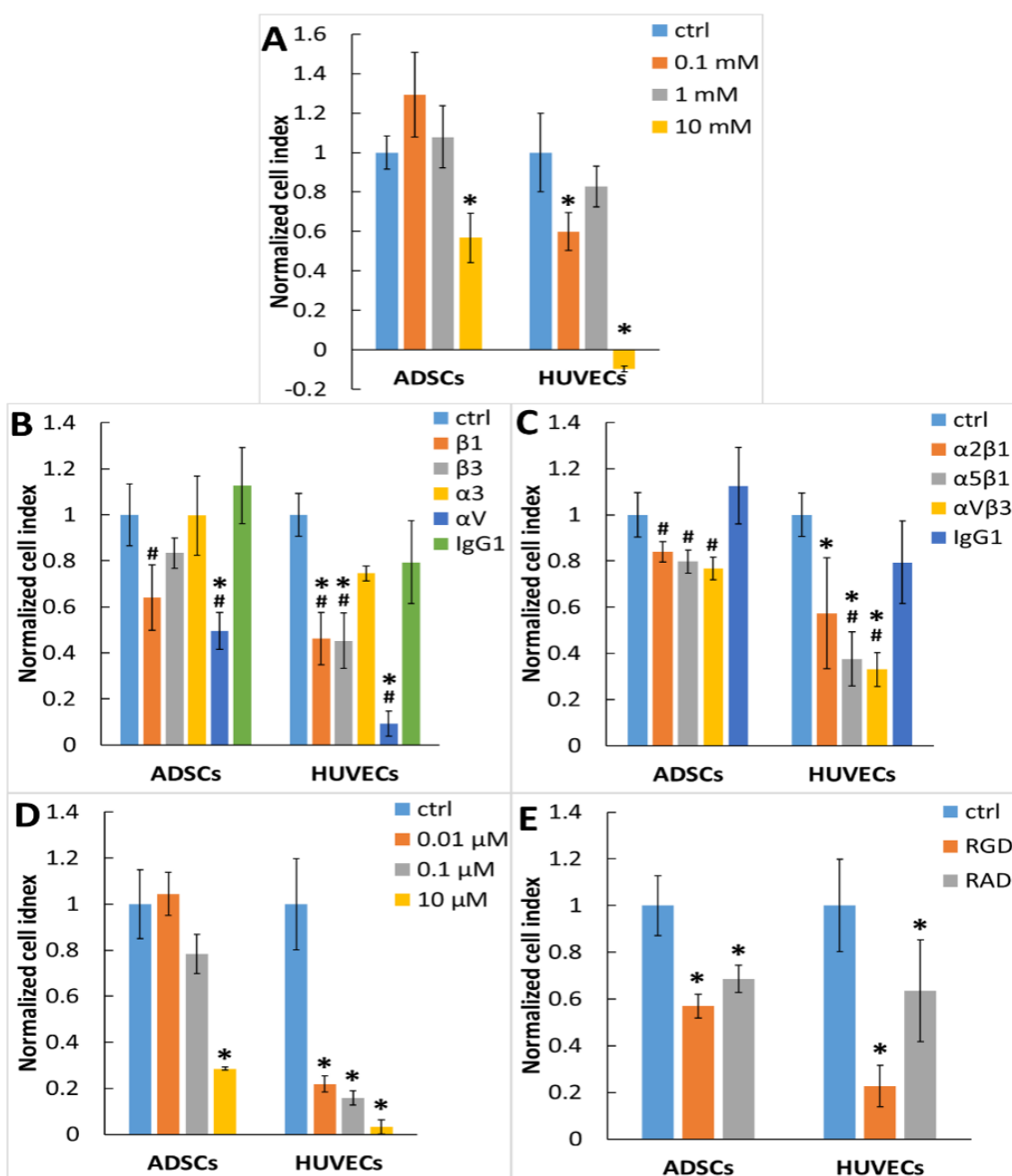


Figure 7. Role of integrins in the initial adhesion of ADSCs and HUVECs to substrate-immobilized Gal-3 (1 h after seeding). (A) The cells were seeded in a medium containing EDTA in concentrations ranging from 0.1 to 10 mM. (B) The cells were seeded in the medium containing antibodies against the 1, 3, 3, and V integrin subunits. The antibody against V integrin subunit was used in a 1:25 dilution, and the other antibodies were used in a concentration of 20 g/mL. Nonspecific mouse IgG1 was used as an isotype control. (C) The cells were seeded in the medium containing antibodies against 21, 51, or V3 integrin receptors. Nonspecific mouse IgG1 was used as an isotype control. Antibodies were used in a concentration of 20 g/mL. (D) The cells were seeded in a medium containing the V1 inhibitor in concentrations ranging from 0.01 to 10 M. (E) The cells were seeded in a medium containing the GRGDSP peptide. The GRADSP peptide was used as a negative control. Both peptides were used in a concentration of 200 M. Before cell seeding, the wells were coated with 1 M Gal-3 and blocked with 0.5% w/v BSA. The cell index values were normalized to the untreated sample in a pure medium without any additive (ctrl). Mean ± SD from 3 wells. Holm-Sidak test, $p < 0.05$. The samples were statistically compared within the group of the indicated cell type. * Statistically significant difference in comparison with the control cells (ctrl). # Statistically significant difference in comparison with the cells incubated with the isotype control (IgG1).

Integrin receptors can be divided into specific groups according to their affinity to various ECM proteins or various amino acid sequences within these proteins. There are RGD-binding integrins recognizing fibronectin (e.g., 51) or vitronectin (e.g., V3), collagen-binding receptors (e.g., 11 or 21), or laminin-binding receptors (e.g., 61 or 71 [29]). Since the laminin-binding receptors 61 or 71 are weakly expressed in ADSCs [30], we decided to test the most widespread receptors from the remaining groups. For this aim, we used antibodies against the 21 integrin (collagen I receptor), and also against the 51 and V3 integrins, which are receptors for fibronectin and vitronectin. These two blood serum-derived proteins are the main proteins mediating cell–substrate adhesion *in vitro*. Thus, it may be supposed that integrin receptors for fibronectin and vitronectin would be highly expressed in cultured cells. As proven by flow cytometry, the 21, 51, and V3 integrins were highly expressed in ADSCs and HUVECs in our study (Figures S4 and S5 in the Supplementary Materials). Apparently, the 21, 51, and V3 integrin antibodies had only a slightly negative influence on the adhesion of ADSCs. On the other hand, the inhibitory effect of these antibodies on the adhesion of HUVECs was more pronounced. Four hours after seeding, both cell types showed the lowest cell index values after blocking with the 51 and V3 integrin antibodies (Figure S3C). However, the reduction of the cell index values was relatively small, especially in the V3 antibody. This suggests that 51 and V3 were not the only receptors responsible for recognizing the substrate-bound Gal-3. From the previous results (Figure 7B), it is obvious that the adhesion to Gal-3 is inhibited mainly by the V and 1 integrin subunits. This led us to the hypothesis that the V1 integrin could be another receptor with affinity to Gal-3. Since there is no commercially available antibody specific to the V1 integrin, we tested a novel peptide inhibitor of the V1 integrin, which was shown to suppress the V1 integrin-mediated adhesion of fibroblasts in nanomolar concentrations, and also to attenuate the experimentally induced lung and liver fibrosis in mice [31]. When applied in concentrations of 0.01, 0.1, and 10 M, the inhibitor significantly decreased the Gal-3-mediated adhesion and spreading in HUVECs in a concentration-dependent manner (Figure 7D and Figure S3D). It is tempting to say that the cell adhesion to Gal-3 is mediated mainly by the V1 integrin; however, the adhesion of ADSCs was significantly blocked only by the 10 M concentration of the inhibitor. Moreover, at the 10 M concentration, the adhesion of ADSCs was also blocked at comparable levels in collagen I, vitronectin, or fibronectin-coated wells (Figure S6 in the Supplementary Materials). In addition, this integrin inhibitor has also been shown to interact with other RGD-binding integrins (e.g., V3, 51, or 81) when applied at micromolar concentrations [32]. The possible role of RGD-binding integrins in Gal-3-mediated cell adhesion was further confirmed by incubating the cells with the RGD-containing peptide. It was found that the cell adhesion and spreading were decreased by the RGD peptide in both ADSCs and HUVECs (Figure 7E and Figure S3E). Interestingly, the cell adhesion to substrate-bound Gal-3 was also partially inhibited with a peptide-containing RAD sequence, which was supposed to serve as a negative control.

2.8. Cell Morphology on the Surface Preadsorbed with Gal-3

To visualize the morphology of the cells adhered to the Gal-3-coated surface, we adsorbed Gal-3 on the 96-well glass plate and blocked the nonspecific binding sites with BSA. The reference wells were either left uncoated or coated with fibronectin or collagen I and blocked with BSA or only blocked with BSA. The cells were fixed four hours after seeding into the pure medium. Changes in the cell morphology on various adhesion substrates were also quantified by evaluation of the cell morphology characteristics (i.e., cell area, perimeter, circularity, and solidity; Figure S9 in the Supplementary Materials).

ADSCs on Gal-3 showed similar morphology characteristics to the cells on pristine, uncoated glass with a slightly better-developed actin cytoskeleton (Figures S7A, S8A, and S9 in the Supplementary Materials). ADSCs on fibronectin were more spread out (Figure S9A,B), with visible vinculin-containing focal adhesions located at the cell periphery. The cells

on collagen I showed a lower amount of focal adhesions than on fibronectin. Blocking the pristine glass surface with BSA prevented the ADSCs from spreading adequately and forming a well-developed actin cytoskeleton.

HUVECs on the control pristine glass displayed more rounded morphology than ADSCs (Figure S9C, a relatively high circularity parameter), but they were still relatively well-spread with the actin cytoskeleton and focal adhesions at the cell periphery (Figures S7B and S8B in the Supplementary Materials). HUVECs seeded on Gal-3 formed clusters of cells. In contrast to the relatively well-spread ADSCs on the Gal-3-coated surface, HUVECs displayed a stellate-like morphology with a poorly developed actin cytoskeleton, located mainly in the cell protrusions, which was also manifested in a smaller average cell spreading area, a shorter cell perimeter, and also in a relatively low solidity, i.e., a high occurrence of cell protrusions (Figure S9). HUVECs on fibronectin-coated glass showed well-formed vinculin-containing focal adhesions homogeneously distributed throughout the entire substrate-contacting cell membrane and a strong actin cytoskeleton. HUVECs on collagen I displayed a well-developed cytoskeleton, but the cytoskeletal structure was slightly worse than the one on fibronectin. The cells on pristine glass blocked with BSA were poorly spread out and were not able to form almost any cytoskeletal structures (Figures S7B, S8B and S9 in the Supplementary Materials).

3. Discussion

The aim of this work was to investigate Gal-3 as an adhesion receptor on the cell surface and as an extracellular ligand binding to the cell surface receptors. Our results show that ADSCs express higher amounts of Gal-3 than HUVECs. It is in accordance with earlier findings that stem cells and other immature cell types often contain a higher amount of Gal-3 than more mature cells [22,33]. However, when exposed to Gal-3 in the cell culture medium, HUVECs reached a considerably higher intensity of fluorescence signal than ADSCs (Figure 2). It could therefore be concluded that HUVECs showed a stronger ability to bind Gal-3 than ADSCs, at least at higher Gal-3 concentrations in the extracellular environment. Gal-3 interacts with the cell surface receptors mainly by binding to glycans on proteins [34], and its binding activity depends on the glycosylation pattern on the cell surface [35,36]. The binding of Gal-3 to the cell surface glycoproteins is mediated by terminal -galactoside groups of N-glycans [35], and it is negatively regulated by sialylation [35,37]. Supposedly, ADSCs contain lower amounts of -galactoside groups available for Gal-3 binding compared to HUVECs. Thus, the difference between Gal-3 binding to ADSCs and HUVECs can be explained by different glycosylation patterns in their cell surface glycoproteins. Our preliminary experiment with tunicamycin (an inhibitor of N-glycosylation) showed that the association of Gal-3 with the cell surface of ADSCs is independent of the tunicamycin treatment (up to 10 g/mL, which was already detrimental to the cells; data not shown). In future experiments, it would be interesting to treat the cells with other glycosylation inhibitors (e.g., swainsonine or benzyl N-acetyl--D-galactosaminide) to obtain a deeper insight into the influence of glycosylation on the association of Gal-3 with the cell plasma membrane.

In addition, ADSCs and HUVECs may differ in the further processing of Gal-3 after its binding to the cell surface. After binding to cells, Gal-3 is rapidly internalized by endocytosis, which is either carbohydrate-dependent (as in nonphagocytic cells) or independent (as in cells capable of phagocytosis; [38]). After endocytosis, some Gal-3 molecules are trafficked into various intracellular compartments, including lysosomes, while some of them are recycled on the cell membrane [39]. Galectins can also counteract the endocytic uptake by forming lattices on the plasma membrane, which depends also on the concentration and structure of the glycoprotein and glycolipid Gal-3 ligands [40].

Gal-3 (28 kDa) consists of an N-terminal collagen-like domain that enables protein oligomerization and a C-terminal domain (carbohydrate recognition domain; CRD) binding -galactosides [41]. We found that Gal-3 binds to the surface of HUVECs in a manner inhibitable by carbohydrates, such as LacdiNAc. LacdiNAc is a -galactoside naturally

present in a variety of glycoproteins that acts as a specific ligand for Gal-3 [17,21,25]. Naturally occurring -galactosides (e.g., lactose) have also been shown to inhibit the binding of Gal-3 to the cell surface [34], as well as inhibit the subsequent biological effects triggered by Gal-3 [4,34]. Besides, there is a broad variety of other carbohydrate-based Gal-3 inhibitors [4,13,20,42,43].

The -galactoside LacdiNAc, chosen for this study, can bind not only to Gal-3 but, to some extent, also to other proteins from the galectin family (e.g., Gal-2 or -7; [44]). On the other hand, LacdiNAc has a low binding affinity to Gal-1 or Gal-4 [25,44]. Of the twelve types of human galectins identified so far [5], only four types of galectin are expressed abundantly (e.g., Gal-1, -3, -8, and -9) in HUVECs, while the expression of the other galectins is only faint or undetectable [45]. A similar expression pattern was also observed in mesenchymal stem cells [46]. Therefore, in our experimental setup where excess amounts of exogenous Gal-3 were applied, we can consider any possible interaction of LacdiNAc with other proteins from the galectin family insignificant.

Our study also revealed that even the highest concentration of LacdiNAc (100 mM) did not stop the association of recombinant Gal-3 with the plasma membrane of HUVECs completely. This finding correlates with a study where the treatment of the plasma membrane with lactose led to the detachment only of a small part of membrane-associated Gal-3 [47]. This phenomenon was also observed in other studies [16,34,40,44], and it should be taken into account when LacdiNAc is used therapeutically in Gal-3-overexpressing tissues [11]. We hypothesized that the inability to detach all membrane-associated Gal-3 with the LacdiNAc ligand is caused either by the presence of high-affinity binding sites for Gal-3 on the cell surface by the involvement of a noncanonical binding site on Gal-3 CRD [48–50] or, possibly, by the presence of another binding site on the Gal-3 molecule. The two binding sites on Gal-3 CRD (canonical and noncanonical) can be occupied by the ligands at the same time.

Our results showed that Gal-3 optimally enhanced the cell adhesion when adsorbed to the plastic surface in the concentration of 1 M. Previous research showed both inhibitory and enhancing effects of Gal-3 in the culture medium on the cell adhesion to a cultivation substrate [1,51]. These contradictory results could be explained by the ability of Gal-3 to form oligomeric structures. When present in a solution at lower concentrations, Gal-3 stays in its monomeric form and binds in a monovalent manner to the cell surface or extracellular matrix proteins, creating steric hindrance and lowering the strength of the cell adhesion. In higher concentrations, Gal-3 can form oligomeric complexes and binds to the cell surface and extracellular matrix glycoproteins simultaneously, functioning as an “adhesion glue” (or a crosslinking agent) and enhancing the cell adhesion mediated by specific adhesion sequences on extracellular glycoproteins. When present in amounts exceeding the concentrations of the carbohydrate ligands on the extracellular matrix or cell surface, Gal-3 tends to bind the ligands in a monovalent manner, which leads to the inhibition of cell adhesion [1]. The concentration at which Gal-3 switches from its inhibitory to adhesion-enhancing activity and vice versa is micromolar [51]. Interestingly, our results showed that relatively high concentrations of adsorbed Gal-3 (i.e., 3–33 M) were not optimal for cell adhesion. When adsorbed at high concentrations (tens of micromoles per liter) to the surface, Gal-3 was supposed to form multivalent oligomeric complexes [52]. However, we suggest that a high concentration of Gal-3 in the solution led to the formation of clustered Gal-3 molecules bound in a high density on the substrate, which caused steric inhibition of the correct interaction of Gal-3 with the adhesion receptors on the cell surface, thus decreasing the cell adhesion intensity. The negative effect of the excess of the adhesion ligands was observed before [53] with the RGD ligands. Our results showed that the adsorbed Gal-3 mediated the cell adhesion of both HUVECs and ADSCs. The adhesion could not be inhibited by LacdiNAc, which suggests the involvement of another cell adhesion-mediating mechanism than the interaction of the Gal-3 CRD canonical binding site with carbohydrates. It has been reported that the cells can bind Gal-3 in other alternative ways, such as by integrin adhesion receptors α_{11} , α_{31} , and α_{71} . Other cell

membrane-associated molecules binding galectin include CD7 (an immunoglobulin found on thymocytes and mature T cells), CD43 (sialophorin), and CD45 (tyrosine phosphatase on hematopoietic cells), fibronectin, vitronectin, laminin, and also lysosome-associated membrane proteins LAMP-1 and LAMP-2 [1–3]. In the cited studies, Gal-3 was believed to interact with the carbohydrate components of all the mentioned molecules, but it is questionable whether this interaction is always mediated by the CRD canonical binding site in the Gal-3 molecule. Alternative binding molecules for Gal-3 on cell surfaces could also include proteins.

In the search for alternative binding sites for Gal-3 on the cell surface, we concentrated on the integrin adhesion receptors on cells, which have been shown to be involved in Gal-3-mediated cell–matrix adhesion [1–3]. Integrin adhesion receptors comprise at least 18 - and 8 -subunits, which can assemble into at least 24 unique integrin receptors [29]. Thus, we used antibodies against the mentioned subunits, and also against the 3 subunit, which is a component of the so-called “vitronectin receptor”- the V3 integrin, widely expressed in immature and proliferating cells, including the cells grown in conventional serum-supplemented cell culture systems. The mentioned integrin subunits are expressed in many cell types, including ADSCs and HUVECs, as shown by the flow cytometry analysis (Figures S4 and S5 in the Supplementary Materials) in our study, and also elsewhere [54–56]. Our results showed that cell adhesion was blocked by antibodies against the V and 1 integrin subunits but not substantially by the anti-3 subunit antibody.

Our observations that the cell adhesion to Gal-3 is mediated mainly by the integrin subunits V and 1 are also in good correlation with the study by Zhuo et al. (2008) [37]. They observed a significant decrease in the adhesion of colonocytes to Gal-3 when incubated with an integrin 1 functional blocking antibody. Moreover, they found that the adhesion is negatively regulated by the sialylation of the 1 integrin subunit. The role of 1 integrin as a surface receptor for Gal-3 was also proven in a study by Fukumori et al., performed on T cells [34].

Our results further showed that the adhesion to substrate-bound Gal-3 is mediated, at least partially, by integrins 51 and V3. These integrins are present on both ADSCs and HUVECs (Figures S4 and S5 in the Supplementary Materials). They are receptors for fibronectin and vitronectin, playing an important role in angiogenesis [57]. Another integrin involved in cell adhesion to substrate-bound Gal-3 was the V1 integrin, but its involvement was more pronounced in HUVECs than in ADSCs, as indicated by the blocking experiments (Figure 7D). Interestingly, the involvement of the 51 and V3 integrins and their subunits, such as 1, 3, and V, was also more pronounced in HUVECs (Figure 7B,C), although the flow cytometry showed comparable amounts of this molecule in the HUVECs and ADSCs (Figures S4 and S5 in the Supplementary Materials). On the other hand, the 3 integrin subunit (representing the 31 integrin receptor), which is expressed mainly in HUVECs (Figures S4 and S5 in the Supplementary Materials), appeared to be involved in Gal-3-mediated adhesion to a lesser extent. These results suggest that the cell type is an important factor affecting the role of integrins in Gal-3-mediated cell adhesion. This phenomenon may deserve further investigation in the future.

The 51, V3, and also V1 integrins typically recognize the RGD motif within the ECM molecules. Therefore, it can be hypothesized that the adhesion of ADSCs and HUVECs to Gal-3 is mediated by a specific amino acid adhesion sequence in the Gal-3 structure, which binds to integrin receptors. This is in accordance with our results where the adhesion of the cells to Gal-3 was significantly blocked by the 10 M V1 inhibitor, which is of an oligopeptidic RGD-like nature. In micromolar concentrations, this inhibitor can block a wide range of RGD-binding integrins [32]. The RGD sequence itself can also block cell adhesion to Gal-3 [58]. Surprisingly, the adhesion of ADSCs and HUVECs was partially inhibited by the RGD-containing peptide (Figure 7E), albeit there was no RGD motif in Gal-3 primary structure. However, it is not uncommon in the integrin superfamily that a specific type of integrin can bind to different ECM ligands in a “promiscuous” manner and different types of integrins can bind to the same ligand [59]. Therefore, it

cannot be excluded that some other amino acid sequence(s) in the Gal-3 molecule may take part in the integrin–Gal-3 interactions. Another possibility would be the involvement of a noncanonical binding site on Gal-3 CRD, which was shown to be independent of the blocking of the canonical binding site with -galactosides [49].

When adhered to glass coated with Gal-3, ADSCs showed a similar morphology to the untreated glass. In contrast, HUVECs on the Gal-3-coated surface exhibited a distinct morphology when compared with the cells on fibronectin coating or with untreated glass. HUVECs formed clusters of cells with the poorly developed cytoskeleton and “stellate-like” morphology. Similarly, the formation of “stellate-like” morphology with numerous lamellipodia and filopodia was observed in epithelial cells after incubation with Gal-3 [60]. There, the Gal-3-induced changes in the cell morphology were mediated by the $\alpha_3\beta_1$ integrin. In our study, the strong expression of the $\alpha_3\beta_1$ integrin was observed in HUVECs; in contrast, only a mild expression of this integrin was detected in ADSCs. This would explain the differences in the cell morphology of these two cell types on the Gal-3-coated surface. All these results suggest that, although Gal-3 interacts with the integrin receptors and enhances cell adhesion, it is not able to trigger specific integrin-mediated cytoskeletal formation. It can be explained by the fact that Gal-3 is not a “classical” ligand for integrin receptors, such as specific oligopeptide sequences within ECM molecules (e.g., RGD) that bind both α and β chains within the integrin receptor [59]. As shown in our experiments, Gal-3 can bind only a single subunit of the integrin receptor, e.g., the V subunit within the $\alpha_3\beta_1$ integrin, as documented in a relatively high inhibitory activity of the V blockers and no activity of the β_1 blockers. Such a partial binding cannot ensure a fully functional cell adhesion to Gal-3, at least in some cell types.

Our findings on cell–material adhesion mediated by the optimal concentration of Gal-3 adsorbed on the material surface may be applied in vascular tissue engineering. Gal-3 biofunctionalization of relatively bioinert materials used for vascular prostheses could lead to a better cell adhesion, as observed in the case of ADSCs and HUVECs in our in vitro experiments. The biofunctionalization of biomaterials with Gal-3 could be used as a novel alternative approach to the functionalization with short ECM-derived oligopeptides, which serve as ligands for integrin adhesion receptors and which have been widely investigated for the improved endothelialization of vascular replacements based on synthetic polymers [61,62] or decellularized matrices [63]. Furthermore, due to its positive role in angiogenesis [16], Gal-3 could also be utilized in broader tissue engineering applications. The Gal-3 biofunctionalization of 3D scaffolds (e.g., for bone or skin tissue engineering) could attract endothelial cells, facilitate their adhesion, potentiate capillary formation, and thus support the vascularization process of a scaffold that is very important for the long-term survival and proper functioning of the newly engineered tissues.

4. Materials and Methods

4.1. Preparation of Human Recombinant Gal-3

A recombinant His-tagged construct of Gal-3 was produced and purified as described previously [21]. Gal-3 was recombinantly expressed in the cells of *E. coli* Rosetta 2 (DE3) pLysS. The cultivation of precultures (60 mL in 0.5 L baffled flasks) was done overnight in Lysogeny broth (LB) medium (0.5% w/v yeast extract, 1.0% w/v tryptone, and 0.5% w/v NaCl; pH 7.4) at 220 rpm and 37 °C. The medium contained ampicillin (100 mg/L) and chloramphenicol (34 mg/L). After 17 h, the main cultures (600 mL in 3 L baffled flasks) in Terrific broth (TB) medium (2.4% w/v yeast extract, 1.2% w/v tryptone, 0.4% v/v glycerin, 17 mM KH_2PO_4 , and 72 mM K_2HPO_4 ; pH 7.0) containing antibiotics were inoculated with precultures and incubated at 37 °C and 150 rpm until they reached an optical density (OD_{600}) of 0.6–0.8. Then, the expression of Gal-3 was induced by isopropyl 1-thio- β -D-galactopyranoside (0.5 mM). After 24 h, the cells were centrifuged (5000 rpm, 20 min, 4 °C) and frozen at –20 °C. For the purification of Gal-3, *E. coli* cells were suspended in an ice-cold equilibration buffer (20 mM Na_2HPO_4 , 500 mM NaCl, and 20-mM imidazole; pH 7.4) and sonicated on ice (six 30 s cycles, 52% amplitude). After removing the cell debris

(centrifugation at 13,400 rpm, 15 min, 10 C), the supernatant was filtered through a 0.8 m syringe filter and loaded on a HisTrap™ HP 5-mL column (GE Healthcare, Chicago, IL, USA), according to the manufacturer's instructions, in an equilibration buffer. Gal-3 was eluted with elution buffer (20 mM Na₂HPO₄, 500 mM NaCl, and 500 mM imidazole; pH 7.4). The combined fractions containing galectin were dialyzed in SnakeSkin™ Dialysis Tubing (10 kDa MWCO, Thermo Fisher Scientific, Waltham, MA, USA) overnight against EPBS buffer (50 mM NaH₂PO₄, 150 mM NaCl, and 2 mM ethylenediaminetetraacetic acid; pH 7.5) and for an additional 4 h against PBS buffer (50 mM NaH₂PO₄ and 150 mM NaCl; pH 7.5). The usual yield was ca 7–10 g of cells per 1 L of medium and 5 mg of pure Gal-3 per 1 g of cells. After sterile filtration, Gal-3 (100–200 M solutions) was stable for 1 to 2 months at 4 C.

4.2. Preparation and Characterization of LacdiNAc Ligand for Gal-3

The disaccharide epitope LacdiNAc, which acts as a selective ligand for Gal-3, was prepared and structurally characterized as described in our recent work [25].

4.3. Cell Models

Human adipose tissue-derived stem cells (ADSCs) were isolated from a lipoaspirate obtained by liposuction from the thigh region of a patient (woman, aged 46 years) at a negative pressure of 200 mmHg. The isolation was conducted in compliance with the tenets of the Declaration of Helsinki for experiments involving human tissues and under the ethical approval issued by the Ethics Committee in Na Bulovce Hospital (Budínova 2, CZ 180 00 Prague 8). Written informed consent was obtained from the patient before the liposuction procedure. The ADSCs were isolated by a method described by Estes et al. (2010) [64] with the slight modifications reported in our earlier studies [65,66]. Briefly, the lipoaspirate was rinsed several times in phosphate-buffered saline (PBS) to remove the blood cells, digested by 0.1% type I collagenase in PBS for 1 h at 37 C, and centrifuged. The obtained vascular–stromal fraction was washed two times, and it was filtered using a filter with 100-µm pores (Cell Strainer; BD Falcon, Franklin Lakes, NJ, USA). After the final washing and centrifugation, the cells were seeded into tissue culture polystyrene flasks (75 cm²; TPP, Trasadingen, Switzerland) at a density of 0.16 mL of the original lipoaspirate per cm². The cells were expanded in Dulbecco's modified Eagle's medium (DMEM; Gibco, Thermo Fisher Scientific, Waltham, MA, USA) supplemented with 10% fetal bovine serum (FBS; Gibco, Thermo Fisher Scientific, Waltham, MA, USA), 40 µg/mL of gentamicin, and 10 ng/mL of FGF-2 (GenScript Biotech Co., Piscataway, NJ, USA, Cat. No. Z03116-1). In passage 2, the cells were characterized by flow cytometry (Accuri C6 Flow Cytometer, BD Biosciences, San Jose, CA, USA), which revealed the presence of standard surface markers of ASCs, namely CD105 (99.9%), CD90 (99.5%), CD73 (100%), and also, CD29 (100%). However, the ASCs were negative or almost negative for CD31 (0.5%), for CD34 (0.2%), CD45 (3.8%), and for CD146 (4.7%).

Human umbilical vein endothelial cells (HUVECs) were purchased from Lonza, Basel, Switzerland (Cat. No. C2517A, passage 3). The cells were expanded in endothelial cell growth medium 2 (EGM-2), which was prepared from endothelial cell basal medium 2 (EBM-2, PromoCell, Heidelberg, Germany, Cat. No. C-22111), supplemented with 1% antibiotic antimycotic solution (v/v, A5955, Sigma-Aldrich, St. Louis, MO, USA) and the growth medium 2 supplement pack (PromoCell, Heidelberg, Germany, Cat. No. C-39211) containing hydrocortisone, heparin, ascorbic acid, EGF, VEGF, IGF-1, FGF-2, and 2% FBS.

4.4. Natural Presence of Gal-3 in ADSCs and HUVECs

The natural presence of Gal-3 in the cell types used in this study was determined by immunofluorescence staining. The cells were fixed with 4% paraformaldehyde in phosphate-buffered saline (PBS) for 20 min at room temperature (RT). For staining of Gal-3 on the cell plasma membrane, the cells were incubated with PBS containing 1% w/v BSA for 20 min at RT. BSA was used for blocking the nonspecific-binding sites for the

antibodies. After rinsing with PBS, the cells were incubated with a primary anti-Gal-3 antibody, produced in rabbit (Sigma-Aldrich, St. Louis, MO, USA; Cat. No. SAB4501746). The antibody was diluted in PBS at a ratio of 1:400, and the cells were incubated overnight at 4 C. After washing with PBS, the cells were incubated for 1 h at RT in the dark with the secondary antibody Alexa Fluor[®] 488 F(ab')₂ fragment of goat anti-rabbit IgG (H+L), Invitrogen, Carlsbad, CA, USA, Cat. No. A11070; diluted in PBS at a ratio of 1:400. To stain the intracellular Gal-3, the cells were permeabilized by incubation with PBS containing 1% w/v BSA and 0.1% Triton X-100 for 20 min at RT, followed by incubation with PBS containing 1% Tween for another 20 min at RT. Then, the cells were incubated with an anti-Gal-3 primary antibody (Sigma-Aldrich, St. Louis, MO, USA; Cat. No. SAB4501746) and Alexa Fluor[®] 546 goat anti-rabbit IgG (H + L), Invitrogen, Carlsbad, CA, USA, Cat. No. A11010, to visualize the intracellular Gal-3. The presence and distribution of Gal-3 in the cells were then evaluated using the Andor Dragonfly 503 scanning disc confocal microscope equipped with a Zyla 4.2 PLUS sCMOS camera and objective HC PL APO 40/1.10 W CORR CS2 (Andor Technology Ltd., Belfast, UK).

The cytosolic fraction of the ADSCs and HUVECs was isolated using the Qproteome cell compartment kit (Qiagen, Germantown, MD, USA) according to the manufacturer's instructions. Briefly, after harvesting, approximately 4×10^6 cells were washed twice with PBS, resuspended in 1 mL of ice-cold Lysis buffer, and swayed for 10 min at 4 C. After centrifugation at 1000 g for 10 min at 4 C, the supernatant (cytosolic proteins) was transferred into a fresh tube. The proteins were precipitated in acetone for 30 min on ice and dissolved in 200 L of SDS-PAGE loading buffer. An equal amount of dissolved cytosolic proteins (18 L of ADSCs and 20 L of HUVECs) was loaded on 12% SDS-polyacrylamide gel and separated by electrophoresis (15 mA for a gel). Next, the proteins were transferred onto a 0.45-m nitrocellulose membrane (100 V, 2 h, 4 C). After washing with Tris-buffered saline with Tween 20 (TBS-T; 20 mM Tris, 14-mM NaCl, and 0.1% Tween 20; pH 8.0), the membrane was blocked with 10% milk in TBS-T for 2 h at room temperature. Subsequently, the membrane was incubated with a primary antibody against human Gal-3 (D4I2R, 1:1000, Cell Signaling Technology, Danvers, MA, USA) at 4 C overnight in 5% milk in TBS-T and, then, with the HRP-conjugated anti-rabbit secondary antibody (1:5000, Abcam, Cambridge, UK). The signal was developed in the SuperSignal West Femto Maximum Sensitivity Substrate (Thermo Fisher Scientific, Waltham, MA, USA) and documented using the G:BOX Chemi XRQ gel doc system with GeneTools software (Syngene, Synoptics Group, Cambridge, UK).

4.5. Association of Free Gal-3 with the Cell Surface

HUVECs or ADSCs were grown to confluence in 96-well tissue culture polystyrene plates (TPP; Trasadingen, Switzerland, Cat. No. 92096). Then, the medium was removed, and the cells were incubated in 50 L of fresh EGM-2 containing Gal-3 in concentrations of 0, 0.03, 0.1, 0.3, 1, 3, 10, or 30 M for 1 h at 37 C. The cells were then fixed with paraformaldehyde without permeabilization and were stained by immunofluorescence for Gal-3 bound on the cell cytoplasmic membrane, as described in Section 4.4, using the anti-Gal-3 antibody (EP2775Y) produced in rabbits (Abcam, Cambridge, UK; Cat. No. ab76245). The amount of Gal-3 on the cell surface was then estimated spectrophotometrically using a Synergy[™] HT Multi-Mode Microplate reader (BioTek, Winooski, VT, USA) by measuring the fluorescence intensity of the stained Gal-3 bound to the cell membrane (Ex./Em. = 485/528 nm). The microphotographs were taken using an Olympus IX 71 epifluorescence microscope equipped with a DP 70 digital camera (Olympus, Tokyo, Japan).

Potential blocking of the association of Gal-3 with the cell membrane with LacdiNac was then investigated. First, Gal-3 was diluted in the EGM-2 medium to the concentration of 30 M (which proved to be the optimum concentration for the association of Gal-3 with the cell surface, as indicated by Figures 2 and 3). Gal-3 was then incubated with LacdiNac added to the same medium in 0, 0.01, 0.1, 1, 10, 50, or 100 mM concentrations for 1 h at 37 C. After that, 50 L of the media, with a combination of Gal-3 and each concentration

of LacdiNAC, were added to the confluent layers of HUVECs in 96-well plates and were incubated with the cells for another 1 h at 37 C.

The optimum concentration of LacdiNAC for blocking the association of Gal-3 with cells was then selected (1 mM; Figure 4) and used for further blocking experiments, in which Gal-3 and LacdiNAC were added to the cells in a different order. In these experiments, the cells were first incubated with 30 M Gal-3 for 1 h, then were rinsed with PBS and incubated for an additional 1 h with 1 mM LacdiNAC or contrariwise. A group of cell samples was also incubated with a mixture of 30 M Gal-3 and 1 mM LacdiNAC. Reference cell samples were incubated for 1 h either with Gal-3 (30 M) alone or with LacdiNAC (1 mM) alone. The cells were then fixed with paraformaldehyde and stained for the cytoplasmic membrane-bound Gal-3. The amount of Gal-3 was then estimated spectrophotometrically, as mentioned above.

4.6. Cell Adhesion to Gal-3 Immobilized on Cultivation Substrate

For studies on the effect of Gal-3 as a cell adhesion ligand, this protein was adsorbed from a PBS solution overnight at 4 C on the bottom of the wells in xCELLigence 96-well E-plates (E-plate view 96 PET, Cat. No. 300600910, ACEA Biosciences, San Diego, CA, USA). The PBS solutions contained 0, 0.1, 0.33, 1, 3.3, 10, or 33 M Gal-3. For each concentration, six wells were used. One-half of these wells were blocked with 0.5% w/v bovine serum albumin (BSA) in PBS for 1 h at 37 C, and the other half was left unblocked. The wells were then rinsed twice with PBS to remove unbound Gal-3 and BSA molecules and seeded with ADSCs or HUVECs at a density of 10^4 cells/well in 200 L of the cell culture medium. Pure DMEM and pure EBM-2 without any additives were used for the ADSCs and HUVECs, respectively. The cells in the plates were then incubated for 4 h at 37 C in a humidified atmosphere containing 5% CO₂ in the air, and the cell adhesion was monitored every 3 min for 4 h with a sensory xCELLigence system (Agilent Technologies, Waltham, MA, USA). This system enables the label-free, real-time monitoring of cell adhesion and growth based on electrical impedance, which is generated by the cells adhering to the bottoms of the sensory E-plates with interdigitated gold electrodes. During the first day after cell seeding, this impedance is generated mainly by cells initially attached to the well bottom and by the subsequent cell spreading, whereas, in the following days, the impedance is mainly attributed to the increase in the cell number, i.e., to the cell proliferation. The relative changes of the impedance in time are calculated by RTCA software (ACEA Biosciences, San Diego, CA, USA) as the cell index (CI). The cell index is defined as follows: $CI = (\text{impedance at time point } n) - (\text{impedance in the absence of cells}) / (\text{nominal impedance value})$. The normalized cell index value represents the cell index value of a sample normalized to the control sample (ctrl); thus, the cell index values of the samples are calculated proportionally to the cell index value of the control, which is set to 1.

The potential blocking of cell adhesion on substrate-immobilized Gal-3 with LacdiNAC was also investigated. The wells in an xCELLigence E-plate were preadsorbed with Gal-3 at a 1 M concentration, which proved as the optimum concentration for the adhesion of both ADSCs and HUVECs (see below in Figure 5 and Table S1 in the Supplementary Materials). The wells were then blocked with 0.5% w/v BSA in PBS and were preincubated with 100 L of pure DMEM containing LacdiNAC in concentrations of 0, 1, 2, 4, 10, 20, and 40 mM at 37 C. After 1 h, the wells were seeded with ADSCs at a density of 10^4 cells/well in 100 L of pure DMEM containing the respective concentration of LacdiNAC. The cells were incubated at 37 C in a humidified air atmosphere containing 5% CO₂ in the xCELLigence system, where the cell adhesion was monitored every 15 min for 4 h.

4.7. The Role of Integrin Adhesion Receptors in Gal-3-Mediated Cell Adhesion

To study the role of integrin receptors in Gal-3-mediated cell adhesion, the wells in an xCELLigence E-plate were coated with 1 M Gal-3 and blocked with 0.5% w/v BSA as described above. The ADSCs or HUVECs were trypsinized and resuspended in a pure medium to a final concentration of 10^5 cells/mL. The cell suspension was then incubated

in wells of non-tissue culture-treated 24-well polystyrene plates (Corning Inc., Corning, NY, USA, Cat. No. 351147) at 37 °C for 30 min in a rotary shaker (300 rpm) with ethylenediaminetetraacetic acid (EDTA), a potent chelator of calcium, which is indispensable for the adhesion function of integrin receptors. The cells were incubated with EDTA in 0.1, 1, and 10 mM concentrations. To observe the role of the RGD-binding integrins in Gal-3-mediated cell adhesion, the cells were incubated with the GRGDSP peptide (SCP0157, Sigma-Aldrich, St. Louis, MO, USA) at the concentration of 200 M. The GRADSP peptide (SCP0156, Sigma-Aldrich, St. Louis, MO, USA) was used as a negative control. To specify the type of integrin receptor that was involved in Gal-3-mediated cell adhesion, the cells were incubated with antibodies against the integrin subunit V (Millipore, Burlington, MA, USA, MAB2021Z, clone AV1, which binds to the V integrin subunit [67] and blocked the adhesion to various substrates [68]); subunit 3 (Millipore, Burlington, MA, USA, MAB1952Z, clone P1B5, which specifically binds to the 3 subunit and inhibits the adhesion to collagen, fibronectin, or laminin [69]); subunit 1 (Millipore, Burlington, MA, USA, MAB2253, clone 6S6, which binds specifically to the 1 integrin subunit [70] and blocks the adhesion to collagen or fibronectin [71]); subunit 3 (Millipore, Burlington, MA, USA, MAB2023Z, clone B3A, which is specific to the 3 subunit and inhibits cell adhesion [72,73]); against integrin V3 (Millipore, Burlington, MA, USA, MAB1976, clone LM609, which specifically recognizes an epitope on the V3 heterodimer and prevents the adhesion to vitronectin, fibrinogen, or the von Willebrand factor [74]); integrin 51 (Millipore, Burlington, MA, USA, MAB1969, clone JBS5, which recognizes an epitope on the 51 integrin heterodimer [75] and inhibits the adhesion to fibronectin [76]); or integrin 21 (Millipore, Burlington, MA, USA, MAB1998, clone BHA2.1, which specifically recognizes the 21 heterodimer, is unable to bind the integrin receptor-lacking I-domain, and blocks the adhesion to collagen or laminin [77]); or with an V1 integrin inhibitor (MedChemExpress, Monmouth Junction, NJ, USA, HY-100445A). Mouse monoclonal IgG1 (Millipore, Burlington, MA, USA, MABC002) was used as the isotype control. The antibody against the V integrin subunit was used in the 1:25 dilution, and the other antibodies were used in a concentration of 20 g/mL. The V1 integrin inhibitor was used in the concentrations of 0.01, 0.1, and 10 g/mL. The cells were then seeded in wells of xCELLigence E-plates into 100 L of medium (10^4 cells/well), and the initial cell adhesion was measured for 4 h.

To analyze the expression of integrin adhesion receptors on the cell surface, the antibodies against integrin subunits V (MAB2021Z), 3 (MAB1952Z), 1 (MAB2253), 3 (MAB2023Z), and against integrins V3 (MAB1976), 51 (MAB1969), and 21 (MAB1998), were used. All these antibodies were purchased from Millipore, Burlington, MA, USA. The ADSCs and HUVECs were trypsinized and resuspended in PBS containing 0.5% w/v BSA. The cells were incubated with primary antibodies on ice for 20 min. The antibody against the V integrin subunit was used in the dilution 1:50, and the other primary antibodies were used in a concentration of 10 g/mL. Then, the cells were centrifuged and washed in 0.5% w/v BSA and incubated with anti-mouse IgG conjugated with Alexa Fluor 488 (10 g/mL, Cat. No. A11017, Thermo Fisher Scientific, Waltham, MA, USA) for another 15 min on ice. The cells were centrifuged and washed in 0.5% w/v BSA. The presence of integrins on the cell surface was analyzed using a NovoCyte® Flow Cytometer (ACEA Biosciences, Agilent, Santa Clara, CA, USA). At least 30,000 ADSCs and 15,000 HUVECs were analyzed per sample. To determine the background fluorescence signal, the cells were left unstained or incubated with nonspecific mouse monoclonal IgG1 (Millipore, Burlington, MA, USA, MABC002) and, then, with the secondary antibody.

4.8. Comparison of Gal-3 with Other Adhesion Ligands and Cell Morphology

To compare the cell adhesion-promoting ability of Gal-3 with the other extracellular proteins commonly used for material surface coatings, 96-well glass plates (Cellvis, Mountain View, CA, USA, P96-1.5H-N) were preadsorbed with Gal-3 (1 M in PBS), fibronectin (20 g/mL in PBS), or collagen I (50 g/mL in 0.02 M acetic acid) overnight at 4 °C and

then blocked with 0.5% w/v BSA for 1 h at 37 C. The ADSCs or HUVECs were seeded at a density of 7.5×10^3 cells/well in 200 L of the pure medium (DMEM or EBM-2, respectively). After 4 h of incubation at 37 C, the cells were fixed, permeabilized, and stained to visualize vinculin-containing focal adhesions in the cell membrane and filamentous actin (F-actin) cytoskeleton.

For visualizing the vinculin-containing focal adhesions, the cells were fixed and permeabilized as described in Section 2.4. The cells were then stained with an antibody against vinculin, an integrin-associated focal adhesion protein (mouse monoclonal antibody, Cat. No. V9131, Sigma-Aldrich; dilution 1:400) overnight at 4 C. The cells were washed with PBS and were incubated with anti-mouse IgG conjugated with Alexa Fluor 488 (Cat. No. A11017, Thermo Fisher Scientific, Burlington, MA, USA; dilution 1:400) for 1 h at RT in the dark. At the same time, the F-actin cytoskeleton was stained with phalloidin-TRITC (0.1 g/mL in PBS, Sigma-Aldrich, St. Louis, MO, USA), and the cell nuclei were counterstained with Hoechst 33,258 (10 g/mL in PBS) for 1 h at RT (both dyes were added into the secondary antibody solution).

The stained cells were observed through the Olympus epifluorescence microscope IX71 (DP71 digital camera, objective magnification 20, 40, or 100). The morphology characteristics, such as cell area, perimeter, circularity, and solidity (i.e., a parameter inversely correlated with the presence of protrusions on the cell surface), were evaluated from microphotographs using ImageJ software (National Institutes of Health, Bethesda, MD, USA; version FIJI 2.0.0-rc-68/1.52 h).

4.9. Statistics

The data in the graphs are shown as the mean \pm SD from three wells. The data depicted in Figure S9 in the Supplementary Materials (comparisons of the morphology characteristics of the cells) were statistically analyzed using ANOVA on Ranks, Dunn's method, $p < 0.05$. The data in the remaining figures were analyzed with the use of one-way ANOVA, Holm-Sidak test, $p < 0.05$. The data were analyzed with SigmaPlot 14.0 software (Systat Software Inc., San José, CA, USA).

5. Conclusions

We found that Gal-3 is naturally present on the surface of human adipose tissue-derived stem cells (ADSCs) and human umbilical vein endothelial cells (HUVECs). Gal-3 from extracellular environments, e.g., from the culture medium, can associate with these cells in a concentration-dependent manner, and this association can be significantly reduced by LacdiNac, a selective ligand for Gal-3, bound to the canonical binding site on the carbohydrate recognition domain (CRD) of the Gal-3 molecule. Moreover, LacdiNac can detach the newly associated Gal-3 from the cells in a concentration-dependent manner. These results indicate that free extracellular Gal-3 can associate with cells through its CRD domain.

Another important finding of this study is that Gal-3 acts as an extracellular ligand mediating cell adhesion. After the adsorption on tissue culture well plates and blocking the nonspecific binding sites with BSA (which is a nonadhesive for cells), Gal-3 promoted the initial adhesion of ADSCs and HUVECs, and LacdiNac was not able to block this adhesion when incubated with the adsorbed Gal-3 before cell seeding or when added into the cell culture medium. Therefore, cell adhesion to extracellular Gal-3 seems to be mediated by a binding site different from the carbohydrate-binding site on the CRD, which has not been observed so far and should be further investigated. On the cell membrane, the cell adhesion to the substrate-bound Gal-3 is mediated, at least partially, by integrins with the V and 1 chains—namely, with the 51, V3, and V1 integrins, as revealed by integrin-blocking experiments with specific anti-integrin antibodies.

Supplementary Materials: The following are available online at <https://www.mdpi.com/article/10.3390/ijms22105144/s1>: Figure S1: Spreading of ADSCs and HUVECs on wells of E-plates in the xCELLigence system four hours after seeding. Figure S2: The effect of LacdiNAc on the spreading of ADSCs four hours after seeding into untreated wells or wells preadsorbed with 1 M Gal-3 and blocked with BSA. Figure S3: Role of integrins in the spreading of ADSCs and HUVECs on substrate-immobilized Gal-3 (four hours after seeding). Figure S4: Cell surface expression of integrins on ADSCs. Figure S5: Cell surface expression of integrins on HUVECs. Figure S6: Adhesion of ADSCs on wells one hour after seeding in a medium containing various concentrations of the V1 inhibitor. Figure S7: Fluorescence staining of ADSCs and HUVECs adhered to various protein-coated glass surfaces 4 h after cell seeding (objective magnification 40). Figure S8: Fluorescence staining of ADSCs and HUVECs adhered to various protein-coated glass surfaces four hours after cell seeding (objective magnification 100). Figure S9: The morphology characteristics of ADSCs and HUVECs adhered to various protein-coated glass surfaces four hours after seeding.

Author Contributions: Conceptualization, P.B. and L.B.; methodology, A.S., M.V. and P.B.; software, A.S.; validation, K.S., P.B., M.T. and L.B.; formal analysis, A.S. and M.T.; investigation, A.S., M.V. and M.T.; data curation, M.T.; writing—original draft preparation, A.S. and M.T.; writing—review and editing, P.B., K.S., V.K. and L.B.; supervision, V.K., and L.B.; project administration, L.B., V.K.; and funding acquisition, P.B. and V.K. All authors have read and agreed to the published version of the manuscript.

Funding: This work was supported by the Czech Science Foundation (grant No. 18-01163S) and by the Ministry of Education, Sports, and Youth of the Czech Republic (mobility projects LTC18041 (COST Action CA16225) and LTC18038 (COST Action CA16122)).

Institutional Review Board Statement: The study on human ADSCs was conducted according to the guidelines of the Declaration of Helsinki, and approved by the Ethics Committee of “Na Bulovce” Hospital in Prague (11 June 2019).

Informed Consent Statement: Written informed consent has been obtained from the patient(s) to publish this paper.

Data Availability Statement: The data presented in this study are available on request from the corresponding authors.

Acknowledgments: The authors acknowledge the Light Microscopy Core Facility, IMG CAS, Prague, Czech Republic, supported by grants “National Infrastructure for Biological and Medical Imaging” (MEYS—LM2018129), “Modernization of the national infrastructure for biological and medical imaging Czech-BioImaging” (MEYS—CZ.02.1.01/0.0/0.0/18_046/0016045), and formal National Program of Sustainability NPUI LO1220 and LO1419 (RVO: 68378050-KAV-NPUI), for their support with the confocal imaging presented herein.

Conflicts of Interest: The authors declare no conflict of interest.

Abbreviations

ADSC	Adipose tissue-derived stem cells
BSA	Bovine serum albumin
CI	Cell index
CRD	Carbohydrate recognition domain
EBM-2	Endothelial cell basal medium-2
ECM	Extracellular matrix
EGF	Epidermal growth factor
EGM-2	Endothelial cell growth medium-2
EPC	Endothelial progenitor cell
FBS	Fetal bovine serum
FGF-2	Fibroblast growth factor-2
Gal-3	Galectin-3
GRGDSP	Gly-Arg-Gly-Asp-Ser-Pro integrin-blocking RGD-based peptide
HIV	Human immunodeficiency virus

HPMA	N-(2-Hydroxypropyl) methacrylamide
HUVEC	Human umbilical vein endothelial cell
IGF-1	Insulin-like growth factor-1
LacdiNAc	2-Acetamido-2-deoxy--D-galactopyranosyl-(1!4)-2-acetamido-2-deoxy-D-glucopyranose
LacNAc	-D-Galactopyranosyl-(1!4)-2-acetamido-2-deoxy-D-glucopyranose
PBS	Phosphate-buffered saline
RGD	Arg-Gly-Asp binding motif
RT	Room temperature

References

- Hughes, R.C. Galectins as modulators of cell adhesion. *Biochimie* **2001**, *83*, 667–676. [[CrossRef](#)]
- Cummings, R.D.; Liu, F.T. Galectins. In *Essentials of Glycobiology*, 2nd ed.; Varki, A., Cummings, R.D., Esko, J.D., Freeze, H.H., Stanley, P., Bertozzi, C.R., Hart, G.W., Etzler, M.E., Eds.; Cold Spring Harbor: New York, NY, USA, 2009; ISBN 9780879697709.
- Xin, M.; Dong, X.W.; Guo, X.L. Role of the interaction between galectin-3 and cell adhesion molecules in cancer metastasis. *Biomed. Pharmacother.* **2015**, *69*, 179–185. [[CrossRef](#)]
- Barman, S.A.; Li, X.Y.; Haigh, S.; Kondrikov, D.; Mahboubi, K.; Bordan, Z.; Stepp, D.W.; Zhou, J.L.; Wang, Y.S.; Weintraub, D.S.; et al. Galectin-3 is expressed in vascular smooth muscle cells and promotes pulmonary hypertension through changes in proliferation, apoptosis, and fibrosis. *Am. J. Physiol.-Lung Cell. Mol. Physiol.* **2019**, *316*, L784–L797. [[CrossRef](#)]
- Brinchmann, M.F.; Patel, D.M.; Iversen, M.H. The role of galectins as modulators of metabolism and inflammation. *Mediat. Inflamm.* **2018**, *2018*, 9186940. [[CrossRef](#)]
- Zick, Y.; Eisenstein, M.; Goren, R.A.; Hadari, Y.R.; Levy, Y.; Ronen, D. Role of galectin-8 as a modulator of cell adhesion and cell growth. *Glycoconj. J.* **2002**, *19*, 517–526. [[CrossRef](#)]
- Bojarová, P.; Křen, V. Sugared biomaterial binding lectins: Achievements and perspectives. *Biomater. Sci.* **2016**, *4*, 1142–1160. [[CrossRef](#)] [[PubMed](#)]
- Johannes, L.; Jacob, R.; Leffler, H. Galectins at a glance. *J. Cell Sci.* **2018**, *131*, jcs208884. [[CrossRef](#)]
- Liu, F.T.; Wan, L. Galectin-3 and inflammation. *Glycobiol. Insights* **2016**, *6*, 1–9. [[CrossRef](#)]
- Fashanu, O.E.; Heckbert, S.R.; Aguilar, D.; Jensen, P.N.; Ballantyne, C.M.; Basu, S.; Hoogeveen, R.C.; deFilippi, C.; Cushman, M.; Folsom, A.R. Galectin-3 and venous thromboembolism incidence: The atherosclerosis risk in communities (ARIC) study. *Res. Pract. Thromb. Haemost.* **2017**, *1*, 223–230. [[CrossRef](#)]
- Bojarová, P.; Tavares, M.R.; Laaf, D.; Bumba, L.; Petrásková, L.; Konefal, R.; Bláhová, M.; Pelantová, H.; Elling, L.; Etrych, T.; et al. Biocompatible glyconanomaterials based on HPMA-copolymer for specific targeting of galectin-3. *J. Nanobiotechnol.* **2018**, *16*, 73. [[CrossRef](#)] [[PubMed](#)]
- Laaf, D.; Bojarová, P.; Pelantová, H.; Křen, V.; Elling, L. Tailored multivalent neo-glycoproteins: Synthesis, evaluation, and application of a library of galectin-3-binding glycan ligands. *Bioconjug. Chem.* **2017**, *28*, 2832–2840. [[CrossRef](#)] [[PubMed](#)]
- Laaf, D.; Bojarová, P.; Elling, L.; Křen, V. Galectin-carbohydrate interactions in biomedicine and biotechnology. *Trends Biotechnol.* **2019**, *37*, 402–415. [[CrossRef](#)]
- Panjwani, N. Role of galectins in re-epithelialization of wounds. *Ann. Transl. Med.* **2014**, *2*, 89. [[CrossRef](#)]
- Iacobini, C.; Menini, S.; Ricci, C.; Scipioni, A.; Sansoni, V.; Cordone, S.; Taurino, M.; Serino, M.; Marano, G.; Federici, M.; et al. Accelerated lipid-induced atherogenesis in galectin-3-deficient mice: Role of lipoxidation via receptor-mediated mechanisms. *Arterioscler. Thromb. Vasc. Biol.* **2009**, *29*, 831–836. [[CrossRef](#)]
- Nangia-Makker, P.; Honjo, Y.; Sarvis, R.; Akahani, S.; Hogan, V.; Pienta, K.J.; Raz, A. Galectin-3 induces endothelial cell morphogenesis and angiogenesis. *Am. J. Pathol.* **2000**, *156*, 899–909. [[CrossRef](#)]
- Laaf, D.; Bojarová, P.; Mikulová, B.; Pelantová, H.; Křen, V.; Elling, L. Two-step enzymatic synthesis of β -D-N-acetylgalactosamine-(1!4)-D-N-acetylglucosamine (LacdiNAc) chitooligomers for deciphering galectin binding behavior. *Adv. Synth. Catal.* **2017**, *359*, 2101–2108. [[CrossRef](#)]
- Tavares, M.R.; Bláhová, M.; Sedláková, L.; Elling, L.; Pelantová, H.; Konefal, R.; Etrych, T.; Křen, V.; Bojarová, P.; Chytil, P. High-affinity N-(2-hydroxypropyl) methacrylamide copolymers with tailored N-acetyllactosamine presentation discriminate between galectins. *Biomacromolecules* **2020**, *21*, 641–652. [[CrossRef](#)]
- Bratteby, K.; Torkelsson, E.; L'Estrade, E.T.; Peterson, K.; Shalgunov, V.; Xiong, M.F.; Leffler, H.; Zetterberg, F.R.; Olsson, T.G.; Gillings, N.; et al. In Vivo veritas: F-18-radiolabeled glycomimetics allow insights into the pharmacological fate of galectin-3 inhibitors. *J. Med. Chem.* **2020**, *63*, 747–755. [[CrossRef](#)]
- Vašíček, T.; Spiwok, V.; Červený, J.; Petrásková, L.; Bumba, L.; Vrbata, D.; Pelantová, H.; Křen, V.; Bojarová, P. Regioselective 3-O-substitution of unprotected thiodigalactosides: Direct route to galectin inhibitors. *Chem. Eur. J.* **2020**, *26*, 9620–9631. [[CrossRef](#)] [[PubMed](#)]
- Bumba, L.; Laaf, D.; Spiwok, V.; Elling, L.; Křen, V.; Bojarová, P. Poly-N-acetyllactosamine neo-glycoproteins as nanomolar ligands of human galectin-3: Binding kinetics and modeling. *Int. J. Mol. Sci.* **2018**, *19*, 372. [[CrossRef](#)]

22. Furuhata, S.; Ando, K.; Oki, M.; Aoki, K.; Ohnishi, S.; Aoyagi, K.; Sasaki, H.; Sakamoto, H.; Yoshida, T.; Ohnami, S. Gene expression profiles of endothelial progenitor cells by oligonucleotide microarray analysis. *Mol. Cell. Biochem.* **2007**, *298*, 125–138. [[CrossRef](#)]
23. Chen, W.T.; Zhang, F.; Zhao, X.Q.; Yu, B.; Wang, B.W. Galectin-3 and TRIM16 coregulate osteogenic differentiation of human bone marrow-derived mesenchymal stem cells at least partly via enhancing autophagy. *Bone* **2020**, *131*. [[CrossRef](#)] [[PubMed](#)]
24. Li, Y.J.; Xu, X.; Wang, L.H.; Liu, G.J.; Li, Y.Q.; Wu, X.B.; Jing, Y.G.; Li, H.Y.; Wang, G.H. Senescent mesenchymal stem cells promote colorectal cancer cells growth via galectin-3 expression. *Cell. Biosci.* **2015**, *5*, 21. [[CrossRef](#)] [[PubMed](#)]
25. Šimonová, A.; Kupper, C.E.; Böcker, S.; Müller, A.; Hofbauerová, K.; Pelantová, H.; Elling, L.; Křen, V.; Bojarová, P. Chemo-enzymatic synthesis of LacdiNAC dimers of varying length as novel galectin ligands. *J. Mol. Catal. B Enzym.* **2014**, *101*, 47–55. [[CrossRef](#)]
26. Hutchings, H.; Ortega, N.; Plouet, J. Extracellular matrix-bound vascular endothelial growth factor promotes endothelial cell adhesion, migration, and survival through integrin ligation. *FASEB J.* **2003**, *17*, 1520–1522. [[CrossRef](#)]
27. Lee, M.H.; Brass, D.A.; Morris, R.; Composto, R.J.; Ducheyne, P. The effect of non-specific interactions on cellular adhesion using model surfaces. *Biomaterials* **2005**, *26*, 1721–1730. [[CrossRef](#)] [[PubMed](#)]
28. da Silva, R.G.; Tavora, B.; Robinson, S.D.; Reynolds, L.E.; Szekeres, C.; Lamar, J.; Batista, S.; Kostourou, V.; Germain, M.A.; Reynolds, A.R.; et al. Endothelial alpha3beta1-integrin represses pathological angiogenesis and sustains endothelial-VEGF. *Am. J. Pathol.* **2010**, *177*, 1534–1548. [[CrossRef](#)]
29. Hynes, R.O. Integrins: Bidirectional, allosteric signaling machines. *Cell* **2002**, *110*, 673–687. [[CrossRef](#)]
30. Goessler, U.R.; Bugert, P.; Bieback, K.; Stern-Straeter, J.; Bran, G.; Hormann, K.; Riedel, F. Integrin expression in stem cells from bone marrow and adipose tissue during chondrogenic differentiation. *Int. J. Mol. Med.* **2008**, *21*, 271–279. [[CrossRef](#)] [[PubMed](#)]
31. Reed, N.I.; Jo, H.; Chen, C.; Tsujino, K.; Arnold, T.D.; DeGrado, W.F.; Sheppard, D. The v1 integrin plays a critical in vivo role in tissue fibrosis. *Sci. Transl. Med.* **2015**, *7*, 288ra79. [[CrossRef](#)]
32. Wilkinson, A.L.; Barrett, J.W.; Slack, R.J. Pharmacological characterisation of a tool v1 integrin small molecule RGD-mimetic inhibitor. *Eur. J. Pharmacol.* **2019**, *842*, 239–247. [[CrossRef](#)]
33. Ahrens, I.; Domeij, H.; Topcic, D.; Haviv, I.; Merivirta, R.M.; Agrotis, A.; Leitner, E.; Jowett, J.B.; Bode, C.; Lappas, M.; et al. Successful in vitro expansion and differentiation of cord blood derived CD34+ cells into early endothelial progenitor cells reveals highly differential gene expression. *PLoS ONE* **2011**, *6*, e23210. [[CrossRef](#)]
34. Fukumori, T.; Takenaka, Y.; Yoshii, T.; Kim, H.R.C.; Hogan, V.; Inohara, H.; Kagawa, S.; Raz, A. CD29 and CD7 mediate galectin-3-induced type II T-cell apoptosis. *Cancer Res.* **2003**, *63*, 8302–8311. [[PubMed](#)]
35. Suzuki, O.; Abe, M. Cell surface N-glycosylation and sialylation regulate galectin-3-induced apoptosis in human diffuse large B cell lymphoma. *Oncol. Rep.* **2008**, *19*, 743–748. [[CrossRef](#)]
36. Tadokoro, T.; Ikekita, M.; Toda, T.; Ito, H.; Sato, T.; Nakatani, R.; Hamaguchi, Y.; Furukawa, K. Involvement of galectin-3 with vascular cell adhesion molecule-1 in growth regulation of mouse BALB/3T3 cells. *J. Biol. Chem.* **2009**, *284*, 35556–35563. [[CrossRef](#)]
37. Zhuo, Y.; Chammas, R.; Bellis, S.L. Sialylation of 1 Integrins blocks cell adhesion to galectin-3 and protects cells against galectin-3-induced apoptosis. *J. Biol. Chem.* **2008**, *283*, 22177–22185. [[CrossRef](#)] [[PubMed](#)]
38. Lepur, A.; Carlsson, M.C.; Novak, R.; Dumic, J.; Nilsson, U.J.; Leffler, H. Galectin-3 endocytosis by carbohydrate independent and dependent pathways in different macrophage like cell types. *Biochim. Biophys. Acta Gen. Subj.* **2012**, *1820*, 804–818. [[CrossRef](#)]
39. Gao, X.G.; Liu, D.; Fan, Y.Y.; Li, X.Z.; Xue, H.T.; Ma, Y.Y.; Zhou, Y.F.; Tai, G.H. The two endocytic pathways mediated by the carbohydrate recognition domain and regulated by the collagen-like domain of galectin-3 in vascular endothelial cells. *PLoS ONE* **2012**, *7*, e52430. [[CrossRef](#)]
40. Gao, X.G.; Zhi, Y.; Sun, L.; Peng, X.X.; Zhang, T.; Xue, H.T.; Tai, G.H.; Zhou, Y.F. The inhibitory effects of a rhamnogalacturonan I (RG-I) domain from ginseng pectin on galectin-3 and its structure-activity relationship. *J. Biol. Chem.* **2013**, *288*, 33953–33965. [[CrossRef](#)]
41. John, C.M.; Leffler, H.; Kahl-Knutsson, B.; Svensson, I.; Jarvis, G.A. Truncated galectin-3 inhibits tumor growth and metastasis in orthotopic nude mouse model of human breast cancer. *Clin. Cancer Res.* **2003**, *9*, 2374–2383. [[PubMed](#)]
42. Filipová, M.; Bojarová, P.; Tavares, M.R.; Bumba, L.; Elling, L.; Chytil, P.; Gunár, K.; Křen, V.; Etrych, T.; Janoušková, O. Glycopolymers for efficient inhibition of galectin-3: In Vitro proof of efficacy using suppression of T lymphocyte apoptosis and tumor cell migration. *Biomacromolecules* **2020**, *21*, 3122–3133. [[CrossRef](#)]
43. MacKinnon, A.C.; Gibbons, M.A.; Farnworth, S.L.; Leffler, H.; Nilsson, U.J.; Delaine, T.; Simpson, A.J.; Forbes, S.J.; Hirani, N.; Gauldie, J.; et al. Regulation of transforming growth factor-1-driven lung fibrosis by galectin-3. *J. Respir. Crit. Care Med.* **2012**, *185*, 537–546. [[CrossRef](#)]
44. Ludwig, A.K.; Michalak, M.; Xiao, Q.; Gilles, U.; Medrano, F.J.; Ma, H.; FitzGerald, F.G.; Hasley, W.D.; Melendez-Davila, A.; Liu, M.; et al. Design-functionality relationships for adhesion/growth-regulatory galectins. *Proc. Natl. Acad. Sci. USA* **2019**, *116*, 2837–2842. [[CrossRef](#)] [[PubMed](#)]
45. Thijssen, V.L.; Hulsmans, S.; Griffioen, A.W. The galectin profile of the endothelium—Altered expression and localization in activated and tumor endothelial cells. *Am. J. Pathol.* **2008**, *172*, 545–553. [[CrossRef](#)]
46. Gieseke, F.; Bohringer, J.; Bussolari, R.; Dominici, M.; Handgretinger, R.; Muller, I. Human multipotent mesenchymal stromal cells use galectin-1 to inhibit immune effector cells. *Blood* **2010**, *116*, 3770–3779. [[CrossRef](#)]

47. Gonen, T.; Donaldson, P.; Kistler, J. Galectin-3 is associated with the plasma membrane of lens fiber cells. *Investig. Ophthalm. Vis. Sci.* **2000**, *41*, 199–203. [[PubMed](#)]
48. Miller, M.C.; Ippel, H.; Suylen, D.; Klyosov, A.A.; Traber, P.G.; Hackeng, T.; Mayo, K.H. Binding of polysaccharides to human galectin-3 at a noncanonical site in its carbohydrate recognition domain. *Glycobiology* **2016**, *26*, 88–99. [[CrossRef](#)]
49. Stegmayr, J.; Lepur, A.; Kahl-Knutson, B.; Aguilar-Moncayo, M.; Klyosov, A.A.; Field, R.A.; Oredsson, S.; Nilsson, U.J.; Leffler, H. Low or no inhibitory potency of the canonical galectin carbohydrate-binding site by pectins and galactomannans. *J. Biol. Chem.* **2016**, *291*, 13318–13334. [[CrossRef](#)]
50. Zhang, Z.Y.; Miller, M.C.; Xu, X.J.; Song, C.C.; Zhang, F.; Zheng, Y.; Zhou, Y.F.; Tai, G.H.; Mayo, K.H. NMR-based insight into galectin-3 binding to endothelial cell adhesion molecule CD146: Evidence for noncanonical interactions with the lectin's CRD beta-sandwich F-face. *Glycobiology* **2019**, *29*, 608–618. [[CrossRef](#)]
51. LeMarer, N.; Hughes, R.C. Effects of the carbohydrate-binding protein galectin-3 on the invasiveness of human breast carcinoma cells. *Cell. Physiol.* **1996**, *168*, 51–58. [[CrossRef](#)]
52. Birdsall, B.; Feeney, J.; Burdett, I.D.J.; Bawumia, S.; Barboni, E.A.M.; Hughes, R.C. NMR solution studies of hamster galectin-3 and electron microscopic visualization of surface-adsorbed complexes: Evidence for interactions between the N- and C-terminal domains. *Biochemistry* **2001**, *40*, 4859–4866. [[CrossRef](#)]
53. Benitez, P.L.; Mascharak, S.; Proctor, A.C.; Heilshorn, S.C. Use of protein-engineered fabrics to identify design rules for integrin ligand clustering in biomaterials. *Integr. Biol.* **2016**, *8*, 50–61. [[CrossRef](#)]
54. Morandi, E.M.; Verstappen, R.; Zwierzina, M.E.; Geley, S.; Pierer, G.; Ploner, C. ITGAV and ITGA5 diversely regulate proliferation and adipogenic differentiation of human adipose derived stem cells. *Sci. Rep.* **2016**, *6*, 28889. [[CrossRef](#)]
55. Fang, J.; Wei, Y.D.; Lv, C.R.; Peng, S.; Zhao, S.T.; Hua, J.L. CD61 promotes the differentiation of canine ADMSCs into PGC-like cells through modulation of TGF-beta signaling. *Sci. Rep.* **2017**, *7*, 43851. [[CrossRef](#)] [[PubMed](#)]
56. Rico, P.; Rodrigo-Navarro, A.; de la Pena, M.; Moulisova, V.; Costell, M.; Salmeron-Sanchez, M. Simultaneous boron ion-channel/growth factor receptor activation for enhanced vascularization. *Adv. Biosyst.* **2019**, *3*, e1800220. [[CrossRef](#)]
57. Foubert, P.; Varner, J.A. Integrins in tumor angiogenesis and lymphangiogenesis. *Methods Mol. Biol.* **2011**, *757*, 471–486. [[CrossRef](#)]
58. Suzuki, O.; Abe, M.; Hashimoto, Y. Sialylation and glycosylation modulate cell adhesion and invasion to extracellular matrix in human malignant lymphoma: Dependency on integrin and the Rho GTPase family. *Int. J. Oncol.* **2015**, *47*, 2091–2099. [[CrossRef](#)] [[PubMed](#)]
59. Horton, M.A. The v3 integrin “vitronectin receptor”. *Int. J. Biochem. Cell B* **1997**, *29*, 721–725. [[CrossRef](#)]
60. Saravanan, C.; Liu, F.T.; Gipson, I.K.; Panjwani, N. Galectin-3 promotes lamellipodia formation in epithelial cells by interacting with complex N-glycans on alpha3beta1 integrin. *J. Cell Sci.* **2009**, *122*, 3684–3693. [[CrossRef](#)] [[PubMed](#)]
61. Sivkova, R.; Taborska, J.; Reparaz, A.; de Los Santos Pereira, A.; Kotelnikov, I.; Proks, V.; Kucka, J.; Svoboda, J.; Riedel, T.; Pop-Georgievski, O. Surface design of antifouling vascular constructs bearing biofunctional peptides for tissue regeneration applications. *Int. J. Mol. Sci.* **2020**, *21*, 6800. [[CrossRef](#)]
62. Tang, D.; Chen, S.; Hou, D.; Gao, J.; Jiang, L.; Shi, J.; Liang, Q.; Kong, D.; Wang, S. Regulation of macrophage polarization and promotion of endothelialization by NO generating and PEG-YIGSR modified vascular graft. *Mater. Sci. Eng. C Mater. Biol. Appl.* **2018**, *84*, 1–11. [[CrossRef](#)]
63. Devalliere, J.; Chen, Y.; Dooley, K.; Yarmush, M.L.; Uygun, B.E. Improving functional re-endothelialization of acellular liver scaffold using REDV cell-binding domain. *Acta Biomater.* **2018**, *78*, 151–164. [[CrossRef](#)]
64. Estes, B.T.; Diekman, B.O.; Gimble, J.M.; Guilak, F. Isolation of adipose-derived stem cells and their induction to a chondrogenic phenotype. *Nat. Protoc.* **2010**, *5*, 1294–1311. [[CrossRef](#)] [[PubMed](#)]
65. Bačáková, L.; Zárubová, J.; Trávníčková, M.; Musířková, J.; Pajorová, J.; Slepíčka, P.; Kasářková, N.S.; Švorčík, V.; Kolská, Z.; Motarjemi, H.; et al. Stem cells: Their source, potency and use in regenerative therapies with focus on adipose-derived stem cells—A review. *Biotechnol. Adv.* **2018**, *36*, 1111–1126. [[CrossRef](#)] [[PubMed](#)]
66. Trávníčková, M.; Pajorová, J.; Zárubová, J.; Kročilová, N.; Molitor, M.; Bačáková, L. The influence of negative pressure and of the harvesting site on the characteristics of human adipose tissue-derived stromal cells from lipoaspirates. *Stem Cells Int.* **2020**, *2020*, 1016231. [[CrossRef](#)] [[PubMed](#)]
67. Ratnikov, B.I.; Rozanov, D.V.; Postnova, T.I.; Baci, P.G.; Zhang, H.; DiScipio, R.G.; Chestukhina, G.G.; Smith, J.W.; Deryugina, E.I.; Strongin, A.Y. An alternative processing of integrin alpha(v) subunit in tumor cells by membrane type-1 matrix metalloproteinase. *J. Biol. Chem.* **2002**, *277*, 7377–7385. [[CrossRef](#)]
68. Benoit, Y.D.; Lussier, C.; Ducharme, P.A.; Sivret, S.; Schnapp, L.M.; Basora, N.; Beaulieu, J.F. Integrin alpha 8 beta 1 regulates adhesion, migration and proliferation of human intestinal crypt cells via a predominant RhoA/ROCK-dependent mechanism. *Biol. Cell* **2009**, *101*, 695–708. [[CrossRef](#)] [[PubMed](#)]
69. Wayner, E.A.; Carter, W.G. Identification of multiple cell-adhesion receptors for collagen and fibronectin in human fibrosarcoma cells possessing unique alpha-subunits and common beta-subunits. *J. Cell Biol.* **1987**, *105*, 1873–1884. [[CrossRef](#)]
70. Wilkins, J.A.; Li, A.L.; Ni, H.Y.; Stupack, D.G.; Shen, C.X. Control of beta(1) integrin function—Localization of stimulatory epitopes. *J. Biol. Chem.* **1996**, *271*, 3046–3051. [[CrossRef](#)]
71. Nguyen, T.T.B.; Ward, J.P.T.; Hirst, S.J. Beta 1-integrins mediate enhancement of airway smooth muscle proliferation by collagen and fibronectin. *Am. J. Respir. Crit. Care* **2005**, *171*, 217–223. [[CrossRef](#)]

72. Maeshima, Y.; Yerramalla, U.L.; Dhanabal, M.; Holthaus, K.A.; Barbashov, S.; Kharbanda, S.; Reimer, C.; Manfredi, M.; Dickerson, W.M.; Kalluri, R. Extracellular matrix-derived peptide binds to alpha(v)beta(3) integrin and inhibits angiogenesis. *J. Biol. Chem.* **2001**, *276*, 31959–31968. [[CrossRef](#)]
73. Irigoyen, M.; Pajares, M.J.; Agorreta, J.; Ponz-Sarvisé, M.; Salvo, E.; Lozano, M.D.; Pio, R.; Gil-Bazo, I.; Rouzaut, A. TGFBI expression is associated with a better response to chemotherapy in NSCLC. *Mol. Cancer* **2010**, *9*, 130. [[CrossRef](#)]
74. Cheresh, D.A.; Spiro, R.C. Biosynthetic and functional-properties of an Arg-Gly-Asp-directed receptor involved in human-melanoma cell attachment to vitronectin, fibrinogen, and vonwillebrand-factor. *J. Biol. Chem.* **1987**, *262*, 17703–17711. [[CrossRef](#)] [[PubMed](#)]
75. Mould, A.P.; Garratt, A.N.; Puzon-McLaughlin, W.; Takada, Y.; Humphries, M.J. Regulation of integrin function: Evidence that bivalent-cation-induced conformational changes lead to the unmasking of ligand-binding sites within integrin alpha 5 beta 1. *Biochem. J.* **1998**, *331*, 821–828. [[CrossRef](#)] [[PubMed](#)]
76. Imoto, E.; Kakuta, S.; Hori, M.; Yagami, K.; Nagumo, M. Adhesion of a chondrocytic cell line (USAC) to fibronectin and its regulation by proteoglycan. *J. Oral Pathol. Med.* **2002**, *31*, 35–44. [[CrossRef](#)] [[PubMed](#)]
77. Hangan, D.; Uniyal, S.; Morris, V.L.; MacDonald, I.C.; vonBallestrem, C.; Chau, T.; Schmidt, E.E.; Chambers, A.F.; Groom, A.C.; Chan, B.M.C. Integrin VLA-2 (alpha(2)beta(1)) function in postextravasation movement of human rhabdomyosarcoma RD cells in the liver. *Cancer Res.* **1996**, *56*, 3142–3149. [[PubMed](#)]


Biomedical Materials



PAPER

Differentiation of adipose tissue-derived stem cells towards vascular smooth muscle cells on modified poly(L-lactide) foils

RECEIVED
9 January 2020REVISED
4 August 2020ACCEPTED FOR PUBLICATION
14 August 2020PUBLISHED
17 February 2021

Martina Travnickova^{1,2} , Nikola Slepickova Kasalkova³, Antonin Sedlar¹, Martin Molitor⁴, Jana Musilkova¹, Petr Slepicka³, Vaclav Svorcik³ and Lucie Bacakova¹

¹ Department of Biomaterials and Tissue Engineering, Institute of Physiology of the Czech Academy of Sciences, Videnska 1083, 142 20, Prague 4, Czech Republic

² Second Faculty of Medicine, Charles University, V Uvalu 84, 150 06, Prague 5, Czech Republic

³ Department of Solid State Engineering, University of Chemistry and Technology, Technicka 5, 166 28, Prague 6, Czech Republic

⁴ Department of Plastic Surgery, Na Bulovce Hospital and First Faculty of Medicine, Charles University, Budinova 67/2, 180 81, Prague 8, Czech Republic

E-mail: martina.travnickova@fgu.cas.cz

Keywords: Poly(L-lactic acid) (PLLA), plasma treatment, dextran, polyethylene glycol (PEG), adipose tissue-derived stem cells (ADSCs), differentiation, vascular smooth muscle cells (VSMCs)

Supplementary material for this article is available [online](#)

Abstract

The aim of our research was to study the behaviour of adipose tissue-derived stem cells (ADSCs) and vascular smooth muscle cells (VSMCs) on variously modified poly(L-lactide) (PLLA) foils, namely on pristine PLLA, plasma-treated PLLA, PLLA grafted with polyethylene glycol (PEG), PLLA grafted with dextran (Dex), and the tissue culture polystyrene (PS) control. On these materials, the ADSCs were biochemically differentiated towards VSMCs by a medium supplemented with TGF β 1, BMP4 and ascorbic acid (i.e. differentiation medium). ADSCs cultured in a non-differentiation medium were used as a negative control. Mature VSMCs cultured in both types of medium were used as a positive control. The impact of the variously modified PLLA foils and/or differences in the composition of the medium were studied with reference to cell adhesion, growth and differentiation. We observed similar adhesion and growth of ADSCs on all PLLA samples when they were cultured in the non-differentiation medium. The differentiation medium supported the expression of specific early, mid-term and/or late markers of differentiation (i.e. type I collagen, α SMA, calponin, smoothelin, and smooth muscle myosin heavy chain) in ADSCs on all tested samples. Moreover, ADSCs cultured in the differentiation medium revealed significant differences in cell growth among the samples that were similar to the differences observed in the cultures of VSMCs. The round morphology of the VSMCs indicated worse adhesion to pristine PLLA, and this sample was also characterized by the lowest cell proliferation. Culturing VSMCs in the differentiation medium inhibited their metabolic activity and reduced the cell numbers. Both cell types formed the most stable monolayer on plasma-treated PLLA and on the PS control. The behaviour of ADSCs and VSMCs on the tested PLLA foils differed according to the specific cell type and culture conditions. The suitable biocompatibility of both cell types on the tested PLLA foils seems to be favourable for vascular tissue engineering purposes.

1. Introduction

Cardiovascular diseases have a high incidence in many countries, and are responsible for almost one third of all deaths worldwide. Atherosclerosis is a very frequent degenerative disorder of the blood vessels, characterized by the impaired

function of endothelial cells (ECs) leading to abundant storage of low-density lipoprotein particles. Non-invasive treatment of atherosclerosis usually involves adjusting nutrition habits and medication. However, when there is excessive vessel degeneration, surgical vascular replacement often becomes necessary.

Current vascular replacement options include biological and synthetic vascular grafts. Biological grafts are mainly represented by autologous grafts. Allografts and xenografts are less routinely used. Autologous grafts can be harvested from arteries (e.g. from *arteria thoracica interna* or *arteria radialis*) or from superficial veins (e.g. *vena saphena*). These grafts are widely used. They are the ideal choice for small-diameter vascular replacements (i.e. <5 mm), which are associated with a high risk of thrombosis (for a review, see Carrabba *et al* 2018). Although autologous grafts provide ideal properties, the opportunities for harvesting a vessel graft in good condition and of sufficient size are very limited, and the required surgery can increase patient morbidity. Unmodified allografts or xenografts can evoke an immunogenic response in the host organism. However, procedures for decellularizing these grafts seem to be an interesting approach to the use of a low-immunogenicity scaffold composed of natural extracellular matrix (ECM), which can be seeded with the patient's autologous cells. Nevertheless, the unavailability of suitable biological grafts continues to intensify the demand for novel synthetic vascular grafts.

For decades, synthetic scaffolds for clinically-used vascular grafts have been made of non-degradable polyethylene terephthalate or polytetrafluorethylene (for a review, see Chlupac *et al* 2009). These materials are non-toxic *per se*, but they are hydrophobic and bio-inert, with a limited bioactive capacity to somehow remodel or support the cell–material interaction. New biodegradable natural or synthetic compounds have therefore been studied with a view to improving the properties of the graft (i.e. by improving the mechanical properties of the graft, by supporting cell attachment and growth, by finding ways to avoid activating the blood coagulation cascade and thrombosis formation, or by improving the gradual controlled bio-degradation of the biomaterial) (Chlupac *et al* 2009). The list of promising compounds includes various forms of polyurethanes, polycaprolactone, poly(L-lactide) (PLLA), poly(glycolic acid), polyvinyl alcohol, alginate, chitosan, and some copolymers of these compounds, such as poly(DL-lactic acid-co-glycolic acid) (PLGA) (for a review, see Pashneh-Tala *et al* 2016, Hielscher *et al* 2018). These polymers can be used in various ways to create mono-, bi- or tri-layer scaffolds (for a review, see Goins *et al* 2019). In addition, the biomaterial itself can be improved with the use of various natural components and coatings (e.g. collagen, fibrin, fibronectin, laminin or dextran (Dex) coating), which can mimic the naturally present ECM and other molecules, and can support the adhesion, growth and differentiation of vascular cells (Goins *et al* 2019, Pashneh-Tala *et al* 2016, Filová *et al* 2014). Moreover, various growth factors (e.g. VEGF, FGF2, PDGF), biologically active

molecules (e.g. heparin, Dex, sirolimus, simvastatin), and various amino acid sequences, which serve as ligands for cell adhesion receptors, e.g. RGD, can be incorporated into the coatings in order to ameliorate the bioactivity of the grafts (for a review, see Strobel *et al* 2018). Last but not least, scaffold-free approaches suggest the use of cell-sheets only (i.e. confluent layers of cells to create appropriate tissue-engineered vascular grafts (TEVGs) (Carrabba and Madeddu 2018).

PLLA is a semi-crystalline polyester with a wide range of biomedical applications thanks to its biocompatibility, its relatively slow biodegradability and high mechanical strength (for a review, see Gritsch *et al* 2019). PLLA can be fabricated into scaffolds of various shapes and with various properties (e.g. fibres, membranes, films, foils). However, the material is relatively highly hydrophobic. This property can restrict the biomedical applications of PLLA, due to the impaired cell–material interactions (Gritsch *et al* 2019).

Plasma treatment is generally used to modify the chemical and physical properties of polymers. Various gases, e.g. air, oxygen (O₂), argon (Ar), nitrogen (N₂), NH₃, C₃F₈, can be applied as plasma sources to create reactive functional groups on an originally inert biomaterial. These functional groups can enhance the attachment of other biomolecules, such as peptide molecules or natural polymers. In addition, these changes reduce the water contact angle (CA), i.e. they increase the wettability of the material, which is known to affect the subsequent cell adhesion, morphology, viability or growth (Wan *et al* 2003, Nakagawa *et al* 2006).

Polyethylene glycol (PEG) is a hydrophilic polymer without or with low levels of toxicity and immunogenicity, which is advantageous for biomedical applications. Depending on its molecular weight, it can be used for surface modifications, as a component of particles for transporting various molecules, or as a hydrogel compound that can be further modified to achieve better bioactive properties (Zhu 2010). PEG can serve as an inhibitor of protein adsorption (Alcantar *et al* 2000) and cell attachment, which gives anti-adhesive and anti-bacterial characteristics to this material (Mas-Moruno *et al* 2019). PEG is also suitable for vascular engineering, due to its non-thrombogenic and highly elastic properties (Hahn *et al* 2007).

Dex is a hydrophilic polysaccharide that can be present in a wide range of molecular weights. It provides suitable biodegradable and biocompatible properties in biomedical applications, with multiple positive effects specifically in vascular applications, similarly to PEG. It has been reported that Dex provides an anti-thrombogenic effect by inhibiting the activation of blood coagulation (Alexandre *et al* 2015) and, similarly to PEG, it has also been used as a

plasma expander that lowers the viscosity of the blood (Chatpun and Cabrales 2011).

Current vascular tissue engineering aims to create cellular TEVGs characterized by zero or at least low immunogenicity, by non-thrombogenicity or anti-thrombogenicity, and also by appropriate biodegradable and mechanical properties. Patient autologous cells are believed to potentially ameliorate the acceptance of vascular grafts. However, autologous mature cells, i.e. ECs and vascular smooth muscle cells (VSMCs), can be used for graft seeding only in limited quantities. New sources of immature pluripotent or multipotent stem cells have therefore been investigated.

VSMCs are the main component of *tunica media* (i.e. the middle layer of arteries), and they are responsible for the contractile function of blood vessels. The ability to contract is very important for maintaining appropriate blood pressure levels (Chang *et al* 2014).

Adipose tissue-derived stem cells (ADSCs) are adult multipotent stem cells of mesenchymal origin. Currently, adult mesenchymal stem cells seem to be one of the most promising sources of stem cells for vascular tissue engineering (Zhang *et al* 2017, Hielscher *et al* 2018). The main advantages of ADSCs are their relatively easy accessibility, the availability of sufficient quantities in almost all patients, a high proliferation rate, a low tendency to senescence and, last but not least, the potential to differentiate towards various cell types (for a review, see Travníková and Bačáková 2018, Bacakova *et al* 2018a). ADSCs have also been reported to differentiate towards VSMCs, depending on the composition of the medium, the properties of the biomaterial, and the dynamic culture conditions (Zhang *et al* 2017, Bacakova *et al* 2018b).

The influence of individual polymers and ECM components has been widely studied. However, our work presented here deals with more complex studies of combinations of modified polymers and composite media. Little is known about the interaction of ADSCs and VSMCs with PLLA modified by plasma treatment and subsequent grafting with PEG or Dex, i.e. molecules with positive effects in vascular applications. In particular, the influence of modifications to PLLA on the differentiation of ADSCs towards VSMCs, and the influence of modifications to PLLA together with a differentiation medium on its potential use in TEVG fabrication seems to be an uninvestigated topic.

Our previous study suggested favourable biocompatibility of plasma-treated PLLA foils in short-term interaction with ADSCs (Bacakova *et al* 2018a). The first aim of our present study was therefore to observe the interaction, biocompatibility, longer-term growth, and potential differentiation of ADSCs

towards VSMCs, on the one hand, and the phenotypic maturation of VSMCs on pristine and variably modified PLLA foils, on the other. The second aim of our study was to investigate the cell behaviour on these same materials while culturing them in a differentiation medium.

2. Materials and methods

2.1. Biomaterial preparation

2.1.1. Material

Biopolymer poly(L-lactic acid) (PLLA), crystallinity (60%–70%), density $1.25 \text{ g} \cdot \text{cm}^{-3}$, thickness $50 \mu\text{m}$ ($\pm 20\%$) (purchased from Goodfellow, UK) was used for this experiment. Circular samples with a final diameter of 2 cm were cut from polymer sheets.

2.1.2. Modifications

2.1.2.1. Plasma treatment

The PLLA foils were treated by Ar^+ plasma in Balzers SCD 050 under the following conditions: gas purity 99.997%, pressure 10 Pa, electrode distance 50 mm, power 3 W, treatment time 240 s, room temperature (RT), area of 48 cm^2 , chamber volume of ca 1000 cm^3 and plasma volume of 240 cm^3 .

2.1.2.2. Chemical grafting

Some of the plasma-treated polymer samples were chemically grafted by immersing them into a 2% aqueous solution of PEG (Mr = 20 000, Sigma Aldrich, USA) or into a 2% aqueous solution of Dex (Mr = 9 000–11 000, Sigma Aldrich, USA) for 20 h at RT. The non-bonded PEG or Dex was removed by immersing the samples into distilled water for 24 h. Subsequently the samples were dried for 12 h at RT.

2.1.2.3. Etching

Some of the plasma-treated polymers samples were immersed into deionized water for 20 h immediately after plasma treatment. These samples were used as a control to samples grafted with PEG or Dex.

In this work, we studied several types of polymeric substrates (samples): (i) pristine PLLA, (ii) PLLA plasma-treated for 240 s (PLLA240), (iii) plasma-treated PLLA etched in water, (iv) plasma-treated PLLA grafted with PEG and (v) plasma-treated PLLA grafted with Dex.

2.2. Biomaterial characterization

2.2.1. Surface characterization

Physico-chemical and morphological analyses of the pristine and modified PLLA samples were performed by a variety of measurement techniques. It is known that the water CA of plasma-modified PLLA depends on the period of time after modification. The ageing time was determined by goniometry. The other analyses were performed only on the aged samples (more than 30 d after plasma treatment).

2.2.2. Contact angle

The surface CA was measured using the static water drop CA method. The measurements and the evaluation were performed using the See System (Advex Instruments, CZ). The water drops for the CA measurements were created using drops of distilled water on three samples, at ten different positions on the surface of the material of each sample at RT. The CAs of all modified samples were measured over a period of 50 d after their final modification.

2.2.3. Surface morphology and roughness

The surface morphology and the roughness of the pristine and modified samples were determined using a Dimension ICON (Bruker Corp.), QNM mode in Air, silicon Tip on Nitride Lever SCANASYST-AIR, spring constant 0.4 N m^{-1} and a frequency of 70 kHz was used. NanoScope Analysis software was applied for scan evaluation. The mean roughness value (R_a) represents the arithmetic average of the deviation from the centre plane of the sample. Each sample was measured three times (regions of $10 \times 10 \mu\text{m}^2$), independently.

2.2.4. Chemical composition

The concentrations of the C(1s), N(1s) and O(1s) atoms in the treated surface layer were measured by X-ray Photoelectron Spectroscopy (XPS). An Omicron Nanotechnology ESCAProbeP spectrometer was used to measure the spectra of the modified polymer surfaces. An area of $2 \times 3 \text{ mm}^2$ was analysed. The x-ray source provided monochromatic radiation of 1486.7 eV. The spectra were measured with a step size of 0.05 eV. The spectra were evaluated with the use of CasaXPS software. The concentration of the elements is given as the atomic percentage.

2.3. Cell isolation

2.3.1. ADSCs

The isolation of the cells was performed in compliance with the Declaration of Helsinki and under ethical approval from the Ethics Committee at Na Bulovce Hospital in Prague. Written informed consent approving experimental use of extracted adipose tissue was obtained from the healthy donor before the liposuction procedure was applied. The ADSCs were isolated using collagenase digestion of adipose tissue; for a detailed description of the isolation procedure, see our previous research (Przekora *et al* 2017, Travnickova *et al* 2020). In brief, the lipoaspirate was washed several times with phosphate buffer saline (PBS; Sigma Aldrich) and was digested using a solution of collagenase type I (Worthington Biochemical Corp.). After digesting and subsequent centrifuging, the mature adipocytes and the digested tissue were aspirated, and the remaining stromal vascular fraction containing the ADSCs was seeded into culture flasks. The ADSCs (passage 2) were characterized by flow cytometry (Accuri C6 Flow Cytometer) to

confirm the presence of mesenchymal stem cells and the absence of other cell types. Phycoerythrin, FITC, Alexa488- or Alexa647-conjugated monoclonal antibodies against CD105, CD90, CD73, CD29, CD146, CD45, CD34 and CD31 were used. The percentage of positive cells for specific CD markers was as follows: CD105 (98.3%), CD90 (99.2%), CD73 (100%), CD29 (99.9%), CD146 (81.7%), CD45 (6.9%), CD34 (1.7%), CD31 (1.8%).

2.3.2. VSMCs

The cells were isolated from porcine aorta by the explantation method, according to a protocol previously described in Liskova *et al* (2017). In brief, the porcine aorta was washed with PBS and the outer *tunica adventitia* was gently removed. The aortic wall was longitudinally cut and the *tunica intima*, together with 2/3 of the *tunica media*, was gently separated and cut into small pieces. The cut pieces were digested using collagenase type III (Worthington Biochemical Corp.) and were subsequently seeded into culture flasks. The cells were cultured and were characterized by positive immunofluorescence staining for α -smooth muscle actin (α SMA), calponin, h-caldesmon, desmin and smooth muscle myosin heavy chain (SM-MHC), and were used as a positive control for ADSCs differentiating towards VSMC phenotype. Porcine VSMCs were chosen due to the relatively high similarity of the porcine and human cardiovascular systems, and due to the relatively high stability of the differentiated contractile phenotype in these cells (Christen *et al* 1999). The similarities in morphology and in physiology can be exploited for further preclinical *in vivo* studies of material biocompatibility.

2.4. Cell culturing

For the cell seeding experiments, pristine PLLA, PLLA plasma-treated for 240 s, plasma-treated PLLA grafted with PEG, and plasma-treated PLLA grafted with Dex samples were used. Prior to cell seeding, the samples (PLLA, PLLA240, PEG, and Dex) were sterilized in 70% ethanol for 1 h and were then rinsed with PBS. Subsequently, the samples were inserted in a 12-multiwell plate and were fixed by inert glass circles. Tissue culture polystyrene (PS), represented by the bottoms of the wells in a 12-multiwell plate, was used as the control.

The ADSCs (passage 2) were seeded at a density of 8000 cells per cm^2 in 2 ml per well of Dulbecco's Modified Eagle Medium (DMEM; Gibco, Thermo Fisher Scientific) supplemented with 10% (vol vol⁻¹) foetal bovine serum (FBS; Gibco, Thermo Fisher Scientific), gentamicin ($40 \mu\text{g ml}^{-1}$; Sandoz, Novartis) and basic fibroblast growth factor (10 ng mL^{-1} , FGF2; GenScript). After 4 d of cultivation, the medium was changed to trigger differentiation of ADSCs towards VSMCs. The medium referred to as the 'differentiation medium' contained DMEM supplemented with 2% (vol vol⁻¹) FBS, transforming

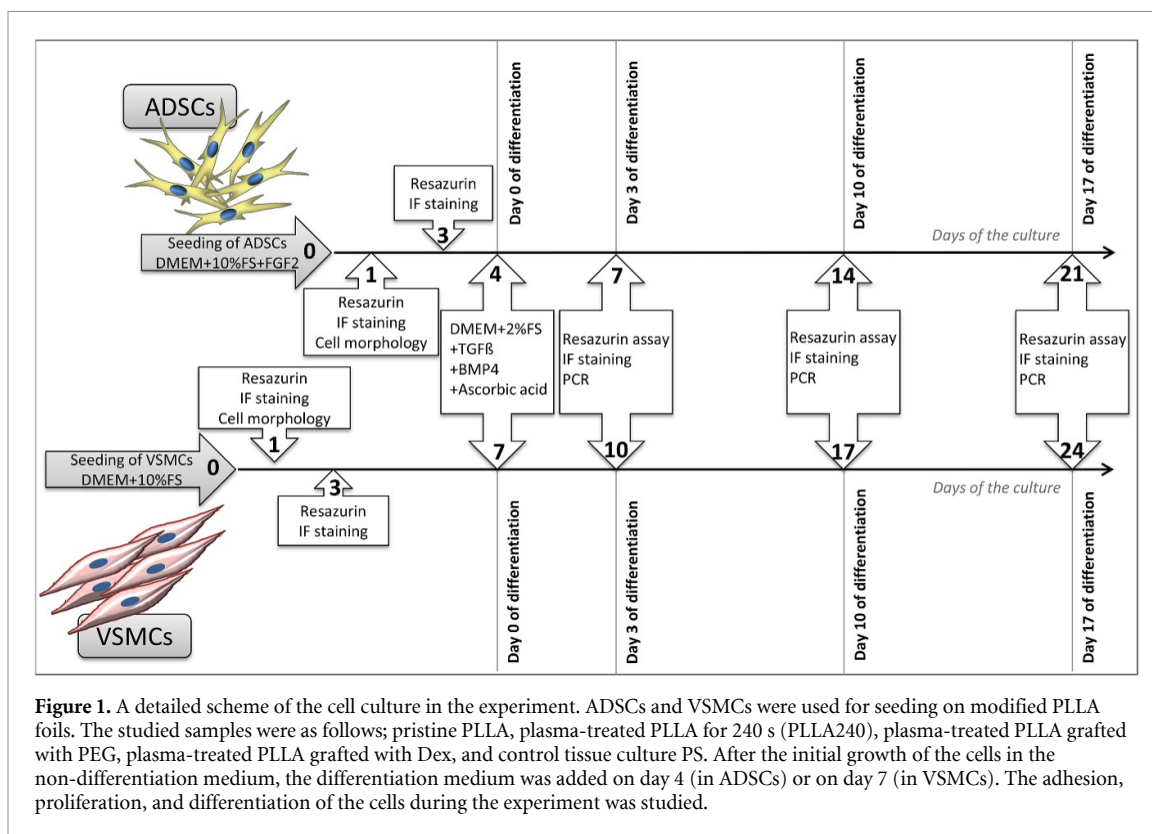


Figure 1. A detailed scheme of the cell culture in the experiment. ADSCs and VSMCs were used for seeding on modified PLLA foils. The studied samples were as follows; pristine PLLA, plasma-treated PLLA for 240 s (PLLA240), plasma-treated PLLA grafted with PEG, plasma-treated PLLA grafted with Dex, and control tissue culture PS. After the initial growth of the cells in the non-differentiation medium, the differentiation medium was added on day 4 (in ADSCs) or on day 7 (in VSMCs). The adhesion, proliferation, and differentiation of the cells during the experiment was studied.

growth factor beta 1 (2.5 ng mL^{-1} , TGF β 1; Abcam), bone morphogenetic protein 4 (2.5 ng mL^{-1} , BMP4; Sigma Aldrich) and ascorbic acid ($150 \text{ }\mu\text{M}$, AA; Sigma Aldrich). The control medium referred to as the ‘non-differentiation medium’ contained DMEM supplemented with 10% (vol vol $^{-1}$) FBS only. The ADSCs were cultured for 21 d in total; i.e. for 17 d with a differentiation medium. For the detailed design of the experiment, see figure 1. The ADSCs cultured in the non-differentiation medium were used as a negative control to ADSCs that were differentiated towards VSMCs.

The VSMCs (passage 4) were seeded at a density of $14\,000$ cells per cm^2 in DMEM supplemented with 10% (vol vol $^{-1}$) FBS. From day 7 of the culture, the medium was changed similarly to ADSCs. The ‘differentiation medium’ contained DMEM supplemented with 2% (vol vol $^{-1}$) FBS, TGF β 1 (2.5 ng mL^{-1}), BMP4 (2.5 ng mL^{-1}), and AA ($150 \text{ }\mu\text{M}$). The control medium, referred to as ‘non-differentiation’, contained DMEM supplemented with 10% (vol vol $^{-1}$) FBS only. Due to the slower initial adhesion and growth of the cells at the beginning of the experiment, the VSMCs were cultured for 24 d in total; however the time period with the differentiation medium was the same as for the ADSCs (i.e. 17 d). For the detailed design of the experiment, see figure 1. The VSMCs cultured in both types of media were used as a positive control for ADSCs differentiating towards the VSMC phenotype.

During cell culturing, the medium was changed twice a week, and both cell types were maintained in an incubator with a humidified atmosphere of 5% CO_2 at a temperature of $37 \text{ }^\circ\text{C}$.

2.5. Metabolic activity of the cells

Conversion of resazurin (Cat. No. R7017, Sigma-Aldrich) was used to measure the metabolic activity of the cells, which is considered as an indirect indicator of cell proliferation. The principle of this redox indicator assay is based on the colorimetric conversion of blue resazurin to pink resorufin, which can be quantified by fluorescence or absorbance measurements. This reduction is induced by the activity of the mitochondrial enzymes of the viable cells. In order to estimate the proliferation activity of the cells, the metabolic activity was measured on days 1, 3, 7, 14, and 21 (for ADSCs) and on days 1, 3, 7, 10, 17, and 24 (for VSMCs). In brief, the stock resazurin solution (4 mM) was added to DMEM without phenol red with 10% (vol vol $^{-1}$) FBS to a final concentration of $40 \text{ }\mu\text{M}$. The samples with the cells were transferred to fresh 12-multiwell plates, were pre-washed with PBS, and 1.5 ml of the resazurin solution was added to the cells in each well. The time of incubation at $37 \text{ }^\circ\text{C}$ was the same on all days; i.e. 3 h and 15 min (for ADSCs) and 3 h and 45 min (for VSMCs). Subsequently, the fluorescence was measured ($E_x/E_m = 530/590 \text{ nm}$) on a SynergyTM HT Multi-Mode Microplate reader (BioTek, U.S.A.). The background control (resazurin solution without cells) was subtracted.

2.6. Immunofluorescence staining and microscopy techniques

Immunofluorescence staining was used to visualize the cells during the process of adhesion, growth and differentiation. Prior to all types of immunofluorescence staining, the cells were fixed with 4% paraformaldehyde (for 10 min), were pre-treated in PBS with 1% (vol vol⁻¹) bovine serum albumin (BSA, Sigma-Aldrich) and 0.1% (vol vol⁻¹) TritonX-100 (for 20 min), and were then incubated in PBS with 1% (vol vol⁻¹) Tween 20 (for 20 min). Washing in a pure PBS solution was applied after each step.

On day 1, the cells were stained with Texas Red C2-maleimide (1.7 µg mL⁻¹ in PBS; Invitrogen) and the cell nuclei were counterstained with Hoechst 33258 (10 µg mL⁻¹ in PBS; B1155, Sigma-Aldrich) for 30 min in order to visualise the morphology of the cells.

On days 1 and 3, the cells were stained with monoclonal anti-vinculin primary antibody (clone hVIN-1, dilution of 1:200 in PBS; V 9131, Sigma-Aldrich) overnight at 4 °C, and then with phalloidin-TRITC (100 ng mL⁻¹ in PBS; Sigma-Aldrich) for 1 h at RT in order to visualize the filamentous actin. The secondary antibody, i.e. anti-mouse IgG conjugated with Alexa Fluor 488 (dilution 1:400; A11017, Thermo Fisher Scientific), and Hoechst 33258 for staining the cell nuclei (10 µg mL⁻¹ in PBS) were applied for 1 h at RT.

On days 7, 14, and 21 (for ADSCs) and on days 10, 17, and 24 (for VSMCs), the cells were stained with primary antibodies against α -smooth muscle actin (α SMA, clone 1A4, dilution 1:200 in PBS; A2547, Sigma Aldrich) or against myosin heavy chain 11 (SM-MHC, MYH11 (G-4), dilution of 1:200; sc-6956, Santa Cruz Biotechnology) overnight at 4 °C. Then anti-calponin (EP798Y, dilution 1:200 in PBS; ab46794, Abcam) or anti-type I collagen (dilution of 1:400 in PBS; LSL-LB-1197, CosmoBio) were applied for 3 h at room temperature. Subsequently, the secondary antibodies were applied; i.e. anti-mouse IgG conjugated with Alexa Fluor 546 (dilution 1:400; A11003, Thermo Fisher Scientific) and anti-rabbit IgG conjugated with Alexa Fluor 488 (dilution 1:400; A11070, Thermo Fisher Scientific) for 1 h at RT. The cell nuclei were counterstained with Hoechst 33258 (10 µg mL⁻¹ in PBS). The Olympus epifluorescence microscope IX71 (DP71 digital camera, objective magnification of 10x, 20x or 40x) was used to take the images.

2.7. Image analysis

Hoechst counterstaining of the nuclei was used to count the cells on days 1, 3, 7, 14 and 21 (for ADSCs) and on days 1, 3, 10, 17 and 24 (for VSMCs). Microphotographs of 6–7 randomly selected microscopic fields were analysed for each sample type. The initial doubling time of ADSCs and VSMCs on the PLLA samples was calculated from the cell numbers

between days 1 and 3 (i.e. 48 h of cell culture) according to the following equation: $DT = t \times \ln(2) / (\ln(N) - \ln(N_0))$, where t represents the duration of the culture, N represents the number of cells on day 3, and N_0 represents the number of cells on day 1.

The spreading area, the circularity, the aspect ratio, and the solidity of the cells were measured in order to analyze the morphology of the ADSCs and VSMCs on day 1. The analyses of these parameters were performed in ImageJ software according to the following calculations; i.e. circularity: $4\pi \times \text{area} / \text{perimeter}^2$, aspect ratio: major axis/minor axis, solidity: area/convex area. From 86 to 248 cells were analysed for each sample.

2.8. RNA isolation and RT-qPCR

Total RNA isolation was performed using a Total RNA Purification Plus Micro Kit (Norgen Biotek) according to the manufacturer's protocol. The RNA concentration and purity was evaluated from measurements of absorbance at 260 nm and 280 nm using a NanoDrop One Spectrophotometer (Thermo Fisher Scientific, USA). Reverse transcription was carried out using an Omniscript Reverse Transcription Kit (Qiagen, Germany) according to the attached instructions with the use of random hexamers (New England Biolabs, USA). The reaction mixture containing aliquots of 1 µg of isolated RNA in a final reaction volume of 20 µl was incubated at 37 °C for 60 min. The synthesized cDNA was then stored at -20 °C for further use.

In human ADSCs, the mRNA levels were measured with 5xHOT FIREPol Probe qPCR Mix Plus (ROX) (Solis BioDyne, Estonia) and TaqMan Gene Expression Assays (Life Technologies) containing hydrolysis probes labelled with FAM reporter dye specific to COL1A1 (Hs00164004_m1), CNN1 (Hs00154543_m1), SMTN (Hs01022259_m1), ACTA2 (Hs00909449_m1), MYH11 (Hs00975796_m1), and B2M (Hs00187842_m1) as a reference gene. In porcine VSMCs, the mRNA levels were quantified with hydrolysis probes specific to ACTA2 (Ss04245588_m1), CNN1 (Ss03392449_g1) and SMTN (Ss03373737_m1). B2M (Ss03391154_m1) was used as a reference gene. qPCR was performed in a 96-well optical reaction plate in a final reaction volume of 20 µl per well using the Viia 7 Real-time PCR System (Thermo Fisher Scientific, USA). The thermal profile consisted of pre-incubation for 2 min at 50 °C, enzyme activation for 10 min at 95 °C and 40 cycles of denaturation (15 s, 95 °C) and annealing/elongation (1 min, 60 °C). The relative gene expression levels were calculated as $-\Delta\Delta C_t$.

2.9. Statistical analysis

The parametric data are expressed as mean + SD, One way ANOVA, Student-Newman-Keuls test, $p \leq 0.05$. The non-parametric data are expressed in box plots as median values, ANOVA on ranks, Dunn's Method,

$p \leq 0.05$. Three parallels from each sample type were used. The statistical comparison among the samples was made on cells cultured in the same medium type and on the same day of the culture. Statistical analyses were performed using SigmaStat 3.5 software and SigmaPlot 10.0 software (Systat Software Inc. USA).

3. Results

3.1. Material wettability

It is known that plasma treatment of polymer macromolecules results in their cleavage, ablation, and alterations to their chemical structure. Plasma treatment thus affects the physicochemical surface properties, e.g. the water CA and the surface wettability. Subsequent grafting with various substances (e.g. biomolecules, nanoparticles, etc) on these plasma-treated surfaces leads to further changes in CA. The change in the surface within the specific time interval from plasma modification is known as ageing (Slepička *et al* 2013, Slepičková Kasálková *et al* 2013). The dependence of CA on ageing time for modified PLLA is shown in figure 2. All modified substrates exhibit a similar trend. The lowest value of CA was detected immediately after modification. During ageing, the CA of all tested samples increased. The increment in the CA values is caused by a rearrangement of the oxygen-containing groups that emerged after exposing the plasma-treated polymer to the ambient atmosphere into a polymer volume or by a rearrangement of grafted substances (Slepička *et al* 2013, Slepičková Kasálková *et al* 2013). In the case of plasma-treated PLLA, 10 d after modification the value of CA is higher than the value of pristine PLLA. The CA values of the grafted substrates are lower than the pristine PLLA values. This may be caused by the fact that there are oxygen-containing substances grafted on to the plasma-activated surface. This usually causes an increase in wettability, because these substances are of hydrophilic character. The ageing time necessary for surface stabilization is 10 d for PLLA modified in plasma discharge, and 15 d for PLLA grafted with PEG or Dex.

3.2. Surface morphology and roughness

Atomic force microscopy (AFM) was used to qualify and quantify the changes in surface morphology and in the roughness of the PLLA samples. The roughness of all tested samples, estimated by the R_a parameter, was in the nanoscale. AFM scans showed slightly higher roughness of the plasma-treated PLLA and Dex-modified PLLA samples than of the pristine PLLA (figure 3). The surface morphology of the pristine PLLA was almost flat, in contrast with the differentiated surface of the plasma-treated PLLA and the single-pillar surface of the Dex-modified PLLA. PEG-modified PLLA showed 5–6 times greater roughness, but the irregularities had a bulging appearance, i.e. they were more rounded and

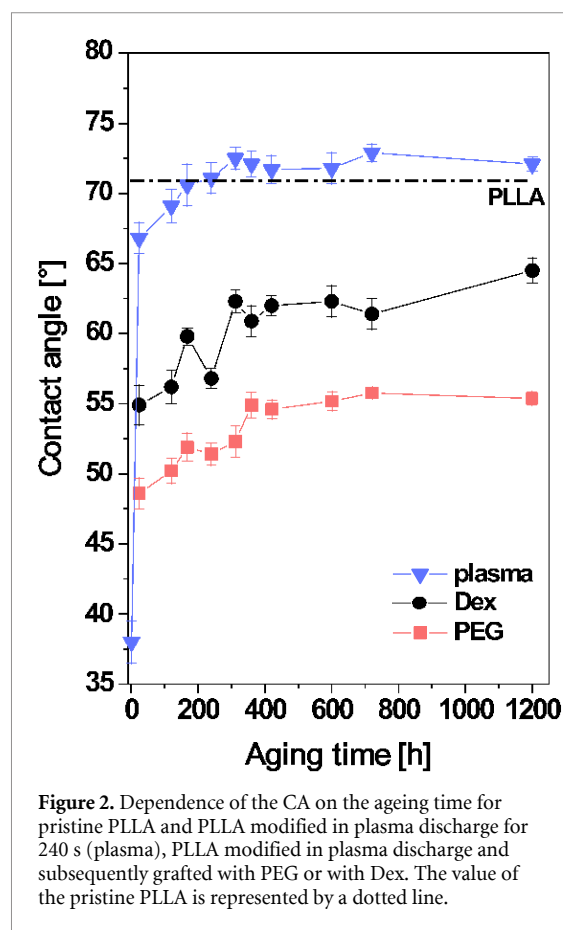


Figure 2. Dependence of the CA on the ageing time for pristine PLLA and PLLA modified in plasma discharge for 240 s (plasma), PLLA modified in plasma discharge and subsequently grafted with PEG or with Dex. The value of the pristine PLLA is represented by a dotted line.

Table 1. Elemental composition of the surface layers of pristine PLLA and PLLA modified by plasma discharge, PLLA modified by plasma discharge and subsequently etched in water or grafted with PEG or Dex.

	Atomic concentration [at.%]		
	O(1s)	N(1s)	
PLLA	63.6	36.4	0
Plasma	65.8	33.4	0.8
Etching	66.5	32.9	0.6
PEG	60.3	38.9	0.5
Dex	62.3	37.2	0.4

less sharp than in the other samples, particularly in the Dex-grafted samples.

3.3. Surface chemistry

The results obtained by goniometry determination of CA are in good agreement with the results of the chemical analysis of the surfaces performed by the XPS method. The atomic concentration of selected elements is shown in table 1.

As has been mentioned above, plasma treatment causes the formation of radicals and double bonds. New functional groups (i.e. carbonyl, carboxyl and ester groups) therefore form after an ‘activated’ surface has been exposed to the ambient oxygen-containing atmosphere. At the same time, plasma modification leads to cleavage of the polymer chains and subsequent surface ablation of PLLA (Slepička

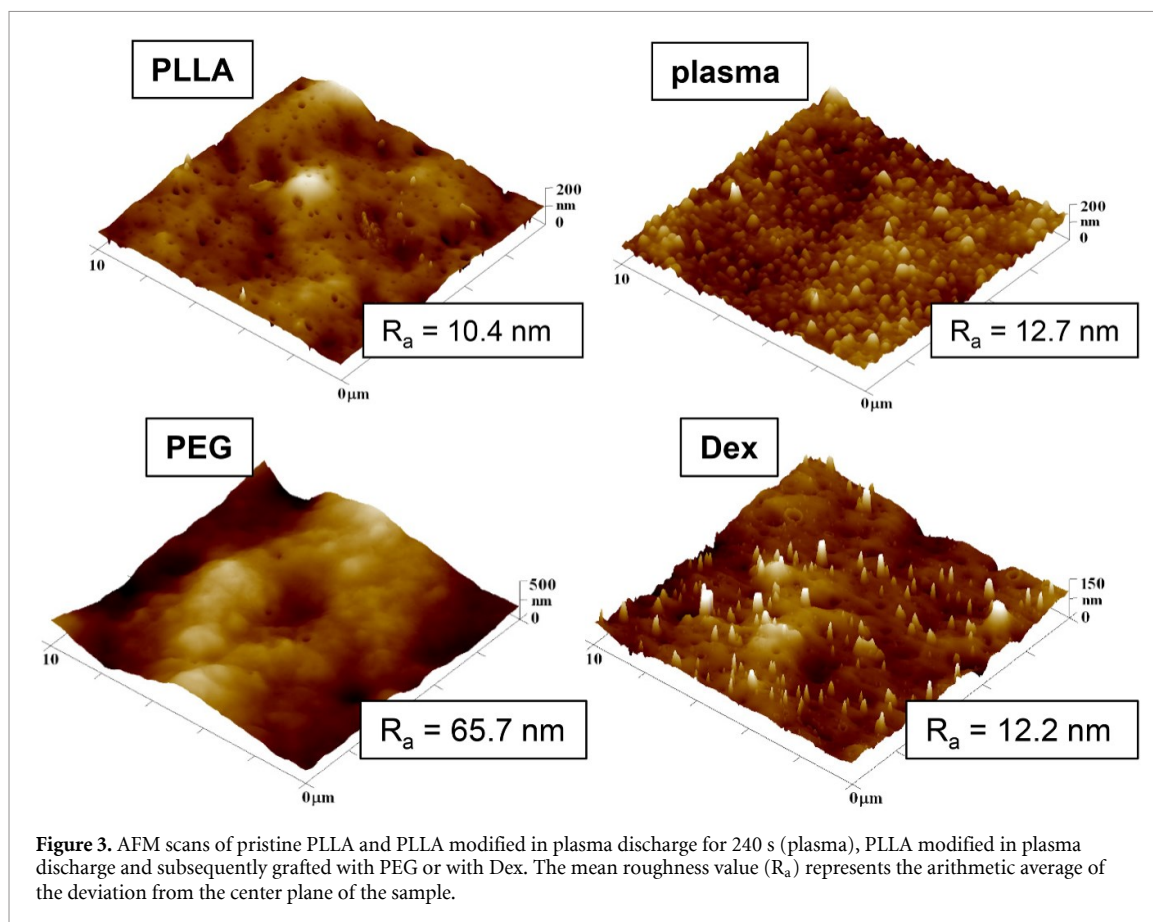


Figure 3. AFM scans of pristine PLLA and PLLA modified in plasma discharge for 240 s (plasma), PLLA modified in plasma discharge and subsequently grafted with PEG or with Dex. The mean roughness value (R_a) represents the arithmetic average of the deviation from the center plane of the sample.

et al 2013, Slepícková Kasálková *et al* 2013). As a result, the oxygen concentration in the surface layer of plasma-modified PLLA decreases. Etching plasma-activated samples removes a part of the newly-formed oxygen-containing groups, and also removes the attached atmospheric nitrogen. Grafting PEG or Dex onto the plasma-modified PLLA surface increases the oxygen concentration, since both compounds contain a large amount of oxygen in their molecules. These results therefore also confirm successful grafting of PEG and Dex on to the surface of PLLA.

3.4. Cell number and doubling time

The initial doubling time was counted from the cell numbers between days 1 and 3 after seeding. The cell numbers were counted from the Hoechst-stained cell nuclei on days 7, 14 and 21 for ADSCs, and on days 10, 17 and 24 for VSMCs, i.e. in time intervals when the cells were being cultured either in a non-differentiation medium or in a differentiation medium.

3.4.1. ADSCs

The initial doubling time of ADSCs on all PLLA samples was similar to the value obtained for the control PS (table 2). Except on day 7, the ADSCs cultured in the non-differentiation medium reached similar cell numbers on all tested samples on the

Table 2. Initial doubling time of ADSCs and VSMCs on pristine PLLA, on PLLA plasma-treated for 240 s (PLLA240), on plasma-treated PLLA grafted with PEG, on plasma-treated PLLA grafted with Dex, and on the control PS counted between days 1 and 3 after seeding.

	Doubling time (hours)	
	ADSCs	VSMCs
PLLA	16.74	39.67
PLLA240	15.00	19.92
PEG	16.86	18.82
Dex	15.12	13.33
PS	14.94	13.42

corresponding day of the culture (figure 4). However, when cultured in the differentiation medium, the ADSCs reached higher values on the PLLA240 and PS samples than on the pristine PLLA, PEG and Dex samples (figure 4). On day 21, the cells were strongly attached and were well-spread on all tested samples when cultured in the non-differentiation medium; however, they started to detach on pristine PLLA, PEG, and Dex when cultured in the differentiation medium. The detachment of ADSCs had a negative influence on the results of nuclei counting.

3.4.2. VSMCs

The initial doubling time of VSMCs on pristine PLLA was almost twice as long as on the other PLLA modifications or on the control PS (table 2). The cell

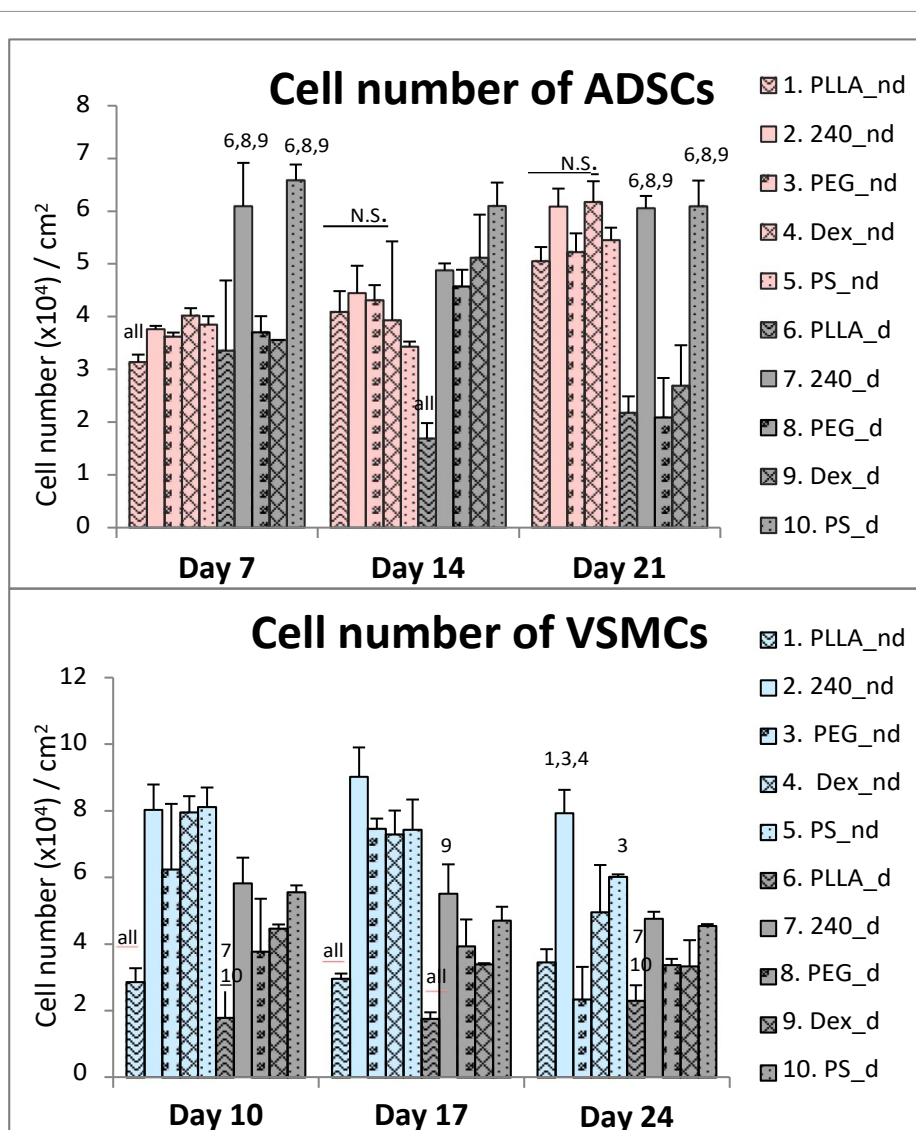


Figure 4. The cell numbers counted from microscopic fields on days 7, 14, and 21 (for ADSCs) and on days 10, 17, and 24 (for VSMCs). The studied samples were as follows; pristine PLLA, plasma-treated PLLA (240), plasma-treated PLLA grafted with PEG, plasma-treated PLLA grafted with Dex, and control tissue culture PS. From day 4 (in ADSCs culture) or from day 7 (in VSMCs culture), the cells were cultivated either in the non-differentiation medium (nd) or in the differentiation medium (d). Mean + SD, one way ANOVA, Student-Newman-Keuls test. The statistical comparison among the samples was made on cells cultured in the same medium type and on the same day of the culture. Statistically significant differences ($p \leq 0.05$) are marked above the columns by the numbers of tested groups of samples. All: statistically significant differences in comparison with all other groups of samples.

number on pristine PLLA was lower than all the other tested samples on all days of the culture, either in the non-differentiation medium or in the differentiation medium (figure 4). The VSMCs cultured in the non-differentiation medium reached almost two times higher cell numbers than the VSMCs cultured in the differentiation medium.

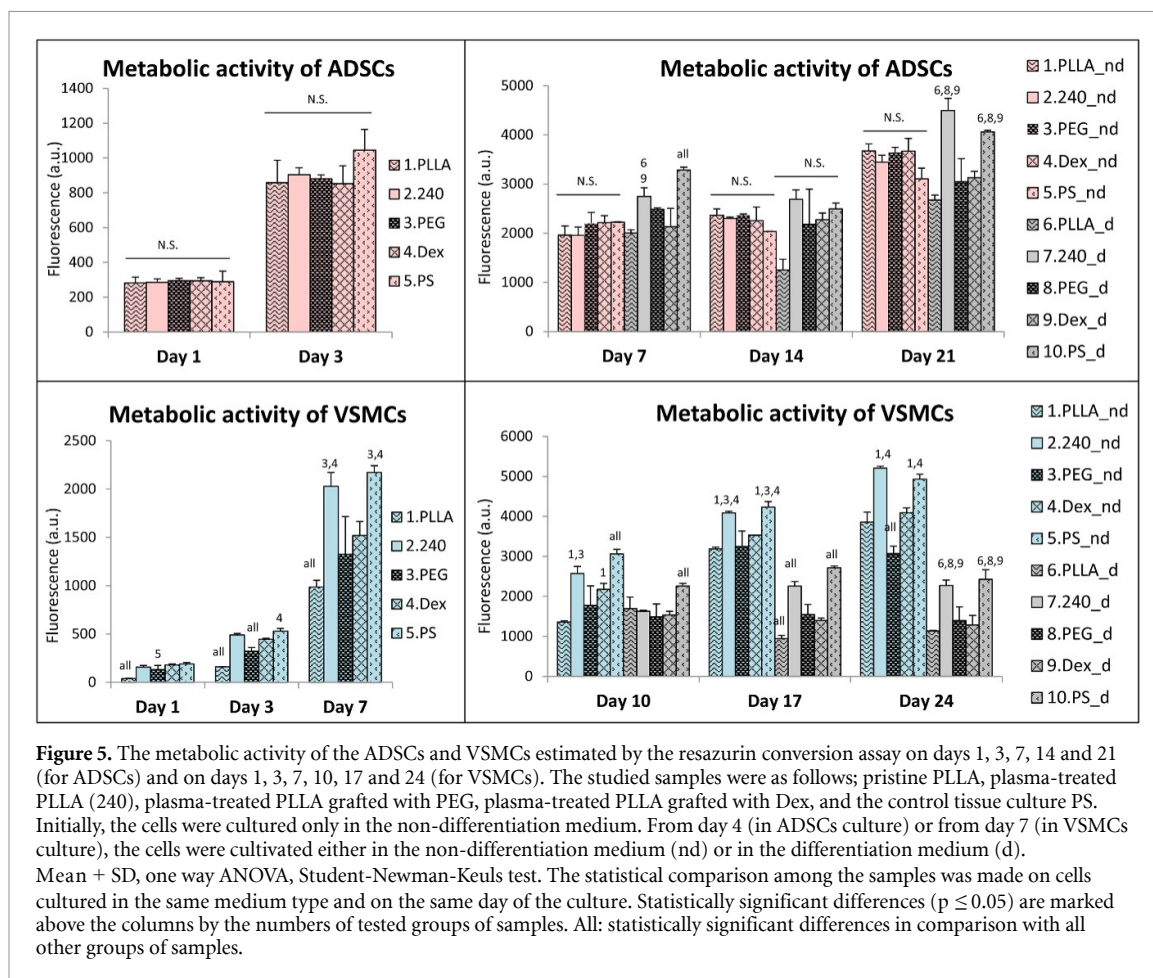
Because the cells had already reached confluence by day 7, the cell numbers further increased only slowly or remained stable, in the case of ADSCs. In the case of VSMCs, the numbers decreased slowly.

3.5. Metabolic activity of cells

The metabolic activity of the ADSCs and VSMCs was estimated by the resazurin conversion assay. The ADSCs showed a similar metabolic activity on all

samples on days 1 and 3 (i.e. before the differentiation medium was added) (figure 5). This trend continued on days 7, 14 and 21, when the ADSCs treated with the non-differentiation medium still showed similar activity on all samples. By contrast, the differences in the metabolic activity of ADSCs on the samples became significant after the differentiation medium had been added, when the PLLA240 and PS samples supported the highest metabolic activity of the cells (figure 5).

Concerning the metabolic activity of VSMCs, all the samples performed better than the pristine PLLA in the initial intervals, i.e. on days 1, 3 and 7 (figure 5). On days 10, 17 and 24, the VSMCs showed a similar trend in metabolic activity to that of the ADSCs grown in the differentiation medium. The



highest cell metabolic activity among the samples was revealed on PLLA240 and on PS, both in the non-differentiation medium and in the differentiation medium (figure 5). However, the VSMCs cultured in the non-differentiation medium reached higher proliferation activity in each interval than the VSMCs cultured in the differentiation medium.

3.6. Initial adhesion, spreading and morphology of the cells

Immunofluorescence staining followed by Image Software analyses was used to characterize the morphology of the cells on the PLLA foils on day 1 after cell seeding. In ADSCs, the smallest cell spreading area was on pristine PLLA (figure 6). In VSMCs, the spreading area was almost the same on all tested PLLA samples; however, the spreading area was significantly lower than on the PS control sample (figure 6). The circularity, the aspect ratio, and the solidity of the ADSCs were similar on all modified PLLA and control PS samples (figure 6). These findings were also in accordance with visual observations, where the cells showed a similar morphology for all samples (figure 7). In contrast to the similar cell spreading area, the VSMCs showed significantly greater circularity and a lower aspect ratio on pristine PLLA and on Dex than on PLLA240, on PEG, and on the control PS sample (figure 6). On days 1 and 3, we

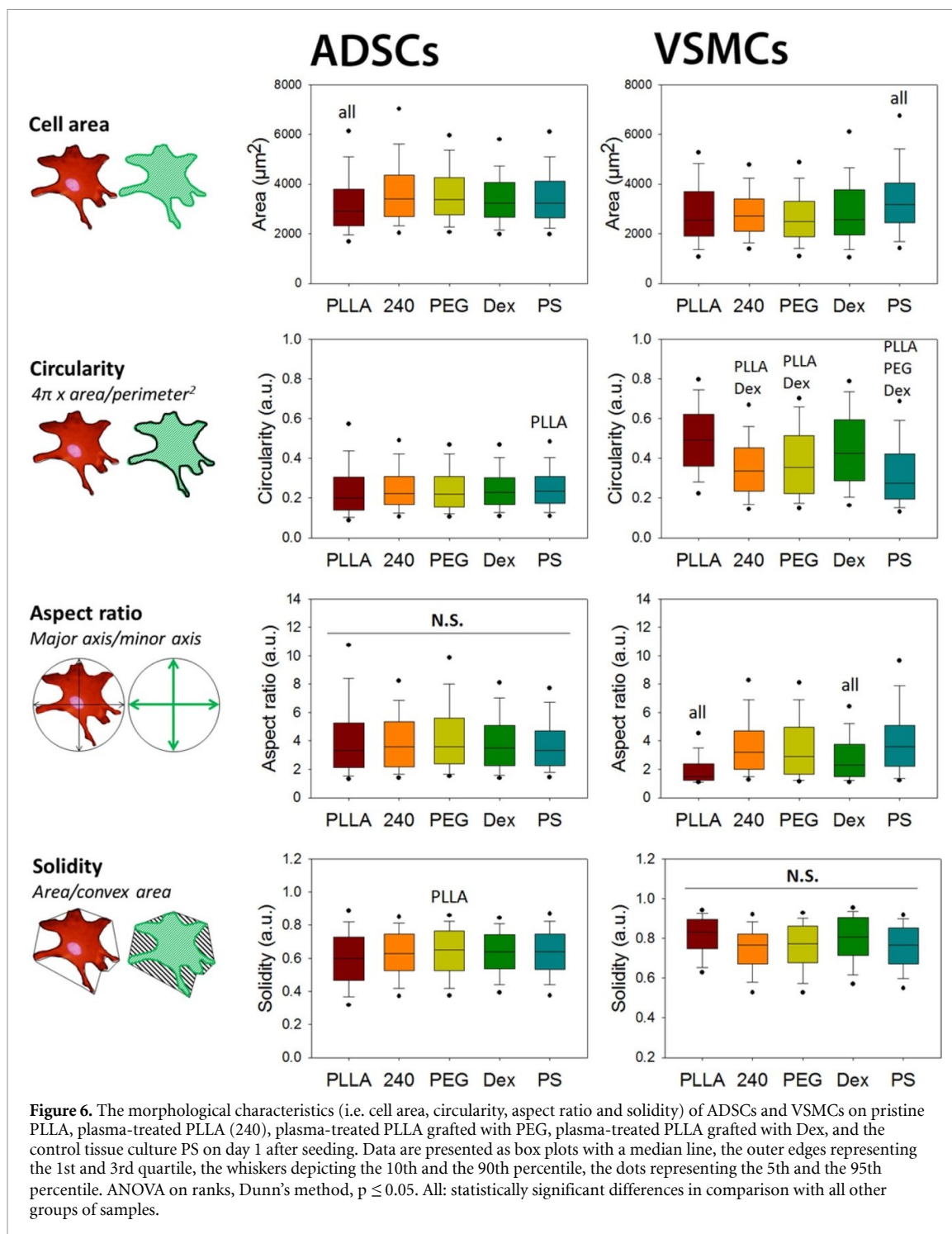
also visually observed more rounded and less-spread cells on pristine PLLA than on the modified PLLA samples, where the cells were better spread and were more elongated (figure 7 and supplementary figure S1 (stacks.iop.org/BMM/16/025016/mmedia)).

3.7. Immunofluorescence staining

Immunofluorescence staining was performed to reveal the presence and the arrangement of various proteins in ADSCs and VSMCs; namely α SMA, calponin, SM-MHC and type I collagen.

3.7.1. ADSCs

Initially, anti- α SMA staining revealed a diffuse signal in ADSCs; however, treatment with the differentiation medium supported the fibrillar structure of α SMA, mainly on days 14 (figure 8) and 21 (figure 9). Anti-calponin staining revealed only sporadic positive cells in ADSCs cultured in the non-differentiation medium, whereas the differentiation medium supported the early formation of variably developed calponin fibres in almost all cells on all tested materials (figure 8). The presence of contractile calponin protein was also stable in later intervals of differentiation (i.e. on days 14 (figure 8) and 21 (figure 9)). The α SMA and calponin fibres were co-localized in some cells, though some of the cells were positive



only for one of these proteins (figure 9). The differentiation medium also supported the formation of type I collagen fibres (figures 9 and S2). Anti-SM-MHC staining revealed sporadically positive cells mainly on day 14 (figures 9 and S2). These SM-MHC-positive cells were observed in cultures treated with the differentiation medium, and were found on all tested samples. Within the ADSCs culture in the non-differentiation medium, the cells only sporadically produced extracellular type I collagen, and no SM-MHC positive cells were observed (supplementary figure S2). The quantity of cells positive for α SMA, calponin and SM-MHC did not visibly differ among

the tested materials, and the main observed influence was dependent on the type of culture medium (i.e. non-differentiation medium vs. differentiation medium). On day 21, the ADSCs cultured in the differentiation medium started to detach from the tested materials.

3.7.2. VSMCs

The cells were positively stained for α SMA and calponin in all observed time intervals on all tested samples, either in the non-differentiation medium or in the differentiation medium. The α SMA and calponin fibres were mostly oriented in the same

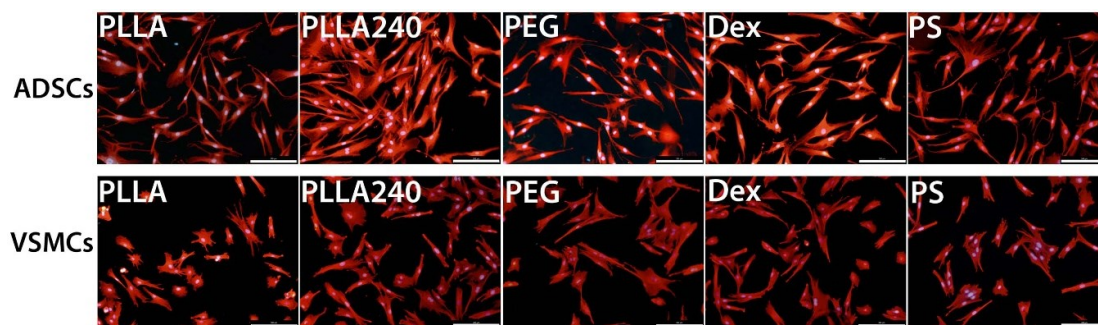


Figure 7. The morphology of ADSCs and VSMCs on day 1 after seeding on pristine PLLA, on plasma-treated PLLA (PLLA240), on plasma-treated PLLA grafted with PEG, on plasma-treated PLLA grafted with Dex, and on the control tissue culture PS. The cells were visualized by Texas Red C2-maleimide. The cell nuclei were counterstained with Hoechst 33258. IX71 Olympus microscope, DP71 digital camera. Objective magnification x10, scale bar 200 μm .

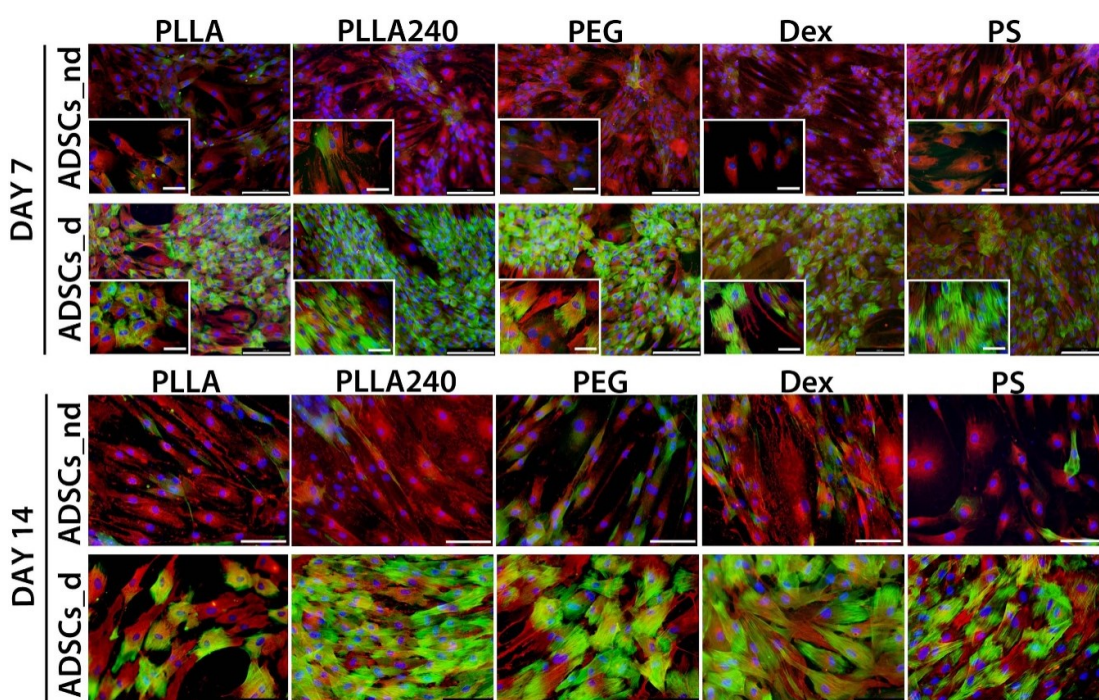


Figure 8. Immunofluorescence staining of αSMA (red) and calponin (green) in ADSCs on day 7 of the culture (i.e. 3 d of differentiation) and on day 14 (i.e. 10 d of differentiation) on pristine PLLA, plasma-treated PLLA (PLLA240), plasma-treated PLLA grafted with PEG, plasma-treated PLLA grafted with Dex, and the control tissue culture PS. ADSCs_nd were cultured in the non-differentiation medium. ADSCs_d were cultured in the differentiation medium. The cell nuclei were counterstained with Hoechst 33258. IX71 Olympus microscope, DP71 digital camera. Objective magnification x10, scale bar 200 μm (day 7) and magnification x20, scale bar 100 μm (day 14). For each sample, a microphotograph under detailed objective magnification x40, scale bar 50 μm is included (day 7).

direction (supplementary figure S3). On days 17 and 24, the VSMCs treated with the non-differentiation medium started to detach from the materials (supplementary figure S3). By contrast, the VSMCs treated in the differentiation medium maintained their elongated morphology until day 24 (with the exception of the pristine PLLA sample, where the cells did not reach the confluence state) (supplementary figure S3).

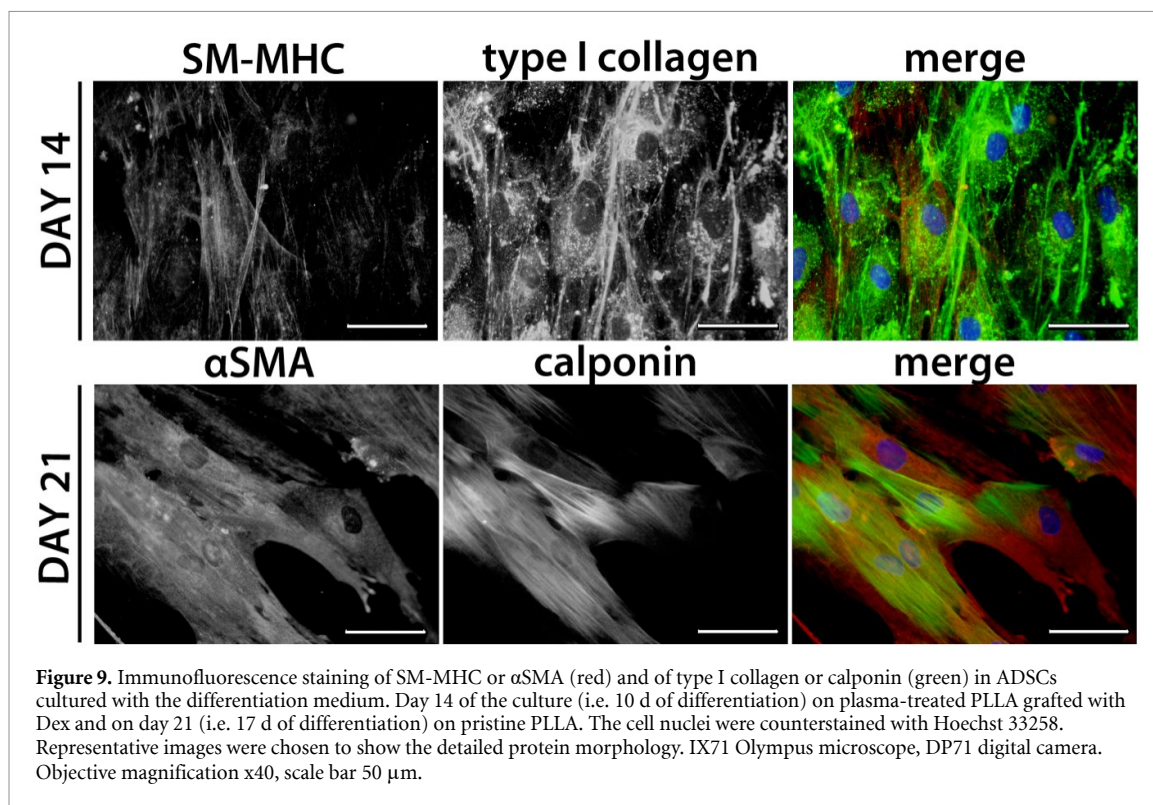
3.8. PCR analysis

Real time qPCR was used to quantify and compare the gene expression of COL1A1, CNN1, SMTN, ACTA2, and MYH11 in cells on the tested samples in the

non-differentiation and differentiation media. The measured values were normalized to the control values obtained in cells on PS treated with the non-differentiation medium for 7 d.

3.8.1. ADSCs

The gene expression of type I collagen (COL1A1) was supported by the presence of the differentiation medium (figure 10(a)). This increased expression of COL1A1 above the control values was almost stable in all time intervals and on all materials. Treatment with the non-differentiation medium led to a decreasing tendency toward COL1A1 expression in cells on all materials in comparison with the control values.



Similarly to type I collagen, the gene expression of calponin (CNN1) was strongly supported by the differentiation medium in cells on all tested samples in all time intervals (figure 10(b)). Moreover, this increased expression caused by the differentiation medium was almost stable throughout the cell culture period. No differences were observed among the tested materials. Treatment with the non-differentiation medium led to decreasing expression of CNN1 in comparison with the control values.

A similar trend was observed in the gene expression of smoothelin (SMTN). The expression of SMTN in ADSCs treated with the differentiation medium was increased throughout the cell culture period. By contrast, there was a decreasing tendency when ADSCs were cultured in the non-differentiation medium (figure 10(c)).

The gene expression of α SMA (ACTA2) was similar in the non-differentiation media and in the differentiation media on all materials on day 7 of cultivation (figure 11(a)). Nevertheless, on days 14 and 21, the difference between the two types of culture media became apparent, when the gene expression increased in ADSCs treated with the differentiation medium (figure 11(a)).

The gene expression of myosin heavy chain 11 (MYH11) in cells grown in the non-differentiation medium was lower in cells cultured on all tested PLLA samples in all time intervals than in the control cells (grown on PS for 7 d in the non-differentiation medium). In ADSCs treated with the differentiation medium, the expression of MYH11 increased, particularly in the cells on plasma-treated PLLA and on

plasma-treated PLLA grafted with PEG or Dex on day 7, and also on plasma-treated and PEG-grafted PLLA on day 21, where the average expression of MYH11 became similar to or slightly higher than in the control cells (figure 11(b)).

3.8.2. VSMCs

Throughout the cell culture period, the gene expression of CNN1 and ACTA2 remained almost unchanged in the VSMCs that were treated with the non-differentiation medium (supplementary figures S4a and S4b). By contrast, treatment with the differentiation medium caused decreasing expression of these genes in cells on all tested materials. The expression of SMTN varied and did not show a specific trend during cell culture. However, the expression was generally lower on days 17 and 21 in cells grown in the differentiation medium than in cells grown in the non-differentiation medium (supplementary figure S4c).

4. Discussion

The set of experiments was performed to study the behaviour of ADSCs and VSMCs (a) on modified PLLA foils and (b) on the modified PLLA foils in combination with the differentiation medium. Our study provides evidence that PLLA foils supported the proliferation and differentiation of ADSCs and VSMCs, both in the non-differentiation culture conditions and in the differentiation culture conditions. These could be promising findings for vascular tissue engineering purposes.

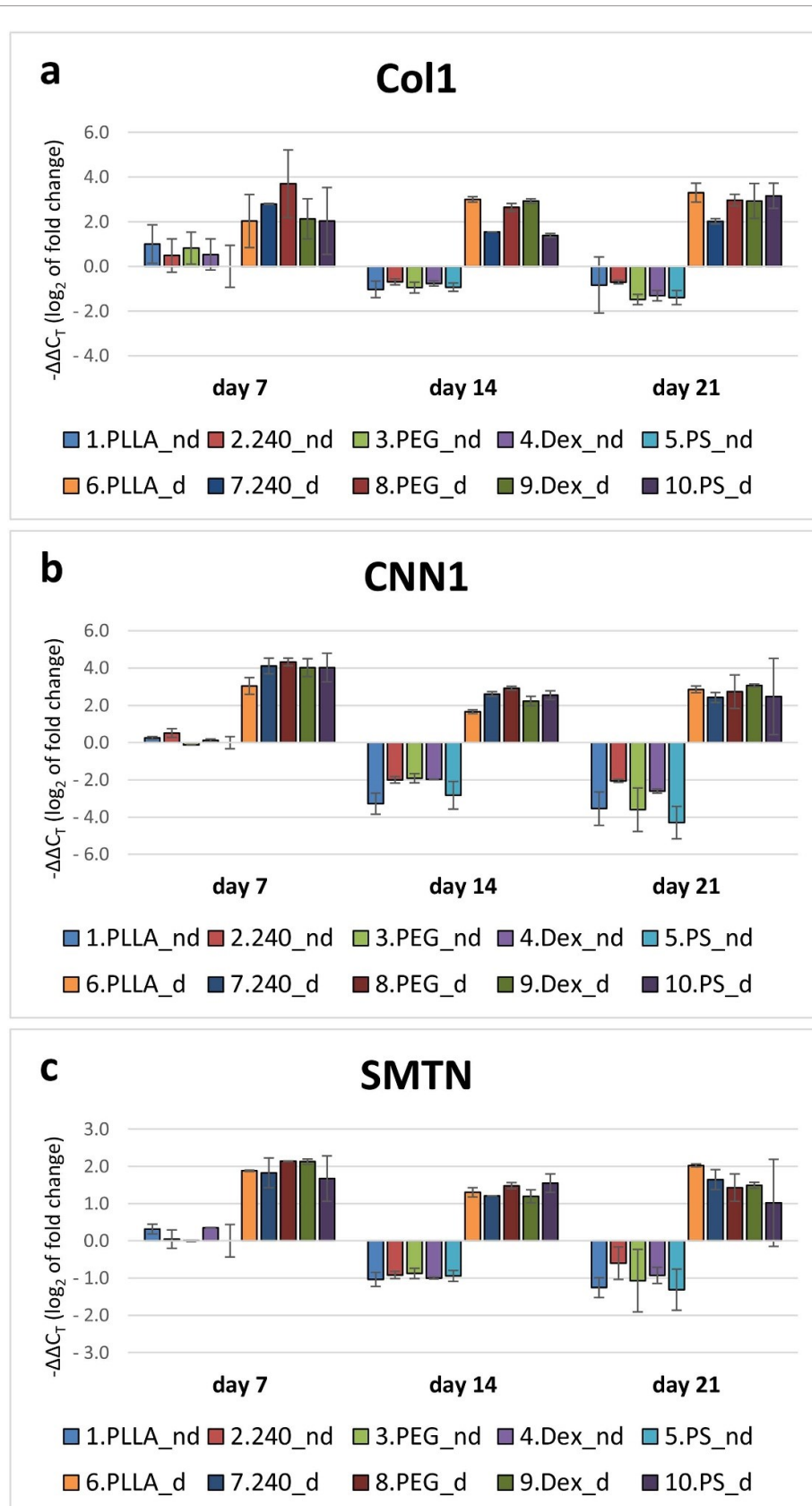
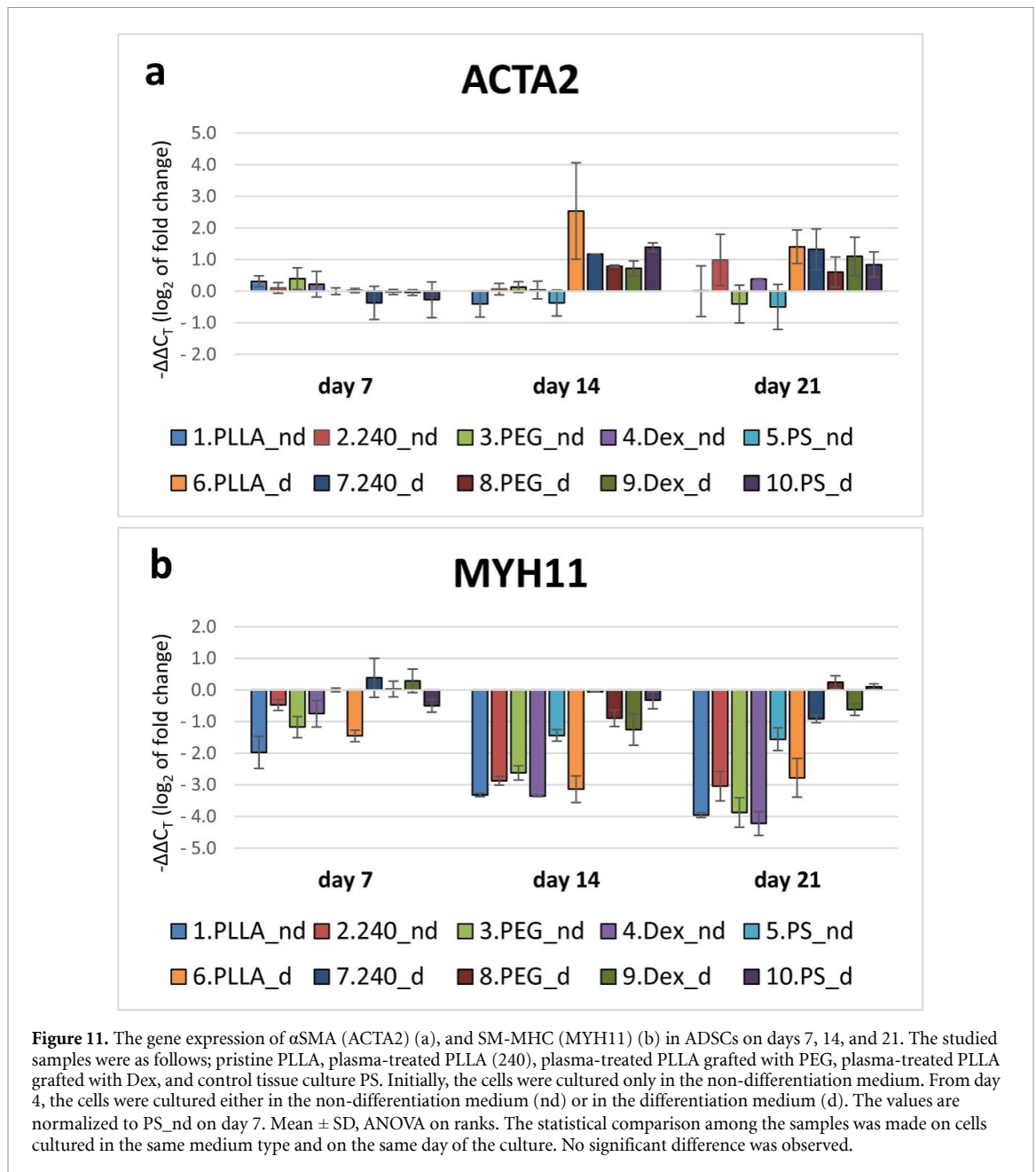


Figure 10. Gene expression of type I collagen (COL1) (a), calponin (CNN1) (b) and smoothelin (SMTN) (c) in ADSCs on days 7, 14, and 21. The studied samples were as follows; pristine PLLA, plasma-treated PLLA (240), plasma-treated PLLA grafted with PEG, plasma-treated PLLA grafted with Dex, and the control tissue culture PS. Initially, the cells were cultured only in the non-differentiation medium. From day 4, the cells were cultured either in the non-differentiation medium (nd) or in the differentiation medium (d). The values are normalized to PS_nd on day 7. Mean \pm SD, ANOVA on ranks. The statistical comparison among the samples was made on cells cultured in the same medium type and on the same day of the culture. No significant difference was observed.



According to many studies, PLLA in the form of nanofibres, microfibres or films is biocompatible with various cell types, including HSVECs, myoblasts, fibroblasts, keratinocytes and ADSCs (Sarasua *et al* 2011, Ballester-Beltrán *et al* 2014, Sabbatier *et al* 2015, Xavier *et al* 2016).

Our study showed similar adhesion, and also subsequent growth and metabolic activity of ADSCs on all tested materials when cultured in the non-differentiation medium. However, ADSCs cultured in the differentiation medium displayed higher cell numbers and higher metabolic activity on PLLA240 and on PS than on the other tested samples. Moreover, on pristine PLLA, PEG and Dex, the ADSCs cultured in the differentiation medium started to partially detach on days 14 and 21. Interestingly, similar cell behaviour as in the case

of differentiated ADSCs was observed for VSMCs. The VSMCs showed worse adhesion, lower growth and lower metabolic activity, especially on pristine PLLA. When VSMCs were cultured in the non-differentiation medium, lower metabolic activity and slightly later detachment of the cells was also observed on the PEG and Dex samples than on PLLA240 and on PS.

Pristine PLLA and its modification by plasma treatment. Pristine PLLA can be burdened with a relatively high level of hydrophobicity, which can impair cell adhesion. It is generally known that, on hydrophobic surfaces, cell adhesion-mediating proteins, e.g. vitronectin and fibronectin, which are present in the serum supplement of cell culture media, are adsorbed in a rigid and denatured conformation, which hampers the accessibility of specific amino

acid sequences in these proteins to cell adhesion receptors (for a review, see Bacakova *et al* 2011). The surface irregularities of PLLA can also influence protein adsorption from FBS, which is important for subsequent cell adhesion. Foldberg *et al* observed higher protein adsorption on PLLA films patterned with circular indentations than on flat pristine PLLA films (Foldberg *et al* 2012). In their study, they observed reduced cell adhesion on both PLLA films than on the control PS; however, the cells subsequently displayed the same growth rate on PLLA films and on the control PS materials. Moreover, cells cultured on PLLA substrates, especially on the patterned substrates, expressed higher mRNA levels of lineage-specific genes than the cells cultured on the control PS material (Foldberg *et al* 2012). The PLLA surfaces could therefore serve as a suitable microenvironment for ADSC growth and differentiation.

Protein adsorption can be further improved by plasma treatment, which is generally known to improve cell adhesion and proliferation (Yamaguchi *et al* 2004). The change in material surface characteristics induced by plasma treatment can better mimic the properties of ECM on the micro- or nanolevel scale (Bacakova *et al* 2011). Ar or O₂ plasma treatment of PLLA membranes can increase the surface roughness and can tailor the hydrophobicity of pristine PLLA. This decrease in the CA can be controlled by the power or the length of time of plasma treatment (Correia *et al* 2016, Bacakova *et al* 2018a, Slepíčka *et al* 2018). According to a study by Argentati *et al*, it seems that O₂ plasma treatment of PLLA films supported higher protein absorption mainly from 10% FBS and blood plasma rather than in the case of pristine PLLA films (Argentati *et al* 2018). Moreover, Argentati *et al* compared the morphology of various stem cell types, i.e. ADSCs, bone marrow stem cells (BM-MSCs) and Wharton's jelly stem cells (WJSCs), and they observed that the cell adhesion to the same PLLA sample seemed to be stem cell type-specific. Specifically, ADSCs cultured on pristine PLLA formed spheroid structures, while ADSCs cultured on plasma-treated PLLA had a fibroblast-like morphology. BM-MSCs maintained their typical fibroblast-like morphology both on pristine PLLA and on plasma-treated PLLA. WJSCs formed spheroid structures both on pristine PLLA and on plasma-treated PLLA (Argentati *et al* 2018).

Similarly, in our previous study, we observed different sizes of the cell spreading area and cell growth on pristine PLLA, on heat-treated carbon coated PLLA, and on the control PS samples, depending on the specific cell type (namely: MG-63, Saos-2, fibroblasts, CPAE, and VSMCs) (Lišková *et al* 2019). The cell type-specific interactions with pristine PLLA are in accordance with our current study, in which our pristine PLLA foils were favourable for the adhesion

of non-differentiated ADSCs but, at the same time, unfavourable for the initial adhesion of VSMCs. These differences in adhesion could also be influenced by the presence of variably expressed surface adhesion molecules and cytoskeleton proteins in non-differentiated ADSCs (for a review, see Argentati *et al* 2019), in differentiated ADSCs, or in mature VSMCs (for a review, see Moiseeva 2001). The quiescent non-proliferative phenotype of VSMCs is characterized by high RNA expression and well-developed protein structures interacting in the cell contraction (i.e. α SMA, calponin, caldesmon and SM-MHC) (Bacakova *et al* 2018c). Logically, our study suggests that, on some PLLA samples, VSMCs could manifest worse adhesion and subsequent higher detachment because of their contractile properties and because of poorly-developed cell-material interactions. These findings are also in accordance with those observed in differentiated ADSCs in our experiment, where the rapid development of contractile proteins was accompanied by a later slight tendency to detach from the same samples, as in case of VSMCs. Stem cells in general are also susceptible to mechanosensing and mechanotransduction signalling, which is usually caused by ECM and/or biomaterial properties. These specific properties (e.g. stiffness, elasticity, tension, etc) can influence the expression of variable adhesion and cytoskeleton proteins, and can drive the stem cell differentiation towards specific cell lineages (Vining and Mooney 2017, Argentati *et al* 2019).

The differences in adhesion and growth of ADSCs and VSMCs on the studied materials could be potentially influenced by the different origin of the cells, i.e. human ADSCs and porcine VSMCs. The porcine cardiovascular system has been reported to have a relatively high similarity to the human cardiovascular system. Moreover, the porcine VSMCs showed a relatively high stability of the differentiated contractile phenotype which makes them suitable for *in vitro* experiments (Christen *et al* 1999). Nevertheless, some differences between porcine and human cells of various types have been reported. For example, porcine mesenchymal stem cells can differ from human mesenchymal stem cells in the cell size or in the presence of some specific CD surface markers such as CD73 or CD105 (Schweizer *et al* 2020). Interestingly, mature human chondrocytes were reported to have a lower proliferation rate and to show a lower expression of β 1-integrins and of vinculin than animal-derived chondrocytes (Schulze-Tanzil *et al* 2009). Beta1-integrins and vinculin are, among others, involved in cell-material interactions, and the specific expression rate could therefore influence the process of cell adhesion in cells from different species. The same authors also reported visual differences in the F-actin cytoskeleton between human and animal-derived chondrocytes (Schulze-Tanzil *et al* 2009).

Interestingly, even the same cell type can display different behaviour on the same sample type, depending on the culture conditions. Wan *et al* (2003) studied the behaviour of mouse fibroblasts on pristine PLLA and on NH₃ plasma-treated PLLA, in static culture conditions and also in dynamic culture conditions. The fibroblasts showed similar initial adhesion to each of the two compared PLLA materials under static conditions. However, the cells cultured on plasma-treated PLLA better withstood the shear stress conditions, while the cells on pristine PLLA detached immediately (Wan *et al* 2003). It seems that plasma treatment provides tighter adhesion cues for cells. This could be advantageous for the production of vascular grafts, because the cells, mainly the ECs, are continually exposed to dynamic shear stress conditions. Stronger adhesion of the cells (both ADSCs and VSMCs) to the plasma-treated samples than to the pristine PLLA samples was also observed in our study, mainly in later time intervals under static culture conditions.

PLLA grafting with PEG and Dex. PEG (also referred to as polyethylene oxide, PEO) is a hydrophilic and biocompatible polymer that is generally referred to as an ‘antifouling’ molecule, because of its negative impact on protein absorption and consequent cell adhesion (Bacakova *et al* 2011). However, it seems that the length of the PEG chain has an important influence on potential cell adhesion and growth. Thus, PEG can act as an anti-adhesive biomaterial coating or as a pro-adhesive biomaterial coating. Grafting the materials with PEG of high molecular weight (i.e. $M_{\text{PEG}} = 20\,000$) induced a lower CA, a more differentiated surface and better growth of VSMCs than grafting the materials with PEG with lower molecular weight (i.e. $M_{\text{PEG}} = 300$ and $M_{\text{PEG}} = 6000$) (Svorcik *et al* 2012). Thus, based on our previous results, $M_{\text{PEG}} = 20\,000$ was our choice for the current study to support suitable cell adhesion and growth.

Similarly, Dex grafting of PLLA foils was used in our study to ameliorate the cell adhesion and growth. Dex is a polysaccharide compound with favourable biocompatible and anti-thrombogenic properties (for a review, see Bacakova *et al* 2014). However, the influence of Dex on the growth of a specific cell type can be ambiguous. Dex derivatives can mimic some heparin effects in blood vessels. Specifically bound Dex copolymers can act as a pro-adhesive surface for ECs, and simultaneously as a low-adhesive surface for VSMCs (Derkaoui *et al* 2010). Nanofibres composed of Dex and pullulan can promote vascular phenotype and can provide a suitable environment for the growth of VSMCs and ECs (Shi *et al* 2012). In addition to the most widely studied polysaccharides in vascular tissue engineering (i.e. Dex and pullulan), cellulose as a similar polysaccharide compound seems to have favourable properties for the growth of VSMCs and/or ECs (Bačáková *et al* 2014).

Composition of culture media. The composition of the media used in our study (i.e. the non-differentiation medium and the differentiation medium) had a non-negligible influence on the behaviour of the ADSCs and VSMCs when cultured on PLLA foils. In general, the differentiation medium (containing BMP4, TGFβ1 and ascorbic acid) induced higher initial metabolic activity of ADSCs than the non-differentiation medium. It also triggered the differentiation of ADSCs towards VSMCs. This was successfully proved by RT-PCR and by immunofluorescence staining of specific early, mid-term and also some late markers of VSMC differentiation on all variably-modified PLLA samples. We also studied the influence of the same composition of the medium on mature VSMCs that were cultured on modified PLLA foils. The differentiation medium (containing BMP4, TGFβ1 and ascorbic acid) caused lower metabolic activity and lower cell numbers of VSMCs on the PLLA foils than the non-differentiation medium. Immunofluorescence staining revealed that all VSMCs were positive for their specific markers when cultured either in the non-differentiation medium or in the differentiation medium. However, we revealed a decrease in the mRNA expression of specific markers in time. Surprisingly, this decrease was greater when the VSMCs were cultured in the differentiation medium. The decrease in the mRNA levels of specific markers and/or the subsequent loss of contractile proteins could be caused by the static *in vitro* culture conditions, which are known to support a synthetic phenotype of VSMCs rather than a contractile phenotype of VSMCs (Chang *et al* 2014). These two phenotypes may have the ability to switch according to the culture conditions (Rensen *et al* 2007).

In addition, it is known that BMP4, TGFβ1 and ascorbic acid in various concentrations can act variably in cell proliferation and differentiation. A strongly positive effect of TGFβ1 and/or BMP4 on stem cell differentiation towards VSMCs has been proved in many studies (for a review, see Zhang *et al* 2017). However, in the case of mature VSMCs, it has been reported that TGFβ1 and BMP4 enhanced the proliferation of pulmonary artery smooth muscle cells (PASMCs) from donors suffering from primary pulmonary hypertension (Morrel *et al* 2001). At the same time, TGFβ1 and BMP4 inhibited the proliferation of PASMCs isolated from healthy control donors and from patients suffering from secondary pulmonary hypertension (Morrell *et al* 2001). Interestingly, the response of VSMCs to BMP4 can be site-specific. BMP4 inhibited the proliferation of PASMCs from proximal segments of the pulmonary artery, but increased the proliferation of PASMCs from peripheral segments of this artery (Yang *et al* 2005). In the same study, BMP4 also promoted the survival of peripheral PASMCs, but not of proximal PASMCs, when exposed to apoptosis-inducing

agents (Yang *et al* 2005). The presence of ascorbic acid in the culture medium is important for the synthesis of collagen fibres, which are one of the basic components of vascular ECM. In our study, the differentiation medium supported the production of extracellular type I collagen, the main component of ECM in *tunica media*, which together with type III collagen is very important for imparting strength to the vascular wall (Wagenseil and Mecham 2009). However, it should be pointed out that overexpression of RNA and abundant formation of ECM proteins can be a sign of vascular fibrosis (Ponticos and Smith 2014).

5. Conclusion

ADSCs and VSMCs confirmed that variously modified PLLA foils in a three-week culture have high biocompatibility, comparable to the level of biocompatibility of the control PS. The most stable monolayer of cells was observed on plasma-treated PLLA and on the PS control, whereas pristine PLLA and PLLA modified with PEG and Dex were characterized by slightly later cell detachment. From this point of view, plasma-treated PLLA seem to be most suitable for obtaining a sufficient amount of cells for vascular wall reconstruction. However, all the PLLA materials supported the growth of ADSCs and their differentiation towards VSMCs. Although the cell behaviour on modified PLLA foils can be influenced by the specific cell type and by the composition of the medium, it seems that PLLA with all the modifications tested here is favourable for the purposes of vascular tissue engineering.

Acknowledgments

Dr Elena Filova (Institute of Physiology) is gratefully acknowledged for helping with isolating VSMCs. The authors would like to acknowledge Mr Robin Healey (Czech Technical University in Prague) for his language revision of the manuscript.

Conflict of interest

The authors declare no conflict of interest.

Funding

This work was supported by the Grant Agency of Charles University (GAUK, Project No. 642217), by the Ministry of Education, Youth and Sports of the Czech Republic within LQ1604 National Sustainability Program II (BIOCEV-FAR Project) and by the project 'BIOCEV' (CZ.1.05/1.1.00/02.0109), and by the Grant Agency of the Czech Republic, Grant No. 17-00885S.

ORCID iD

Martina Travnickova  <https://orcid.org/0000-0002-6348-3607>

References

- Alcantar N A, Aydil E S and Israelachvili J N 2000 Polyethylene glycol-coated biocompatible surfaces *J. Biomed. Mater. Res.* **51** 343–51
- Alexandre N, Costa E, Coimbra S, Silva A, Lopes A, Rodrigues M, Santos M, Mauricio A C, Santos J D and Luís A L 2015 In vitro and in vivo evaluation of blood coagulation activation of polyvinyl alcohol hydrogel plus dextran-based vascular grafts *J. Biomed. Mater. Res. A* **103** 1366–79
- Argentati C *et al* 2018 Surface hydrophilicity of poly(L-Lactide) acid polymer film changes the human adult adipose stem cell architecture *Polymers* **10** E140
- Argentati C, Morena F, Tortorella I, Bazzucchi M, Porcellati S, Emiliani C and Martino S 2019 Insight into mechanobiology: how stem cells feel mechanical forces and orchestrate biological functions *Int. J. Mol. Sci.* **20** 5337
- Bacakova L *et al* 2018a Stem cells: their source, potency and use in regenerative therapies with focus on adipose-derived stem cells - a review *Biotechnol. Adv.* **36** 1111–26
- Bacakova L, Filova E, Parizek M, Ruml T and Svorcik V 2011 Modulation of cell adhesion, proliferation and differentiation on materials designed for body implants *Biotechnol. Adv.* **29** 739–67
- Bačáková L, Novotná K and Pařízek M 2014 Polysaccharides as cell carriers for tissue engineering: the use of cellulose in vascular wall reconstruction *Physiol. Res.* **63** S29–47
- Bacakova L, Travnickova M, Filova E, Matejka R, Stepanovska J, Musilkova J, Zarubova J and Molitor M 2018b Vascular smooth muscle cells (VSMCs) in blood vessel tissue engineering: the use of differentiated cells or stem cells as VSMC precursors *Muscle Cell and Tissue - Current Status of Research Field* (Rijeka: IntechOpen) 289–308
- Bacakova L, Travnickova M, Filova E, Matejka R, Stepanovska J, Musilkova J, Zarubova J and Molitor M 2018c The role of vascular smooth muscle cells in the physiology and pathophysiology of blood vessels in *Muscle Cell and Tissue - Current Status of Research Field* (Rijeka: IntechOpen) 229–57
- Ballester-Beltrán J, Lebourg M, Capella H, Diaz Lantada A and Salmerón-Sánchez M 2014 Robust fabrication of electrospun-like polymer mats to direct cell behaviour *Biofabrication* **6** 035009
- Carrabba M and Madeddu P 2018 Current strategies for the manufacture of small size tissue engineering vascular grafts *Front. Bioeng. Biotechnol.* **6** 41
- Chang S, Song S, Lee J, Yoon J, Park J, Choi S, Park J K, Choi K and Choi C 2014 Phenotypic modulation of primary vascular smooth muscle cells by short-term culture on micropatterned substrate *PLoS One* **9** e88089
- Chatpun S and Cabrales P 2011 Effects on cardiac function of a novel low viscosity plasma expander based on polyethylene glycol conjugated albumin *Minerva Anesthesiol.* **77** 704–14
- Chlupac J, Filova E and Bacakova L 2009 Blood vessel replacement: 50 years of development and tissue engineering paradigms in vascular surgery *Physiol. Res.* **58** S119–39
- Christen T, Bochaton-Piallat M L, Neuville P, Rensen S, Redard M, van Eys G and Gabbiani G 1999 Cultured porcine coronary artery smooth muscle cells. A new model with advanced differentiation *Circ. Res.* **85** 99–107
- Correia D M, Ribeiro C, Botelho G, Borges J, Lopes C, Vaz F, Carabineiro S A C, Machado A V and Lanceros-Mendez S 2016 Superhydrophilic poly(L-lactic acid) electrospun membranes for biomedical applications obtained by argon and oxygen plasma treatment *Appl. Surf. Sci.* **371** 74–82
- Derkaoui S M, Labbé A, Purnama A, Gueguen V, Barbaud C, Avramoglou T and Letourneur D 2010 Films of

- dextran-graft-polybutylmethacrylate to enhance endothelialization of materials *Acta Biomater.* **6** 3506–13
- Filová E, Brynda E, Riedel T, Chlupáč J, Vandrovcová M, Svindrych Z, Lisá V, Houska M, Pirk J and Bačáková L 2014 Improved adhesion and differentiation of endothelial cells on surface-attached fibrin structures containing extracellular matrix proteins *J. Biomed. Mater. Res. A* **102** 698–712
- Foldberg S, Petersen M, Fojan P, Gurevich L, Fink T, Pennisi C P and Zachar V 2012 Patterned poly(lactic acid) films support growth and spontaneous multilineage gene expression of adipose-derived stem cells *Colloids Surf. B* **93** 92–99
- Goins A, Webb A R and Allen J B 2019 Multi-layer approaches to scaffold-based small diameter vessel engineering: A review *Mater. Sci. Eng. C* **97** 896–912
- Gritsch L, Conoscenti G, La Carrubba V, Noeaid P and Boccaccini A R 2019 Poly(lactide)-based materials science strategies to improve tissue-material interface without the use of growth factors or other biological molecules *Mater. Sci. Eng. C* **94** 1083–101
- Hahn M S, Mchale M K, Wang E, Schmedlen R H and West J L 2007 Physiologic pulsatile flow bioreactor conditioning of poly(ethylene glycol)-based tissue engineered vascular grafts *Ann. Biomed. Eng.* **35** 190–200
- Hielscher D, Kaebisch C, Braun B J V, Gray K and Tobiasch E 2018 Stem cell sources and graft material for vascular tissue engineering *Stem Cell Rev. Rep.* **14** 642–67
- Liskova J, Hadraba D, Filova E, Konarik M, Pirk J, Jelen K and Bacakova L 2017 Valve interstitial cell culture: production of mature type I collagen and precise detection *Microsc. Res. Tech.* **80** 936–42
- Lišková J, Slepíčková Kasálková N, Slepíčka P, Švorčík V and Bačáková L 2019 Heat-treated carbon coatings on poly(l-lactide) foils for tissue engineering *Mater. Sci. Eng. C* **100** 117–28
- Mas-Moruno C, Su B and Dalby M J 2019 Multifunctional coatings and nanotopographies: toward cell instructive and antibacterial implants *Adv. Healthcare Mater.* **8** e1801103
- Moiseeva E P 2001 Adhesion receptors of vascular smooth muscle cells and their functions *Cardiovasc. Res.* **52** 372–86
- Morrell N W, Yang X, Upton P D, Jourdan K B, Morgan N, Sheares K K and Trembath R C 2001 Altered growth responses of pulmonary artery smooth muscle cells from patients with primary pulmonary hypertension to transforming growth factor- β 1 and bone morphogenetic proteins *Circulation* **104** 790–5
- Nakagawa M, Teraoka F, Fujimoto S, Hamada Y, Kibayashi H and Takahashi J 2006 Improvement of cell adhesion on poly(L-lactide) by atmospheric plasma treatment *J. Biomed. Mater. Res. A* **77A** 112–8
- Pashneh-Tala S, Macneil S and Claeysens F 2016 The tissue-engineered vascular graft—past, present, and future *Tissue Eng. B* **22** 68–100
- Ponticos M and Smith B D 2014 Extracellular matrix synthesis in vascular disease: hypertension, and atherosclerosis *J. Biomed. Res.* **28** 25–39
- Przekora A, Vandrovcová M, Travnickova M, Pajorova J, Molitor M, Ginalska G and Bacakova L 2017 Evaluation of the potential of chitosan/ β -1,3-glucan/hydroxyapatite material as a scaffold for living bone graft production in vitro by comparison of ADSC and BMDSC behaviour on its surface *Biomed. Mater.* **12** 015030
- Rensen S S, Doevendans P A and van Eys G J 2007 Regulation and characteristics of vascular smooth muscle cell phenotypic diversity *Neth. Heart J.* **15** 100–8
- Sabbatier G, Larrañaga A, Guay-Bégin A A, Fernandez J, Diéval E, Durand B, Sarasua J R and Laroche G 2015 Design, degradation mechanism and long-term cytotoxicity of poly(L-lactide) and poly(Lactide-co- ϵ -caprolactone) terpolymer film and air-spun nanofiber scaffold *Macromol. Biosci.* **15** 1392–410
- Sarasua J R, López-Rodríguez N, Zuza E, Petisco S, Castro B, Del Olmo M, Palomares T and Alonso-Varona A 2011 Crystallinity assessment and in vitro cytotoxicity of polylactide scaffolds for biomedical applications *J. Mater. Sci., Mater. Med.* **22** 2513–23
- Schulze-Tanzil G et al 2009 Differing in vitro biology of equine, ovine, porcine and human articular chondrocytes derived from the knee joint: an immunomorphological study *Histochem. Cell Biol.* **131** 219–29
- Schweizer R et al 2020 Evaluation of porcine versus human mesenchymal stromal cells from three distinct donor locations for cytototherapy *Front. Immunol.* **11** 826
- Shi L, Aid R, Le Visage C and Chew S Y 2012 Biomimicking polysaccharide nanofibers promote vascular phenotypes: a potential application for vascular tissue engineering *Macromol. Biosci.* **12** 395–401
- Slepíčka P, Siegel J, Lyutakov O, Slepíčková Kasálková N, Kolská Z, Bačáková L and Švorčík V 2018 Polymer nanostructures for bioapplications induced by laser treatment *Biotechnol. Adv.* **36** 839–55
- Slepíčka P, Slepíčková Kasálková N, Stránská E, Bačáková L and Švorčík V 2013 Surface characterization of plasma treated polymers for applications as biocompatible carriers *EXPRESS Polym. Lett.* **7** 535–45
- Slepíčková Kasálková N, Slepíčka P, Bačáková L, Sajdl P and Švorčík V 2013 Biocompatibility of plasma nanostructured biopolymers *Nucl. Instrum. Methods Phys. Res. B* **307** 642–6
- Strobel H A, Qendro E I, Alsberg E and Rolle M W 2018 Targeted delivery of bioactive molecules for vascular intervention and tissue engineering *Front. Pharmacol.* **9** 1329
- Svorčík V, Makajová Z, Kasálková-Slepíčková N, Kolská Z and Bačáková L 2012 Plasma-modified and polyethylene glycol-grafted polymers for potential tissue engineering applications *J. Nanosci. Nanotechnol.* **12** 6665–71
- Trávníčková M and Bačáková L 2018 Application of adult mesenchymal stem cells in bone and vascular tissue engineering *Physiol. Res.* **67** 831–50
- Travnickova M, Pajorova J, Zarubova J, Krocilova N, Molitor M and Bacakova L 2020 The influence of negative pressure and of the harvesting site on the characteristics of human adipose tissue-derived stromal cells from lipoaspirates *Stem Cells Int.* **2020** 1016231
- Vining K H and Mooney D J 2017 Mechanical forces direct stem cell behaviour in development and regeneration *Nat. Rev. Mol. Cell Biol.* **18** 728–42
- Wagenseil J E and Mecham R P 2009 Vascular extracellular matrix and arterial mechanics *Physiol. Rev.* **89** 957–89
- Wan Y, Yang J, Yang J, Bei J and Wang S 2003 Cell adhesion on gaseous plasma modified poly-(L-lactide) surface under shear stress field *Biomaterials* **24** 3757–64
- Xavier M V, Macedo M F, Benatti A C B, Jardim A L, Rodrigues A A, Lopes M S, Lambert C S, Filho R M and Kharmandayan P 2016 PLLA synthesis and nanofibers production: viability by human mesenchymal stem cell from adipose tissue *Proc. CIRP* **49** 213–21
- Yamaguchi M, Shinbo T, Kanamori T, Wang P C, Niwa M, Kawakami H, Nagaoka S, Hirakawa K and Kamiya M 2004 Surface modification of poly(L-lactic acid) affects initial cell attachment, cell morphology, and cell growth *J. Artif. Organs* **7** 187–93
- Yang X, Long L, Southwood M, Rudarakanchana N, Upton P D, Jeffery T K, Atkinson C, Chen H, Trembath R C and Morrell N W 2005 Dysfunctional Smad signaling contributes to abnormal smooth muscle cell proliferation in familial pulmonary arterial hypertension *Circ. Res.* **96** 1053–63
- Zhang X, Bendeck M P, Simmons C A and Santerre J P 2017 Deriving vascular smooth muscle cells from mesenchymal stromal cells: evolving differentiation strategies and current understanding of their mechanisms *Biomaterials* **145** 9–22
- Zhu J 2010 Bioactive modification of poly(ethylene glycol) hydrogels for tissue engineering *Biomaterials* **31** 4639–56